SEMMELWEIS EGYETEM DOKTORI ISKOLA

Ph.D. értekezések

3223.

TIBORI KINGA

Patobiokémia

című program

Programvezető: Dr. Csala Miklós, egyetemi tanár

Témavezetők: Dr. Csala Miklós, egyetemi tanár és Dr. Kereszturi Éva, egyetemi docens

Studies on transcriptional control and genetic polymorphism of human stearoyl-CoA desaturase 1

PhD thesis

Kinga Tibori

Molecular Medicine Division Semmelweis University





Supervisors: Éva Kereszturi, Ph.D

Miklós Csala, MD, D.Sc

Official reviewers: Barbara Molnár-Érsek, Ph.D

Ferenc Fekete, Ph.D

Head of the Complex Examination Committee: László Tretter, D.Sc

Members of the Complex Examination Committee: Beáta Törőcsik, Ph.D

Péter Hajdinák, Ph.D

Budapest

2025

Content

List of abbreviations	4
List of figures and tables	7
1. Introduction	9
1.1. Fatty acid desaturation	9
1.1.1. Saturated and unsaturated fatty acids	10
1.1.1.1. Structural features	11
1.1.1.2. Metabolic differences	12
1.1.1.3. Health implications	13
1.1.2. Enzyme systems of desaturation	19
1.1.2.1. Synthesis of monounsaturated and polyunsaturated FAs	20
1.1.2.2. Enzymatic process of desaturation	21
1.1.3. Human acyl-CoA desaturases	21
1.1.3.1. Human Δ9 desaturase isoenzymes	21
1.2. Control of <i>SCD1</i> gene expression	23
1.2.1. Transcriptional regulation	23
1.2.2. Posttranscriptional regulation	25
1.3. <i>SCD1</i> gene polymorphisms	26
1.3.1. Variant of the UTR	26
1.3.2. Variants of the protein coding section	26
1.3.3. Variants of the promoter	27
1.4. Medical significance of <i>SCD1</i> polymorphisms and mutations	27
2. Objectives	30
3. Methods	32
3.1 Chemicals, materials and equipment	32

	3.2.	Web-based tools for <i>in silico</i> analysis	33
	3.3.	Plasmid construction and mutagenesis	33
	3.4.	Cell culture and transfection	35
	3.5.	Cell treatments	35
	3.6.	Preparation of cell lysates	36
	3.7.	Immunoblot analysis	37
	3.8.	Luciferase assay	37
	3.9.	RNA isolation, cDNA synthesis	37
	3.10.	qPCR	38
	3.11.	GC-FID analysis of fatty acid profiles	39
	3.12.	Subjects and genotyping	39
	3.13.	Statistical analysis	41
4	. Res	ults	42
	4.1.	Effects of fatty acids on SCD1 level	42
	4.1.	1. Impact of different dietary FAs on SCD1 expression at the protein level	42
	4.1.	2. Changes in <i>SCD1</i> mRNA level in response to various dietary FAs	43
	4.1.	3. Effects of dietary FAs through <i>SCD1</i> promoter	44
	4.2.	Variations of SCD1 gene	45
	4.2.	1. SNPs of SCD1 promoter	45
	4	2.1.1. Effect of promoter SNPs on FA-dependent modulation of <i>SCD1</i>	
		expression	.47
	4	2.1.2. TF binding modifications of <i>SCD1</i> promoter SNPs:	
		an in silico analysis	.49
	4	2.1.3. Allele-specific effect of ETS1 on SCD1 promoter activity	.50
	4	2.1.4. Modulation of the FA-induced activity of rs1054411_G	
		promoter variants by ETS1	
		2. Variations of the coding region	
	4	.2.2.1. Effect of M224L missense SCD1 SNP on the protein level	.54

	4.2.2.2.	Influence of M224L missense SCD1 SNP on the mRNA level	55
	4.2.2.3.	Protein stability of M224L SCD1 variants	57
	4.2.2.4.	Impact of FAs on the M224L protein variants	58
	4.2.2.5.	Enzymatic activity of M224L desaturase variants	60
	4.2.2.6.	Is the increase in protein level caused by the polymorphism due	
		to the missing methionine or the leucine present?	61
4	.3. Assoc	iation studies	62
5.	Discussion	1	65
5	.1. Impor	tance of different types of FAs and their relationship with	
	SCD1	enzyme	65
5	.2. Polym	norphisms of SCD1	68
	5.2.1. Pro	moter SNPs	68
	5.2.2. M2	24L SNP	69
5	.3. Summ	narizing considerations	70
6.	Conclusion	ns	73
7.	Summary		74
8.	Bibliograp	hy	75
9.	Bibliograp	hy of own publications	86
10.	Acknowle	dgements	87

List of abbreviations

Abbreviation	Definition
AA	arachidonic acid
AP-1	activator protein-1 transcription factor
ATF6	activating transcription factor 6
BSA	bovine serum albumin
CAD	coronary artery disease
$C/EBP\alpha$	CAAT/enhancer binding protein α
CHOP	C/EBP homologous protein
DAG	diacylglycerol
Desat1	desaturase 1
DGAT	diacylglycerol acyl transferase
DHA	docosahexaenoic acid
DMEM	Dulbecco's modified Eagle medium
EGFR	epidermal growth factor receptor
eIF2 $lpha$	eukaryotic translation initiation factor 2α
ELOVL	very long chain fatty acid elongase
EPA	eicosapentaenoic acid
ETS1	ETS proto-oncogene 1, member of the ETS E26 or Erythroblast Transformation Specific family
FA	fatty acid
FADS	fatty acid desaturase
FAT	fatty acid translocase
FATP	fatty acid transport protein
FFA	free fatty acid
FID	flame ionization detector
HEK	human embryonic kidney
HNF4 α	hepatocyte nuclear factor 4 alpha
IL	interleukin
IRE	insulin response element
IRE1	inositol-requiring enzyme 1
IRS1	insulin receptor substrate-1

iTFA industrial trans fatty acid

JAK/STAT Janus kinase/signal transducer and activator of transcription

JNK c-Jun N-terminal kinase
LepRE leptin response element

LTB4 leukotriene B4
LXR liver X receptor

M224L Met→Leu amino acid exchange at position 224

MAF minor allele frequency

MAPK mitogen-activated protein kinase
MCP-1 monocyte chemoattractant protein-1

MFE minimum free energy

MUFA monounsaturated fatty acid

NADH nicotinamide adenine dinucleotide

NADPH nicotinamide adenine dinucleotide phosphate

NAFLD non-alcoholic fatty liver disease
NF-Y nuclear transcription factor Y

NFκB nuclear factor kappa-B

NOX3 NADPH oxidase 3
OGTT oral glucose tolerance test

PERK protein kinase-like ER kinase

PGC-1 α peroxisome proliferator-activated receptor co-activator-1 α

PI3K PI3 kinase

PKC ε protein kinase C epsilon

Pol II RNA polymerase II

PP2A protein phosphatase 2A

PPAR peroxisome proliferator-activated receptor

PUFA polyunsaturated fatty acid

PUFARE polyunsaturated fatty acid response element

ROS reactive oxygen species

rTFA ruminant-derived trans fatty acid

SCD stearoyl-CoA desaturase

SERCA sarco/endoplasmic reticulum Ca²⁺ ATPase

SFA saturated fatty acid

SNP single nucleotide polymorphism

SREBP-1c sterol regulatory element-binding protein-1c

T2DM type 2 diabetes mellitus

T3 triiodothyronine
TF transcription factor
TFA trans fatty acid
TLR Toll-like receptor
TM transmembrane

TNF α tumor necrosis factor- α TR triiodothyronine receptor
UFA unsaturated fatty acid

UPR unfolded protein response
VEP Variant Effect Predictor

VLDL very low-density lipoproteins

XBP1 X-box-binding protein 1

List of figures and tables

Figure 1:	Main cellular mechanisms of lipotoxicity	.9
Figure 2:	Function of SCD enzymes	23
Figure 3:	Transcription factors binding to <i>SCD1</i> promoter	24
Figure 4:	Importance of SCD1 in maintaining a balanced supply of fatty acids2	28
Figure 5:	SCD1 protein expression in FA-treated HEK293T and HepG2 cells4	13
Figure 6:	Impact of different FAs on the <i>SCD1</i> mRNA expression in HEK293T and HepG2 cells	14
Figure 7:	Effect of dietary FAs on <i>SCD1</i> promoter activity in HEK293T and HepG2 cells	1 5
Figure 8:	Location and function of <i>SCD1</i> promoter polymorphisms4	ŀ6
Figure 9:	Modulatory effect of the four most common promoter polymorphisms on FA-dependent <i>SCD1</i> expression in HEK293T cells	↓ 7
Figure 10	: Impact of rs1054411 SNP on SCD1 promoter activity in HepG2 cells4	18
Figure 11	Consensus sequence of ETS1 TF binding site5	50
Figure 12	FA-dependent ETS1 expression in HEK293T cells5	51
Figure 13	: Impact of rs1054411 SNP on the ETS1-mediated stimulation of <i>SCD1</i> promoter activity	52
Figure 14	Interaction between the effect of elaidate treatment and ETS1 overexpression on the activity of rs1054411_C and _G alleles of <i>SCD1</i>	72
Figure 15	promoter	S
T	in two cell lines	14
Figure 16	s SCD1 expression in transiently transfected HEK293T cells determined by aPCR	55

Figure 17:	In silico prediction of the secondary MFE structures of +670A and +670C SCD1 using the RNAfold online tool	56
		.50
Figure 18:	Allele-specific mRNA degradation of the two <i>SCD1</i> variant monitored by qPCR	57
Elouvo 10.		
Figure 19:	Stability of M224L SCD1 variants	.58
Figure 20:	Impact of different FAs on M224L variants of SCD1	.59
Figure 21:	Changes in FA content of cells transfected with M224L SCD1 variants	.60
Figure 22:	Comparison of intracellular Met224 and Ala224 SCD1 protein levels	.61
Figure 23:	Expression and FA-sensitivity of Ala224 SCD1	.62
Figure 24:	Effect of rs1054411 promoter polymorphism on SCD1 expression	.71
Figure 25:	Effect of M224L polymorphism on SCD1 function	.72
Table 1:	The most prevalent long-chain FAs in human diet	.11
Table 2:	Used chemicals, materials and equipment with their manufacturer	.32
Table 3:	Primers used for cloning and mutagenesis	.34
Table 4:	Antibodies used for protein detection	.37
Table 5:	Primers used for qPCR	.38
Table 6:	TaqMan primers and probes	.41
Table 7:	SNPs in SCD1 promoter	.46
Table 8:	List of transcription factors whose binding to SCD1 promoter may be	
	affected by the polymorphisms studied	.49
Table 9:	Comparison of allele, genotype, and genotype combination frequencies	
	of rs1054411 promoter SNP in control and T2DM groups	.63
Table 10:	Comparison of allele, genotype, and genotype combination frequencies	
	of M224L SNP in control and T2DM groups	.64

1. Introduction

1.1. Fatty acid desaturation

Lipids, which are essential for the human body, perform various tasks. They can be membrane constituents, signal molecules in cellular communication or transcriptional regulators of certain genes, they provide opportunity to store energy, and they help many proteins perform their proper functions, for example as chaperones, cofactors, carriers or anchors to membranes. There are simple lipids, in which fatty acids (FAs) form ester bonds with glycerol constituting fats and oils, or with long-chain alcohols creating waxes. Furthermore, and those are the prevalent lipids having diverse biological functions, there are complex lipids which contain additional building blocks beyond FAs and alcohols, such as phosphates, sugars, amino acids, or other functional groups. The main constitutional component of these lipid classes is a diverse range of FAs, which can be classified based on several criteria, including their length of hydrocarbon chain, degree of unsaturation, location and configuration of any double bonds in the chain. Besides their systematic and common names, each FA can be referred to by a shorthand notation containing these four pieces of information [1]: CN:p cis/trans tx, where CN indicates the carbon number (chain length); p stands for the number of double bonds, after which there is information about the double bond(s); t marks the terminus, which can be Δ if the double bond is counted from the carboxylic end or can be ω - or n- if counted from the methyl end; and x represents the position of this double bond, and the configuration may also be marked as cis or trans.

According to chain length, there are four types of FAs [2]. Short-chain FAs containing less than six carbon atoms are typically produced by gut bacteria during the fermentation of dietary fiber in the colon, and are also to be found in dairy products, such as milk, cheese, and yogurt. Medium-chain FAs have six to twelve carbon atoms, and the main representatives, such as caproic acid (6:0), caprylic acid (8:0) and capric acid (10:0), appear in coconut oil and palm kernel oil. Very long-chain FAs with chain length of more than twenty carbon atoms exhibit a wild range of roles, for example in lipid homeostasis, myelin maintenance, spermatogenesis, retinal function and anti-inflammation [3]. Melissic acid (30:0), first found in beeswax, nervonic acid (24:1 *cis* n-9), a FA which is

an essential component of myelin sheath, and the widely studied docosahexaenoic acid (DHA; 22:6 n-3), which is important in the functional development of the brain, belong to this category. In our laboratory, the focus is on long-chain FAs with chain lengths of 12-20 carbon atoms, more specifically C16 and C18 FAs, as these are the most abundant FAs in the human organism. Palmitic acid (16:0), mainly found in palm oil and coconut oil, in products made from animal fat, such as butter, cheese or milk, and in meats, such as beef, pork and chicken, is also added to many processed foods, like bakery products, fried foods or snacks as a preservative or flavor enhancer. Other examples of long-chain FAs include stearic acid (18:0), mainly found in cocoa and shea butter or oleic acid (18:1 $cis \Delta 9$) appearing primarily in natural oils.

The latter three parameters of FA classification – namely the number, location and configuration of double bonds – are related to desaturation, a biochemical process that introduce double bonds into fatty acid molecules. The cis double bonds cause the chain of unsaturated FAs to kink or bend, which affects the physical and chemical properties of these molecules and thus their biological functions. The human body needs not only the right amount, but also the optimally balanced composition of saturated and unsaturated FAs as it defines fundamental cellular processes (such as interactions between lipid assemblies and proteins, or the molecular properties of lipid bilayers), and it plays a crucial role in maintaining overall health and preventing various diseases. The position and the configuration of double bond(s) are also critical – while $cis \omega$ -6, and particularly $cis \omega$ -3 FAs have well-known beneficial effects, several studies highlight the differences in the health effects of cis and trans FAs.

1.1.1. Saturated and unsaturated fatty acids

According to the degree of unsaturation, indicating the number of double bonds in the carbon chain, FAs can be differentiated into saturated fatty acids (SFA), containing only single bonds between carbon atoms, making them "saturated" with hydrogen, and unsaturated FAs (UFA), containing one (monounsaturated FA, MUFA) or more double bonds (polyunsaturated FA, PUFA) in the hydrocarbon chain. The most common long-chain FAs, their degree of desaturation, and their main dietary sources are listed in Table 1. The presence or absence of double bonds affects the physical properties of FAs, such

as melting point and fluidity. The higher the degree of unsaturation, the lower the melting point of the FA. SFAs tend to be solid at room temperature, while UFAs are usually liquid. However, the length of the carbon chain also affects the melting point as longer chains have a greater surface area and stronger intermolecular forces, which require more energy to break apart and melt, *i.e.*, with chain length, the melting point also increases.

Table 1. The most prevalent long-chain FAs in human diet.

Carbon number	Name	Saturation	Cis/Trans	Occurrence
C16	palmitate	16:0 SFA	-	palm oil, butter, cheese, milk, meat, etc.
C16	palmitoleate	16:1 <i>cis</i> Δ9 MUFA (ω -7)	cis	animal fats, vegetable oils, marine oils, macadamia oil
	stearate	18:0 SFA	-	cocoa butter, shea butter
	oleate	18:1, $cis~\Delta 9$ MUFA $(\omega$ -9)	cis	natural oils (avocado, peanut, olive, canola, etc.)
C18	elaidate	18:1 trans Δ 9 MUFA (ω -9)	trans	bovine milk, some meats
CIO	vaccenate	18:1 <i>trans</i> Δ11 MUFA	trans	animal fats and dairy products
	linoleate	18:2 cis $\Delta 9$, $\Delta 12$ PUFA $(\omega ext{-}6)$	cis	essential FA; sunflower, corn oil, soybean oil, sesame, almonds
C20	arachidonic acid	20:4 all-cis Δ 5, Δ 8, Δ 11, Δ 14 PUFA (ω -6)	cis	conditionally essential FA; red meat, fish, eggs, dairy products

1.1.1.1. Structural features

FAs are carboxylic acids with aliphatic hydrocarbon chains and have a general chemical formula: RCOOH. In their favorable, extended conformation, SFAs have a linear, rod-like shape, while UFAs usually have a bent or kinked shape due to the presence of the double bond(s). However, in the case of UFAs, the orientation of the hydrogen atoms around the double bond also affects the structure. The kink is only present in *cis* configuration when hydrogen atoms around the double bond are on the same side of the molecule. In contrast, in *trans* configuration, the hydrogen atoms around the double bond are on opposite sides of the molecule, resulting in a more linear structure, similar to that of an SFA. The *cis* configuration is far more abundant in the human body, since there is no *de novo trans* fatty acid (TFA) synthesis and *cis* isomers are more predominant in the food we consume. However, small amounts of dietary TFAs are also ingested and

incorporated into human lipids. The presence of vaccenic acid (18:1 trans Δ 11), the main representative of TFAs (accounts for 60–80% of total ruminant-derived TFA content [4], and 4–8% of total ruminant-derived FA content [5]) was already proved in 1900's in beef, mutton and butter fat [6]. Later, it was found in other ruminants' fat and milk as well, for instance of cattle and sheep. The rumen of these animals contains a wide range of bacterial species that contribute significantly to lipid metabolism: they carry out certain transformations of dietary lipids. During one of these transformations between linoleic (18:2 n-6) and α -linolenic (18:3 n3) acids to stearic acid (18:0), biohydrogenation gives rise to the formation of TFA intermediates (natural, ruminant-derived TFAs: rTFAs) [5]. TFAs can also derive from industrial processes (iTFAs), such as partial hydrogenation of PUFA-rich oils and fats, which aims to increase shelf life and solidification, and yields margarine and shortening; or deodorization through which live steam is injected into unrefined oils (soybean, palm, canola or fish oils, for instance) under vacuum at high temperature to eliminate unpleasant natural flavor, odor or color [7]. During these processes, the double bond(s) of cis-MUFAs and cis-PUFAs may not only undergo geometric isomerization yielding trans-MUFAs and trans-PUFAs, but their position can also change [8]. Therefore, industrially generated TFAs are abundant in trans $\Delta 9$ and trans $\Delta 10$ isomers of 18 carbon MUFAs, among which the main representative is elaidic acid (18:1 trans Δ 9) – a positional isomer of vaccenic acid and a geometric isomer of the cis-MUFA, oleic acid [9] – which can reach up to 61% of total FA content of foods produced this way [5].

1.1.1.2. Metabolic differences

The presence of UFAs is critical for several reasons. Phospholipid and triglyceride synthesis involves the incorporation of two or three FAs through acylation reactions. Due to the specificity of the acyltransferase enzymes, the first and second carbon atoms of glycerol are normally acylated by a saturated and an unsaturated FA, respectively, and the third carbon atom in triglycerides can receive either a saturated or an unsaturated FA. The right FA composition is essential for the proper physical properties of these lipids. An optimal UFA content not only makes biological membranes properly fluid, flexible and elastic [10, 11], but also allows efficient transmembrane signaling [12]: increased degree of unsaturation enhances the permeability of the bilayer, and, through softening

the membrane and supporting membrane curvature, can help receptor activation and channel formation. In accordance with these physical impacts on membranes, PUFAs were also shown to play an important role in synaptic vesicle recycling [13].

Some PUFAs cannot be synthesized in the human body because we are unable to insert a double bond behind the ω -7 position, *i.e.*, closer than 7 carbon atoms to the end of the chain. Therefore, these so-called essential FAs must be taken in with food. Two FAs are considered essential for humans: the ω -3 α -linolenic acid and the ω -6 linoleic acid. In addition to being important membrane constituents, along with other UFAs, such as oleic acid, they are predominant components of cholesteryl esters [2]. Moreover, these essential PUFAs can be metabolized into various other PUFAs and further to lipid mediators: for instance, arachidonic acid (an ω -6 PUFA made from linoleic acid) is a precursor of countless important regulatory molecules, such as prostaglandins, leukotrienes or thromboxanes [14].

Although there is no human enzyme for geometric isomerization of FAs, TFAs of either ruminant or industrial origin can be metabolized, and their β -oxidation, elongation or further *cis*-desaturation can occur. Health effects of TFAs are controversial. They competitively interfere with the desaturation and elongation of *cis*-PUFAs and the change in membrane fluidity they cause has been reported to contribute to adverse cardiovascular effects [15] – although there might be differences between the impact of iTFAs and rTFAs [16]. These differences may be due to their different abundance – as rTFA can only account for a maximum of 8% of total FA in milk fat, while iTFA can account for up to 61% of total FA in certain pastries or shortenings [5]. Because of the potential negative health effects, many countries have legislated to limit the amount of iTFA allowed in foods. On the other hand, there are studies ascribing beneficial effects to TFAs, such as direct anti-carcinogenic effect of vaccenic acid on MCF-7 human mammary adenocarcinoma cells [4] or positive impact on systemic insulin sensitivity and type 2 diabetes mellitus (T2DM) of *trans*-palmitoleic acid (16:1 *trans* Δ 9) [8].

1.1.1.3. Health implications

While the body stores no proteins and only limited amounts of carbohydrates, fat can be deposited in large quantities in a specialized tissue. In fed state, the liver uses the excess carbohydrates and amino acids to synthesize FAs and build up triglycerides, which are packed in very low-density lipoproteins (VLDLs) to reach the adipose tissue via the blood circulation. Meanwhile, lipids from the food form chylomicrons in the intestinal epithelial cells and are also transported to the adipose tissue through the lymph and blood. Fatty acyl-CoA from these lipoproteins feeds triglyceride synthesis in the adipocytes and get stored in lipid droplets [17]. During starvation or prolonged physical activity, these triglycerides are hydrolyzed into glycerol and FAs, and the latter are delivered to starving cells by the circulation as albumin-associated non-esterified free FAs (FFA).

Glucotoxicity and lipotoxicity

Prolonged oversupply of nutrients can lead to obesity, which is an enlargement of adipose tissue with increased cell number (hyperplasia) and cell size (hypertrophy), although the former shows a genetic boundary [18]. Enlarged fat cells do not have adequate access to nutrients and oxygen, so they secrete adipokines such as monocyte chemoattractant protein-1 (MCP-1) [19] and leukotriene B4 (LTB4) [20], which trigger macrophage differentiation and monocyte chemotaxis, leading to local inflammation. In addition, activated inflammatory T cells secrete cytokines such as interleukins and tumor necrosis factor- α (TNF α), further enhancing the inflammation [21, 22]. Under the influence of these pro-inflammatory cytokines, a variety of signaling pathways are activated. These include the nuclear factor kappa-B (NFkB), Janus kinase/signal transducer and activator of transcription (JAK/STAT) and the c-Jun N-terminal kinase (JNK) pathways. The activation of these pathways, on the one hand, drives cells towards an inflammatory cell response by facilitating transcription of a variety of proinflammatory genes, and on the other hand, damages insulin signaling. Along these pathways, phosphatases and kinases are activated. These enzymes interfere with the function of the insulin receptor substrate-1 (IRS1) protein by removing activating phosphorylations (on tyrosines) and adding inhibitory phosphorylations (on serines/threonines) [23, 24]. Furthermore, as a long-term effect, the expression of IRS1 and the insulin receptor is reduced [25, 26]. Consequently, the local inflammation induces local insulin resistance, thus glucose uptake of the adipocytes decreases, which results in elevated blood glucose level (hyperglycemia). In the meantime, inflammatory cytokines leak from the inflamed adipose tissue into the blood circulation, thus the plasma level of TNF α , IL-6 and IL-1 β increases. Thereby, local inflammation turns into a mild systemic inflammation, damaging the insulin signaling pathway and glucose uptake of other cell

types as well, further elevating plasma glucose levels. Prolonged hyperglycemia increases the demand on β -cells, and increasing insulin production may eventually lead to dysfunction and even death of β -cells. The systemic harmful effect of persistent hyperglycemia is called glucotoxicity. Defective insulin signaling in adipocytes accelerates triglyceride turnover, which increases plasma levels of FFAs. A persistent excess of FFA, in turn, systematically damages the function of the cell – this phenomenon is called lipotoxicity. This means that circulating FFAs have a dual effect on many types of cells, such as muscle cells, β -cells or hepatocytes. They can enter the cells through various FA transporters, for instance fatty acid translocase (FAT/CD36) or fatty acid transport protein 2 (FATP2) – which proteins were proved to be upregulated in rat hepatocytes after FA treatment [27] and in patients with non-alcoholic fatty liver disease or chronic hepatitis C as well [28]. On the other hand, FFAs can enhance inflammation through cell surface receptors in various cells. The main mechanisms of lipotoxicity, including the effects of excessive FAs on oxidative and ER stress, ceramide accumulation and inflammation, are illustrated in Figure 1.

Oxidative stress

FFAs crossing the cell membrane are involved in the cell's metabolism as fatty acyl-CoAs [29]. Through mitochondrial β -oxidation, citrate cycle and oxidative phosphorylation, fatty acyl-CoA provides energy to the cell. In case of overnutrition induced lipotoxicity, cells take up FFAs even when they do not need them. Increased FA oxidation overloads the oxidative capacity of mitochondria, thus over time, incomplete oxidation of FFAs and the excess electrons delivered to the electron transfer chain [30, 31] lead to reactive oxygen species (ROS) production [32], which is one of the main pillars of oxidative stress. Exaggerated ROS generation can directly damage all the macromolecules in the cell, including DNA, moreover, ROS favors apoptosis through the activation of stress-sensitive cascades, such as NFκB, p38 and JNK MAPK pathways [33]. Examining hepatic insulin resistance, Dan Gao *et al.* showed in db/db mice and in HepG2 cell line as well that not only inflammatory cytokines but also NADPH oxidase 3 (NOX3)-derived ROS can activate JNK [34]. Besides, the delicate redox homeostasis of the ER is also exposed to oxidative stress [35].

ER stress

The large amount of acetyl-CoA drives the synthesis of complex lipids, which increases the burden on the ER and requires an increased number of properly folded proteins. Since protein disulfide bond formation increases ROS production [36], oxidative stress is enhanced. The protein overload and the oxidative stress cause ER stress and trigger the unfolded protein response (UPR). There are three transmembrane stress sensors in the ER, which primarily serve adaptation but may also lead to cell death. RNAdependent protein kinase-like ER kinase (PERK) attenuates general protein translation with the inactivating phosphorylation of the eIF2 α . Activating transcription factor 6 (ATF6) induces chaperons and ERAD proteins. And lastly, inositol-requiring enzyme 1 (IRE1) also induces ER chaperons and ERAD proteins and promote lipid synthesis through the activation of the X-box-binding protein 1 (XBP1) transcription factor mRNA. If prolonged UPR fails to rescue ER functions, it drives cell signaling towards apoptosis. ATF6 can induce the proapoptotic CCAAT/enhancer binding protein homologous protein (CHOP), and IRE1 increases the activation of JNK. Interestingly, PERK and IRE1 α are sensitive to increased lipid saturation as well [37, 38]. Thus, if the balance between saturated and unsaturated FAs is greatly shifted, the UPR is more prominent. Unsaturated FAs however, proved to be preventive against ER stress: for example, oleate obstructed the palmitate-induced activation of the UPR in β -cells [39].

Accumulation of DAGs and ceramides

The increased level of acyl-CoA gives a boost to lipid biosynthesis, so that cells other than adipocytes are also under the necessity of synthesizing and storing triglycerides, *i.e.*, forming lipid droplets. Fat accumulation used to be considered damaging to cells, but now the approach is that this process is an escape route to avoid harmful effects of excessive FAs. The appearance of fat droplets in peripheral cells is much more an accompanying phenomenon of lipotoxicity than a cause. Unsaturated FAs protect cells partly by enabling triglyceride synthesis [40]. When the triglyceride synthesizing capacity is saturated, the pressure grows on other lipid synthetic pathways including sphingolipid synthesis, and the accumulation of biosynthetic lipid intermediates, such as diglycerides and ceramides, occurs [41]. Diacylglycerol (DAG) accumulation in hepatocytes was shown to be caused by not only saturated but also unsaturated FAs, which process resulted in PKCε activation and deterioration of insulin-stimulated IRS-2 signaling [42].

While ceramides are the main precursors of other important sphingolipids, such as sphingomyelin or sphingosine, the significantly elevated amount of them after palmitate treatment is in correlation with ER-stress mediated β -cell death [43, 44]. Palmitateinduced ceramide accumulation was also proved to be linked with hepatic insulin resistance [27, 45]. Moreover, in rat L6 skeletal muscle cells [46] and in human muscle cells [47], ceramides were shown to trigger insulin resistance through the inhibition of Akt/PKB by protein phosphatase 2A (PP2A). In addition, ceramide impairs FA oxidation in mitochondria and provokes ER stress via inhibition of the sarco/endoplasmic reticulum Ca²⁺ ATPase (SERCA), through which depletes its calcium storage [48]. Besides insulin resistance and enhancement of lipotoxic effects, elevated ceramide level promotes apoptosis through cytochrome c release from mitochondria [49]. Rescuing effects of unsaturated FAs was shown in the case of lipid intermediates as well. Oleate, the major endogenous MUFA, has been proved by several research groups to be an activator of diacylglycerol acyl transferase (DGAT) that converts DAG to triacylglycerol, protecting against palmitate-induced DAG accumulation [48]. Maedler et al. demonstrated in human β -cells that palmitate and high glucose concentration induce DNA fragmentation and apoptosis, reduce cell proliferation, interfere with insulin secretion and overall disrupt β cell function due to elevated ceramide level and activation of mitochondrial apoptosis. Oleate and palmitoleate, however, prevented these detrimental effects and favored cell proliferation [50]. Henique et al. also verified in skeletal muscle cells that oleate can redirect palmitate towards triglyceride synthesis through enhanced diacylglycerol acyltransferase 2 expression, which decreases the amount of destructive palmitate derivatives, diglycerides and ceramides [51]. Our research group demonstrated in RINm5F rat insulinoma cell line that not only the mono-unsaturated oleate but the two most abundant dietary TFAs, elaidate (18:1 trans Δ 9) and vaccenate (18:1 trans Δ 11) also provide protection against palmitate-induced ceramide and diglyceride accumulation [41].

FAs as inflammation modulating signals

As mentioned above, FFAs can affect cells not only as nutrients or metabolites, but also as signal molecules by binding to cell surface receptors. Saturated FFAs can act on Toll-like receptors (TLR2, TLR4 [52]), which results in the production of inflammatory cytokines like interleukins (IL-1 β , IL-6) or TNF α [21, 22]. These cytokines bind to their

receptors and trigger signaling pathways inducing inflammation and/or apoptosis. These pathways also include the NFkB and JNK cascades. Unsaturated FAs can rescue these adverse effects too. ω -3 PUFAs, like eicosapentaenoic acid (EPA) and docosahexaenoic acid (DHA) found in oily fish, have anti-inflammatory effects as they are capable of decreasing the activation and migration of immune cells such as macrophages and neutrophils, as well as the production of pro-inflammatory cytokines. They were demonstrated in vitro and in vivo to decrease the level of TNF α , and interleukins (IL-1, IL-6, IL-8, and IL-12) in various cell types, such as macrophages, monocytes, endothelial and dendritic cells [53]. This effect is achieved by the inhibition of NF κ B through various options. TLR-4 can activate NFkB with the involvement of NADPH oxidase-dependent ROS and with the help of adaptor proteins recruited into lipid rafts acting as an organized signaling platform [54]. By altering cell membrane phospholipid FA composition, ω -3 PUFAs inhibit SFAs to promote raft formation, thus preventing the interaction between TLR-4 and NF κ B [54]. Another option is through the anti-inflammatory transcription factor, peroxisome proliferator-activated receptor γ (PPAR γ). ω -3 PUFAs are ligands of PPARy which not only can regulate inflammatory gene expression, thus decrease the amount of pro-inflammatory cytokines, but also inhibit the activation of NFkB [55]. Moreover, EPA and DHA are substrates of anti-inflammatory and inflammation resolving lipid mediators, resolvins, protectins and maresins [56]. Arachidonic acid, the most abundant ω -6 PUFA, found mainly in red meat, fish, and egg, however, as mentioned before, can give rise to pro-inflammatory eicosanoids, such as prostaglandins, leukotrienes and thromboxanes.

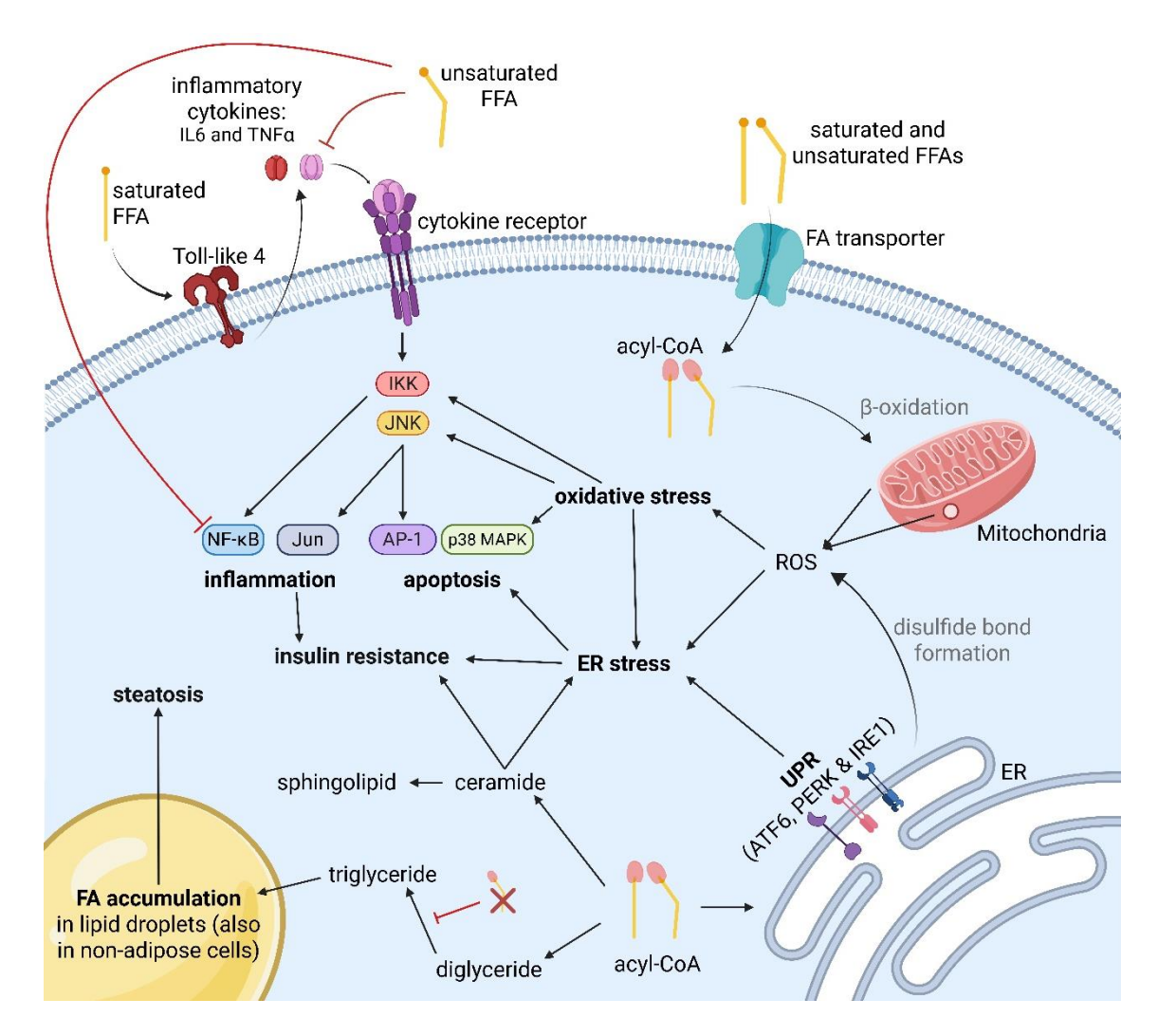


Figure 1. Main cellular mechanisms of lipotoxicity (Created in BioRender). Excessive FA uptake may cause oxidative and ER stress, even apoptosis. Triglycerides are deposited in fat droplets. Accumulating lipid intermediates can promote stress and apoptosis. Saturated FAs induce proinflammatory cytokines through Toll-like receptors, and this effect can be ameliorated by unsaturated FAs. ROS: reactive oxygen species; IKK: inhibitor of nuclear factor-kappa B kinase; NFκB: nuclear factor kappa-B; JNK: c-Jun N-terminal kinase; AP-1: activator protein-1 transcription factor; p38 MAPK: p38 mitogenactivated protein kinase; UPR: unfolded protein response; ATF6: activating transcription factor 6; PERK: RNA-dependent protein kinase-like ER kinase; IRE1: inositol-requiring enzyme 1; IL-6: interleukin 6; TNFα: tumor necrosis factor-α.

1.1.2. Enzyme systems of desaturation

There are several fat-associated human genes whose products take part in the formation of mono- and polyunsaturated FAs, *i.e.*, in desaturation. Namely, stearoyl-CoA desaturase (*SCD*) and fatty acid desaturase (*FADS*) genes code a variety of desaturase enzymes that catalyze oxidation in a FA chain, thus introducing a double bond [57]. The

variety of FAs synthesized in humans is further colored by seven ER-bound elongase enzymes (ELOVL1–7) that can extend both saturated and unsaturated acyl-CoA chains by two (saturated) carbon atoms, thus shifting any double bond back two positions. ELOVL enzymes are specific to acyl-CoAs of different length and degree of saturation. ELOVLs 1, 3, 4, 6 and 7 elongate different SFAs and MUFAs, while ELOVLs 2 and 5 are strictly PUFA-specific enzymes [3].

1.1.2.1. Synthesis of monounsaturated and polyunsaturated FAs

The desaturation process is highly specific, with each desaturase enzyme recognizing and acting on a specific position in the fatty acid chain. Biosynthesis of PUFAs depends on FADS enzymes. Three FADS genes, FADS1, FADS2 and FADS3 are encoded consecutively in chromosome 11 (11q12.2–11q13.1), sharing high level of sequence identity and exon/intron organization similarity with each other [58]. Regarding the proteins they encode, conserved structures typical of membrane-bound desaturases from other species, such as transmembrane domains, an N-terminal cytochrome b5-like domain and three histidine-rich regions, can be found in all of them. The different members of the cluster are responsible for different PUFA synthesis. FADS1, highly expressed in fetal liver, fetal and adult brain and in adrenal gland, is a $\Delta 5$ desaturase (also often referred to as D5D for delta 5 desaturase) that primarily catalyzes the conversion of dihomo-ylinolenic acid (20:3 cis Δ8) to arachidonic acid (20:4 cis Δ5) [59, 60]. FADS2 enzyme functions are more diverse: while it was thought to be a $\Delta 6$ desaturase (also often referred to as D6D for delta 6 desaturase) converting primarily dietary linoleic acid (18:2 $cis \Delta 9$) to γ -linolenic acid (18:3 cis Δ 6), there are studies assigning also Δ 4 [61] desaturase activity to the enzyme. Moreover, it was suggested that FADS2 can act on SFAs as well, converting palmitate to sapienate (16:1 $cis \Delta 6$) in the human skin (sebaceous gland) [62]. FADS3 gene encodes many protein isoforms [63] which biological role is not yet certainly understood. The protein was associated, for instance, with hyperlipidemia [64] and shown to have a $\Delta 13$ desaturase activity on vaccenic acid [65] and a $\Delta 14$ desaturase activity on sphingolipids [66].

While PUFAs can be generated from MUFAs by FADS enzymes, MUFAs are produced from long-chain SFAs by SCD enzymes.

1.1.2.2. Enzymatic process of desaturation

Desaturation of fatty acyl-CoAs occurs in the catalytic center of the desaturase enzymes where a di-iron cofactor helps the elimination of two hydrogen atoms. The enzyme traps the FA into its deep, bent hydrophobic cavity where the two carbon atoms (e.g., the 9th and 10th) get close to the di-iron center [67]. The reaction is aerobe, thus requires molecular oxygen, and electrons from a reducing agent, i.e., nicotinamide adenine dinucleotide (NADH) or nicotinamide adenine dinucleotide phosphate (NADPH). The reducing agents donate electrons through the microsomal electron transfer chain – cytochrome b5 reductase and cytochrome b5. Mediated by the di-iron cluster, molecular oxygen gets activated due to these donated electrons (cytochrome b5 probably binds to the enzyme close to the di-iron center, so as to transfer the electrons effectively [68]). Meanwhile, the two carbon atoms of the fatty acyl chain are positioned in the catalytic center of the desaturase enzyme and each loses a hydrogen. After an initial hydrogen activation step at the carbon atom that is closer to the acidic end [69], the diiron oxidant of the desaturase enzyme detracts two hydrogens from the two carbon atoms. These hydrogens and the activated molecular oxygen are converted to H₂O, while the carbon-carbon double bond is formed [68].

1.1.3. Human acyl-CoA desaturases

 $\Delta 9$ desaturases are key enzymes in the production of unsaturated FAs, as they can introduce the first double bond in an SFA at the $\Delta 9$ position. The MUFAs produced by SCD enzymes can be further desaturated by FADS enzymes with $\Delta 4$, $\Delta 5$, and/or $\Delta 6$ activities.

1.1.3.1. Human $\Delta 9$ desaturase isoenzymes

Since humans cannot produce PUFAs *de novo*, the significance of desaturase enzymes is undeniable. While vertebrates can have plenty of SCD isoforms (mice, for instance have four SCD isoforms, Scd1, Scd2, Scd3 and Scd4), only two types of human SCD have been described [70]. The major human isoform, the 37 kDa SCD1 enzyme is expressed in most human tissues, most prominently in adipose tissue, liver, brain and lung. It was also shown to be induced by high-carbohydrate diet in liver, heart and skeletal muscle [68]. The enzyme is embedded in the ER through four transmembrane (TM) α -

helices forming a cone-like structure with a tight hydrophobic core in the inside. Both amino and carboxy termini are oriented toward the cytosol. The TM helices are connected with two short hydrophilic loops in the ER lumen and with a large hydrophilic loop extending into the cytosol [71]. This latter loop constitutes the main part of the so-called cap domain with the contribution of parts of the N and C termini. In the center of this cap, three histidine-rich segments mediate metal binding, as SCD1 is a desaturase containing two zinc ions, and these histidyl residues may provide ligands to zinc ions at the catalytic site [72]. Interacting with the cap domain, the overhanging cytosolic ends of two TM domains (TM2 and TM4) support metal binding and form a cavity for the acyl chain of the substrate. In fact, the recognition of the acyl-CoA and its positioning within the enzyme is due to various electrostatic and hydrophobic interactions between different segments of the cap domain and different parts of the CoA. Not only the position, but also the *cis* configuration of the introduced double bond is determined by structural features, as SCD1 traps the acyl chain of the substrate into a properly sized, kinked tunnel.

These structural elements are highly conserved in the other human $\Delta 9$ desaturase, SCD5 [73], which is encoded in chromosome 4 (4q21.22). SCD5 is mainly expressed in the brain, adrenal gland and gonads [74], where its expression exceeds that of SCD1 [75]. It is presumably essential for the maintenance of the precise SFA/MUFA ratio in developing tissues as it might be involved in the tightly coordinated sequence of cell division, cell cycle exit, and the onset of neuronal differentiation program [76]. The enzyme has two transcription variants: a five-exon A and a shorter, four-exon B. Due to alternative splicing, variant B uses a former exon with a different polyadenylation site, thus the C termini of the proteins differ in many aspects. We have recently demonstrated in HepG2, HEK293T and SK-N-FI cells, and various human tissues that variant B is indeed transcribed into mRNA, although the corresponding protein is greatly underrepresented compared to variant A in all of the analyzed tissues [77]. As for the function, both SCD isoforms prefer long-chain fatty acyl-CoA substrates with chain lengths of 16 and 18 carbon atoms – palmitoyl-CoA and stearoyl-CoA [78]. Although both enzymes are $\Delta 9$ desaturases (their basic function is depicted in Figure 2), differences in their tissue distribution and regulation led to the hypothesis that SCD1 and SCD5 play different roles in lipid metabolism.

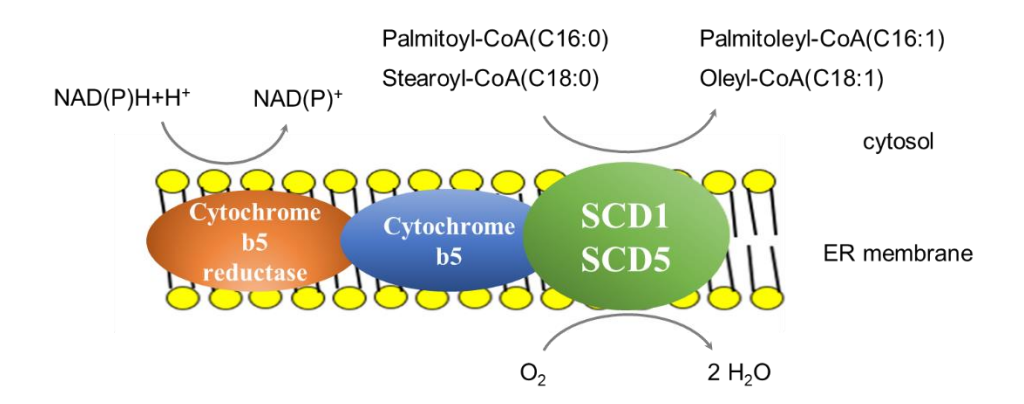


Figure 2. Function of SCD enzymes. Desaturation requires molecular oxygen and electrons provided by an electron transfer chain. Main substrates of SCD1 are palmitoyl-CoA and stearoyl-CoA. They are converted into mono-unsaturated palmitoleyl-CoA and oleyl-CoA, respectively.

1.2. Control of *SCD1* gene expression

SCD1 is encoded by a 17 kb long gene in chromosome 10 (10q24.31). The 359 amino acids of the protein are coded by six exons, separated by five introns in the gene. Interestingly, a very similar sequence in chromosome 17 was discovered by Zhang *et al.* during chromosomal mapping, but it was concluded to be only a fully processed, transcriptionally inactive pseudogene as it lacks introns, has in-frame stop codons and its putative mRNA could not be reverse transcribed by using the corresponding primers [79].

1.2.1. Transcriptional regulation

SCD1 expression is regulated at the level of transcription by several transcription factors (TFs). The pivotal area for promoter activity contains different response elements that are highly conserved among species. In cultured HaCaT keratinocytes, Zhang et al. identified a critical region for promoter activity situated 496-609 upstream from the translation start site with an essential CCAAT box cis element [80]. There is an insulin response element (IRE), containing SREBP1 binding site, where the sterol regulatory element-binding protein-1c (SREBP-1c) can act as mediator of the insulin-induced transcriptional activation of SCD1. Insulin stimulation in chicken embryo hepatocytes and HepG2 cells revealed that upregulation of SCD1 transcription occurs via the PI3 kinase (PI3K), Akt/PKB and mTOR signaling pathway leading to increased binding of SREBP-1c and nuclear transcription factor Y (NF-Y) to this IRE with a 2.5-fold

increment of promoter activity [81]. Leptin enhances the binding of Sp1 and AP-1 transcription factors to the leptin response element (LepRE) located between the aforementioned IRE and the start codon [82] via the Jak2-ERK1/2-p90RSK signal pathway, thereby directly reducing SCD1 expression. There are other important segments in the promoter region of SCD1 as well, such as response elements for the liver X receptor (LXR), peroxisome proliferator-activated receptor α (PPAR α), the C/EBP α and the triiodothyronine receptor (TR) as shown in Figure 3, but most importantly, there is also a PUFA response element (PUFARE) [83].

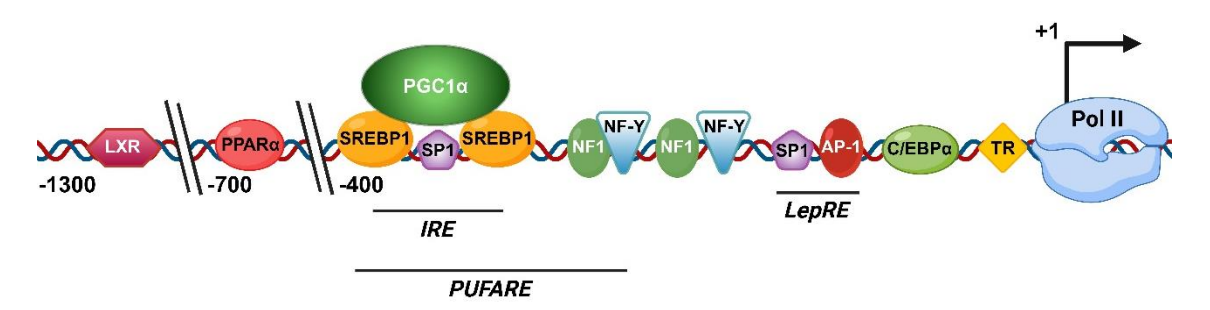


Figure 3. Transcription factors binding to *SCD1* **promoter** (Created in BioRender, based on a figure of [84]). Transcription factor binding sites and regions allowing the fine-tuned regulation of *SCD1* transcription. LXR: liver X receptor, PPAR α : peroxisome proliferator-activated receptor α , SREBP1: sterol regulatory element binding protein 1, SP1: specificity protein 1; PGC-1 α : peroxisome proliferator-activated receptor co-activator-1 α , NF-1/Y: nuclear factor 1/Y, AP-1: activator protein-1; C/EBP α : CAAT/enhancer binding protein α , TR: triiodothyronine receptor, Pol II: RNA polymerase II; IRE: insulin response element, PUFARE: polyunsaturated fatty acid response element; LepRE: leptin response element.

In addition to other activating (e.g., growth factors, peroxisome proliferators, glucose, sucrose or cholesterol) and inhibitory (e.g., glucagon, ghrelin, estrogen or triiodothyronine (T3)) hormones and nutrients as reviewed in 2011 [84], PUFAs are also able to transcriptionally influence the intracellular level of SCD1. For example, docosahexaenoic acid [85], pinolenic acid [86] and conjugated linoleic acid [87] were all shown to decrease the expression of SCD1. Interestingly, while SCD1 is particularly sensitive to changes in the levels of different FAs in the diet, SCD5 is much less responsive to these changes [73]. Our study on SCD5 in HepG2, HEK293T and SK-N-FI cell lines also confirmed this observation [77]. However, treatment with γ -linolenic acid significantly reduced SCD5 levels in a human glioma cell line, suggesting a potential specific regulation of SCD5 by PUFAs [88].

1.2.2. Posttranscriptional regulation

SCD1 expression is also regulated at various posttranscriptional levels. The amount of the protein can fluctuate quickly due to its short half-life, around 3–4 hours [89]. A degradation domain at the N-terminus of the SCD1 [90] was identified in 2000 and redefined two years later, when the same research group proved that replacement of three lysyl residues at positions 33, 35 and 36 with alanine lengthens the half-life of SCD1 [91]. It was presumed that these lysines may be ubiquitinated, thus designating the protein to proteasomal degradation; however, addition of proteasome inhibitors did not lengthen the half-life of the enzyme, suggesting other ways for SCD degradation. Later, a 66-residue N-terminal segment containing two proline (P), glutamic acid (E), serine (S) and threonine (T) rich PEST sequences [92] was described in rat SCD1 and was demonstrated to destabilize SCD1 [89].

Epidermal growth factor receptor (EGFR), an oncogenic driver, was proved to phosphorylate SCD1 at Tyr⁵⁵, thus stabilizing the enzyme in lung cancer cells [93]. Murakami et al. analyzed the effect of different FAs on the level of Desat1, the SCD1 ortholog in Drosophila melanogaster, and identified an N-terminal di-proline motif responsible for the FA-dependent degradation of the enzyme [94]. While MUFAs such as oleate, linoleate and palmitoleate decreased, SFAs did not affect the level of Desat1, suggesting negative feedback by unsaturated FAs on the enzyme. This regulatory effect of yet unknown mechanism occurs at the protein level, since the amount of *Desat1* mRNA remained unchanged. After finding and confirming (with Ala mutations) that the Pro² and Pro³ residues in the N terminal are responsible for the FA-dependent destabilization of Desat1, the research group identified a novel pathway for desaturase degradation. The inhibitors of neither the proteasomal, nor the lysosomal proteolysis hindered the degradation of Desat1, but an inhibitor of the calcium-dependent cysteine protease calpain could effectively increase the half-life of the enzyme. Further experiments proved that this calpain-mediated degradation depends on the presence of MUFAs acting on the di-proline motif. Although in human SCD1 there is only one proline in this N terminal region, it is noteworthy that various effects of FAs on SCD1 protein levels have been revealed in many studies.

The unusually long (~2 kb) 3' untranslated region of *SCD1* mRNA contains several mRNA destabilization motifs, suggesting that *SCD1* can also be regulated at the mRNA level [84].

1.3. SCD1 gene polymorphisms

Despite the obvious importance of SCDs, there are only a few studies on their SNPs (Single Nucleotide Polymorphisms) – most of them are association studies with poorly elucidated molecular mechanisms, often involving intronic variants, which have only a slight chance to drastically modify enzyme functions. However, a mutation in the 3' UTR (untranslated region) and another in the protein coding sequence have been identified and seem to have pathological relevance.

1.3.1. Variant of the UTR

A mutation in the 3' UTR was demonstrated to modify a miRNA binding site [95]. rs41290540 was analyzed in 2064 individuals of Chinese Han population. After finding an inverse correlation between the occurrence of this 3' UTR mutation and the risk of coronary artery disease (CAD), *in silico* methods were applied to predict miRNAs binding to the concerned region. Further examination in a cellular system revealed that the minor (C) rs41290540 allele hinders miR-498 binding. Silencing *SCD1*, miR-498 was found to be upregulated in various cardiovascular diseases, such as congenital heart disease [96], stroke [97] or acute coronary syndrome [95]. Given that the frequency of A→C rs41290540 mutation was significantly lower in the CAD patient group than in the control group and that it was proved to disrupt the miR-498 binding site in the 3' UTR of the *SCD1*, the minor (C) rs41290540 variant was identified as a protective factor against CAD.

1.3.2. Variants of the protein coding section

There is a missense polymorphism (rs2234970) in the coding region of the *SCD1* gene, a swap of adenine to cytosine, resulting in a methionine to leucine exchange at position 224 (M224L). Although the minor allele frequency is relatively high (24–53%) in all populations studied so far, only four research groups have examined associations of

this SNP with diseases to date. Reduction of plasma triglyceride levels was induced by the consumption of dietary docosahexaenoic acid for four weeks in 129 subjects with metabolic syndrome, and the effectivity of this treatment did not show a correlation with the polymorphism [98]. In a mixed population study on 277 Chinese, Malaysian and Indian 4.5-year-old children the accumulation of lipid droplets in skeletal muscle fibers was investigated, and a significant association was found between the occurrence of the major A allele (Met224) and elevated intramyocellular lipid accumulation, which is linked to skeletal muscle insulin resistance and an increased risk of type 2 diabetes [99]. The minor C allele (Leu224) – along with the minor C allele of the intronic SNP, rs3071 - significantly worsened the clinical outcome of stage II colorectal cancer [100]. Finally, in a study involving 210 healthy subjects, the risk of developing cardiometabolic diseases before and after a six-week n-3 PUFA supplementation and its genetic determinants were examined [101]. Both pre and post n-3 PUFA supplementation, the M224L polymorphism showed correlation with higher SCD1 activity on C18 FAs, which could be concluded from a higher unsaturated: saturated FA ratio. Therefore, due to increasing SCD1 activity, the homozygous CC genotype of this polymorphism may represent a higher risk for the development of cardiovascular diseases.

1.3.3. Variants of the promoter

Although databases indicate a large number of single nucleotide polymorphisms in the human *SCD1* promoter region, to date, none of the variants have been reported to have a functional impact and/or health consequence. Two studies involved rs670213, a polymorphism of high minor allele frequency (34–49%) in the position –895 [102, 103], but no association was found with any human pathological state or metabolic trait.

1.4. Medical significance of *SCD1* polymorphisms and mutations

There is strong evidence that SCD1 functioning is a crucial defense mechanism against lipotoxicity-induced cellular damages by converting SFAs into MUFAs [40, 104]. However, by attenuating cellular stress and favoring survival, SCD1 is regarded as a proto-oncogene, and several studies have reported its potential oncogenic effects and high

expression in transformed cells [105, 106]. Alteration in *SCD1* gene expression has also been shown to associate with metabolic syndrome [107], defined by obesity [108] and insulin resistance [109], culminating in type 2 diabetes mellitus [110], aging [111], non-alcoholic fatty liver disease (NAFLD) [112], and cardiac diseases [113]. Therefore, it is presumable that any change that affects the carefully regulated expression or activity of SCD1 is a potential cause of serious diseases (Figure 4).

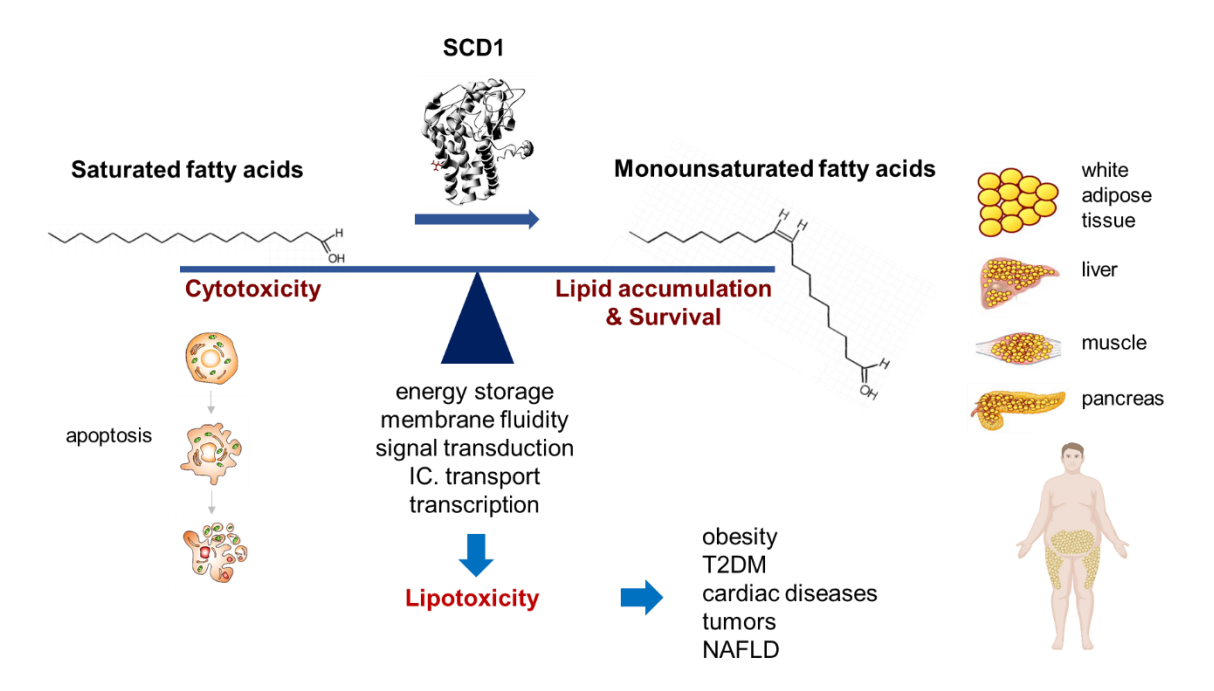


Figure 4. Importance of SCD1 in maintaining a balanced supply of fatty acids. SCD1 maintains the delicate balance between SFAs and MUFAs. If the balance is too tilted in favor of SFAs, their cytotoxic effects will prevail, which may eventually lead to apoptosis. On the other hand, an abundance of MUFAs promotes obesity through excessive lipid accumulation and can eventually lead to tumorigenesis by promoting cell survival. Either way, prolonged high levels of FAs (saturated and unsaturated) due to overnutrition can lead to lipotoxicity, which is a precursor to many diseases, as explained in Chapter 1.1.1.3.

Mutations modulating the regulation of SCD1 expression may occur throughout the gene. Two polymorphisms in intron 5, rs55710213 and rs56334587 have been demonstrated to affect the key regulatory regions of SCD1, where hepatocyte nuclear factor 4 alpha (HNF4 α), a central regulator of glucose and lipid metabolism in the liver, binds [114]. While ordinarily, HNF4 α directly enhances SCD1 expression, the GG haplotype of these polymorphisms disrupts the HNF4 α binding site, thus decreasing SCD1 activity, which underlies diseases associated with reduced hepatic SCD1 levels.

Examining 101 obese adults, Mutch et al. looked for correlation between SCD1 polymorphisms and the effects of dietary oils containing different ratios of SFA/MUFA on blood glucose level [115]. They found three intronic SNPs having statistically significant effect on blood glucose response to the diet: rs1502593 (p = 0.01), rs3071(p = 0.02) and rs522951 (p = 0.03). Moreover, the recessive CC genotype of rs3071 was associated with increased blood glucose level in response to high SFA/low MUFA diet and with reduced blood glucose level when the diet was rich in MUFA. Carrying the dominant A allele, however, was associated with reduced blood glucose response to any kind of oil treatment. The intron variant rs1502593 was also associated with an increased prevalence of the metabolic syndrome in Costa Rican adults [116]. Besides, there seems to be a positive correlation between this SNP and systolic blood pressure and fasting blood sugar levels. Polymorphisms rs2167444 and rs508384 were shown to be associated with an unfavorable profile of cardiometabolic risk factors due to elevated ApoB-48 levels [117]. The minor allele of the 3' UTR variant, rs7849 was correlated with 23% higher insulin sensitivity in elderly Swedish men [118]. To counteract the effects of polymorphisms and mutations that cause SCD1 overexpression or overactivity, not only can a diet rich in n-3 PUFA be followed, as eicosapentaenoic acid (EPA), docosahexaenoic acid (DHA) and arachidonic acid have been proved to reduce SCD levels [85, 119], but pharmaceutical companies are also currently developing SCD downregulator molecules [120].

2. Objectives

Due to the prominent role of SCD1 in lipid metabolism and lipotoxicity, we consider it necessary to get to know as thoroughly as possible the nutritional and genetic factors influencing the expression and activity of the enzyme. We aimed to study the effect of FAs on SCD1 expression and the potential modulating role of *SCD1* gene polymorphism *in vitro* in two cell lines of human origin.

- 1. The FA responsive element located in the *SCD1* promoter suggests that endogenous and dietary FAs may affect the expression of the enzyme. This assumption is also supported by literature data, but the exact impact of certain types of FAs, particularly TFAs is still unclear. Thus, our first goal was to assess the putative effects of SFAs, *cis* and *trans* MUFAs and PUFAs at various levels of SCD1 expression.
- 2. We also aimed to investigate the impact of genetic variations in SCD1. Since the numerous promoter variants of the gene have not yet been investigated and the single known missense SNP in the coding region has only been addressed by association studies, we endeavored the scrutiny of these variants, aiming to compare the expression and enzyme activity of these polymorphic versions, with special regard to their association with type 2 diabetes mellitus.
 - A. After identifying the most common promoter polymorphisms *in silico*, we searched for TFs, the binding of which to the promoter could be affected by these polymorphisms, and created five of these variants by site-directed mutagenesis in reporter constructs to
 - i. assess the effects of these promoter polymorphisms on the expression of the enzyme;
 - ii. determine whether these promoter SNPs modify the control of SCD1 expression by various FAs;
 - iii. validate the *in silico* prediction regarding their effect on TF binding as well as on the promoter activity and its modulation by FAs in the presence of the corresponding TF.

- B. The coding region of SCD1 with either of the two natural variants of M224L (rs2234970) missense SNP as well as an artificial M224A variant was cloned into an expression vector to
 - i. assess the changes in intracellular protein and RNA levels that the SNP may cause;
 - ii. investigate the intracellular degradation of human SCD1 mRNA and protein and find out whether the M224L SNP causes any difference in protein or mRNA stability;
 - iii. compare the effect of FA treatments on the amounts of polymorphic SCD1 proteins and mRNAs;
 - iv. compare the desaturase function of the polymorphic SCD1 enzymes;
 - v. analyze the molecular and structural background of any difference we find in the above experiments.

3. Methods

3.1. Chemicals, materials and equipment

Chemicals, materials and equipment are listed in Table 2. All chemicals used during this work were of analytical grade. All experiments and measurements were carried out by using Millipore ultrapure water.

Table 2. Used chemicals, materials and equipment with their manufacturer.

Chemical / material / equipment	manufacturer	
Culture medium and supplements		
restriction endonucleases (Xho I and Hind III)		
T4 ligase		
Pierce® BCA Protein Assay Kit		
SuperSignal West Pico Chemiluminescent Substrate	Thermo Fisher Scientific	
Varioskan multi-well plate reader		
QuantStudio 12 K Flex Real-Time PCR System		
SuperScript III First-Strand Synthesis System for RT-PCR Kit		
TaqMan assay (C_34192814_10)		
HepG2 and HEK293T cells		
FAs (oleate, palmitate, palmitoleate, linoleate, stearate, vaccenate, elaidate)	Sigma-Aldrich	
Bovine serum albumin, cycloheximide, actinomycin D		
Lipofectamine® 2000, 3000 and P3000	Las situa anna	
RNAqueous®-4PCR Kit	Invitrogen	
iProof [™] High-Fidelity DNA Polymerase	Bio-Rad	
pGL3-Basic plasmid		
Reporter Lysis 5X Buffer	Promega	
Luciferase Assay System kit		
Q5° Site-Directed Mutagenesis Kit	New England BioLabs	
XL10-Gold® Ultracompetent Cells	Agilent	
ETS1 expression plasmid, pcDNA3.1(-) background	BioCat	
Immobilon-P membranes	Millipore	
HRP-conjugated goat polyclonal anti-Actin antibodies		
rabbit polyclonal antibody	Cell Signaling	
HRP-conjugated goat polyclonal anti-rabbit IgG	Cell Signaling	
HRP conjugated mouse monoclonal anti-goat IgG		
C-DiGit [®] Blot Scanner	LI-COR Biotechnology	
Image Studio [®] 5.2 software		
goat polyclonal antibody against Glu-Glu tag	Bethyl Laboratories	
SensiFAST™ cDNA Synthesis Kit	Meridian Bioscience	
ethanol	Molar Chemicals	
RLT buffer	Qiagen	
RNeasy Plus Mini Kit	Qiageii	

3.2. Web-based tools for *in silico* analysis

Stem-loop structure and stability of the *SCD1* mRNA derived from SSCprofiler database were analyzed by using the RNAfold server (http://rna.tbi.univie.ac.at/cgi-bin/RNAfold.cgi, accessed on 24 October 2021) [121]. The application predicts the secondary structure of a single-stranded RNA and calculates the partition function and base pairing probability matrix as well as the minimum free energy (MFE) structure of the molecule.

The 3D structure of human SCD1 was obtained from PBD protein Data Bank (4ZYO, http://www.pdb.org/pdb/home/home.do; accessed on 9 March 2022) [71]. The 3D structure of the Leu224 variant was generated by I-TASSER online prediction program (https://zhanggroup.org/I-TASSER/, accessed on 18 October 2021) [122]. All images were rendered using DeepView/Swiss-Pdb Viewer version 4.0.2 (www.expasy.org/spdbv/, accessed on 13 April 2018).

SCD1 promoter SNPs with minor allele frequency (MAF) above 5% and heterozygosity above 0.095 were selected based on the NCBI and Ensembl databases. To predict the potential effect of rs1054411, rs670213, rs2275657 and rs2275656 polymorphisms on TF binding to the SCD1 promoter, we used JASPAR (http://jaspar.genereg.net/, accessed on 30 June 2022) open-access, nonredundant TF biding profile database [123]. Both allelic variants of each SNP were compared pairwise. TFs showing a score difference of at least 15% between the two variations of the given polymorphism, and a relative score above 80% for at least one of the alleles, were retained for further analysis. The impact of the selected sequence variants was predicted *in silico* using Variant Effect Predictor (https://www.ensembl.org/Homo_sapiens/Tools/ VEP/, accessed on 12 January 2023) [124].

3.3. Plasmid construction and mutagenesis

pcDNA3.1(–) expression and pGL3-Basic (pGL3B) reporter vectors were used. Cloning and mutagenic primer pairs are listed in Table 3. *SCD1* cDNA reverse transcribed from HepG2 cell mRNA was cloned into the pcDNA3.1(–) plasmid between the *Xho* I and *Hind* III restriction sites. Additionally, a 1094 base pair fragment of the upstream

regulatory region of *SCD1* was amplified from human genomic DNA template by iProofTM High-Fidelity DNA Polymerase. After purification and restriction endonuclease digestion, the amplicons were ligated (T4 Ligase) into pGL3B vector between the *Xho* I and *Hind* III restriction endonuclease recognition sites, upstream the luciferase reporter gene. The ETS1 expression plasmid was purchased from BioCat with pcDNA3.1(–) vectorial background.

Table 3. Primers used for cloning and mutagenesis. Bold uppercase letters indicate the recognition sites of the two endonucleases, Xho I and Hind III, respectively. Bold, underlined lowercase letters indicate the mutated bases. T_m : annealing temperature.

Process	Primer	Sequence $(5' \rightarrow 3')$	T _m (°C)
cloning into expression	sense	AAATTT CTCGAG CTCAGCCCCCTGGAAAGTGAT	
vector (pcDNA3.1(–))	antisense	AAATTT AAGCTT GGAACCTGAGGGACCCCAAAC	63
promoter cloning into	sense	AAATTT CTCGAG CAAAACATCCCGCACGCAT	
reporter vector (pGL3B)	antisense	AAATTT AAGCTT GGCATCTTGGCTCTCGGATG	62
M224L	rs2234970 A>C sense	TGGCTTGCTG <u>c</u> TGATGTGCTT	60
mutagenesis	rs2234970 A>C antisense	AAGCACATCAGCAGCCA	60
M224A	sense	TGGCTTGCTG gc GATGTGCTTC	60
mutagenesis	antisense	GGTTTGTAGTACCTCCTC	60
Glu-Glu tag	sense	<u>gaatatatgcctatggaa</u> TGAGTTTGGGGTCCCTCAGGTCC	61
Old Old tag	antisense	<u>ttccataggcatatattc</u> GCCACTCTTGTAGTTTCCATCTCC	57
	rs1054411 C>G sense	TCCCGGCATC <u>g</u> GAGAGCCAAG	68
	rs1054411 C>G antisense	TCACTTTCCAGGGGGCTG	68
	rs670213 T>C sense	GCGTACCGAG <u>c</u> CCCCCGCGCT	72
promoter	rs670213 T>C antisense	CTGCGAACAATGGCTCTGCCCC	72
mutagenesis	rs2275657 G>C sense	GCCGGAGTCC <u>c</u> GTGCGGTCCC	72
	rs2275657 G>C antisense	CGCACACAGGCTGGCTG	72
	rs2275656 G>C sense	GGAGGCGCGG <u>c</u> CTTGGGGATG	71
	rs2275656 G>C antisense	AGGATGCGTGCGGGATGTTTTG	71

The studied natural and artificial mutations and variants as well as the Glu-Glu tagged constructs were generated using Q5[®] Site-Directed Mutagenesis Kit following the manufacturer's instruction. Mutagenic primers (listed in Table 3) were designed using the online NEB primer design software, NEBaseChangerTM. After digestion of the original non-mutated and methylated plasmid by KLD reaction, XL10-Gold[®] Ultracompetent Cells were transformed with an aliquot of the constructs and then screened for positive colonies by PCR. All constructs were verified by Sanger-sequencing.

3.4. Cell culture and transfection

Human embryonic kidney (HEK293T) and hepatocellular carcinoma (HepG2) cells were cultured in 12-well plates (1 × 10⁶ cells per well) in Dulbecco's modified Eagle medium (DMEM) supplemented with 10% fetal bovine serum and 1% penicillin/streptomycin solution at 37 °C in a humidified atmosphere containing 5% CO₂. To investigate the coding region, HEK293T and HepG2 cells were transfected with 0.5–1 μg pcDNA3.1(–)-SCD1 plasmids using 3 μL Lipofectamine 2000 or 3 μL Lipofectamine 3000 supplemented with 2 μL P3000 in 1 mL DMEM. To investigate the promoter region, cells were transfected with 0.5 μg pGL3B-SCD1 promoter constructs using 3 μL Lipofectamine 3000 that was supplemented with 2 μL P3000 in 1 mL DMEM. ETS1 overexpression was obtained with co-transfection of 10, 25, 50, 100 or 200 ng pcDNA3.1(–)-ETS1 expression plasmid. As a transfection control for the luciferase reporter system, 0.5 μg pCMV-β-gal plasmid was co-transfected. Cells were harvested and processed 24–30 h after transfection.

3.5. Cell treatments

For protein stability assay, transfection medium was replaced after overnight incubation at 37 °C with 1 mL DMEM containing the translational inhibitor cycloheximide (50 μ g/mL), and the cells were incubated for 1, 2, 4, or 6 h in 12-well plates. Non-transfected samples and cells transfected with pcDNA3.1(–) "empty" vector were used as control in all experiments.

For mRNA stability assay, transfection medium was replaced after overnight incubation at 37 °C with 1 mL DMEM containing the mRNA synthesis inhibitor

actinomycin D (5 μ g/mL) and the cells were incubated for 0, 1, 2, 4, 8, or 12 h in 12-well plates.

Oleate, palmitate, palmitoleate, linoleate, stearate, elaidate, and vaccenate were diluted in ethanol to a final concentration of 50 mM, conjugated with 4.16 mM FA-free BSA in 1:4 ratio, at 50 °C for 1 h. The working solution for FA treatments was prepared freshly in FBS-free and antibiotic-free medium at 100 µM final concentration. To study the coding region, the culture medium was replaced with FBS-free and antibiotic-free medium 1 h before FA-treatment for 6 h in 12-well plates. To study the promoter, FA treatment was carried out for 24 h in 12-well plates. For luciferase assay, the culture medium was replaced 5 h after transfection and cells were incubated for a further 24 h.

3.6. Preparation of cell lysates

Cell lysates were prepared for immunoblot analysis by removing the medium and washing the cells twice with PBS. 100 μL RIPA lysis buffer (0.1% SDS, 5 mM EDTA, 150 mM NaCl, 50 mM Tris, 1% Tween 20, 1 mM Na₃VO₄, 1 mM PMSF, 10 mM benzamidine, 20 mM NaF, 1 mM pNPP, and protease inhibitor cocktail) was added to each well and the cells were scraped and briefly vortexed. After 50 min incubation on ice, the lysates were centrifuged for 15 min at maximum speed in a benchtop centrifuge at 4 °C to remove cell debris. Protein concentration of the supernatant was measured with Pierce® BCA Protein Assay Kit and the samples were stored at –20 °C until further analysis.

For luciferase reporter assays, cells were washed twice with PBS and then scraped in $100~\mu L$ Reporter Lysis 5X Buffer and vortexed briefly. A single freeze-thaw cycle was followed by centrifuging in a benchtop centrifuge (5 min, max speed, 4 °C). Supernatants were used for enzyme activity determination.

For total RNA isolation, cells were washed twice with PBS and collected in 350 μ L RLT buffer supplemented with 1% β -mercaptoethanol according to manufacturer's protocol. Samples were stored at -80 °C until further analysis.

3.7. Immunoblot analysis

Aliquots of cell lysates (2–20 µg protein per lane) were analyzed by SDS-PAGE on 12% Tris–glycine minigels and transferred onto Immobilon-P membranes. Primary and secondary antibodies were applied overnight at 4 °C and for 1 h at room temperature, respectively. Actin, SCD1, Glu-Glu tag and ETS1 was detected with antibodies listed in Table 4. Horseradish peroxidase (HRP) was detected using the SuperSignal West Pico Chemiluminescent Substrate.

Table 4. Antibodies used for protein detection. HRP: horseradish peroxidase.

Protein	Antibody	Dilution	Secondary antibody	Dilution
Actin	HRP-conjugated goat polyclonal anti-Actin antibody	1:2000	-	-
SCD1	rabbit polyclonal antibody	1:2000	HRP-conjugated goat polyclonal anti-rabbit IgG	1:2000
Glu-Glu tag	goat polyclonal antibody	1:10,000	HRP-conjugated mouse monoclonal anti-goat IgG	1:2000
ETS1	goat polyclonal antibody	1:500	HRP-conjugated mouse monoclonal anti-goat IgG	1:2000

3.8. Luciferase assay

Luciferase activity was detected using Luciferase Assay System kit by adding 15 μ L Luciferin reagent to 5 μ L of all cell extracts. β -galactosidase activity of 20 μ L cell lysates was measured by determining the o-nitrophenyl- β -D-galactopyranoside (at a final concentration of 3 mM) cleavage rate. Luminescence was detected using a Varioskan multi-well plate reader. Values for luciferase activity were normalized to β -galactosidase activity (measured by standard protocol using the same Varioskan plate reader in photometry mode). Each experiment was repeated three times independently, and each sample was analyzed in triplicate.

3.9. RNA isolation, cDNA synthesis

Total RNA was purified from transfected HEK293T and HepG2 cells by using RNeasy Plus Mini Kit following the manufacturer's instruction. Concentrations were measured using NanoDrop1000 spectrophotometer. To assess the integrity and purity of

the isolated total mRNA samples, the ratios of their absorbance at 260/280 and 260/220 nm were determined, and they were also analyzed by agarose gel electrophoresis to visualize bands corresponding to 28S and 18S rRNAs. Possible DNA contamination was removed by DNase I treatment using RNAqueous®-4PCR Kit. cDNA samples were produced by reverse transcription of 0.5 µg DNA-free RNA, using SuperScript III First-Strand Synthesis System for RT-PCR Kit or SensiFASTTM cDNA Synthesis Kit.

3.10. qPCR

Quantitative PCR assay was performed in 20 μ L final volume containing 5 μ L 20 \times diluted cDNA, 1 \times PowerUpTM SYBRTM Green Master Mix, and 0.5 μ M forward and reverse primers using QuantStudio 12 K Flex Real-Time PCR System. Tag-less *SCD1*, Glu-Glu tagged *SCD1* and *ETS1* sequences, and also *GAPDH* cDNA, as an endogenous control, were amplified using primer pairs listed in Table 5.

Table 5. Primers used for qPCR.

Specificity	Primer	Sequence (5' \rightarrow 3')		
SCD1	sense	TTGGGAGCCCTGTATGGGAT		
	antisense	ACATCATTCTGGAATGCCATTGTGT		
Glu-Glu tagged SCD1	sense	CTGGCCTATGACCGGAAGAAA		
	antisense	GACCCCAAACTCATTCCATAGG		
ETS1	sense	AGATGAGGTGGCCAGGAGAT		
	antisense	CTGCAGGTCACACAAAGC		
GAPDH	sense	GTCCACTGGCGTCTTCACCA		
	antisense	GTGGCAGTGATGGCATGGAC		

For increased reliability, RT negative control of each sample was also analyzed in addition to DNase digestion. The first step of the thermocycle was an initial denaturation and enzyme activation at 95 °C for 2 min. It was followed by 40 cycles of 95 °C for 15 s, 55 °C for 15 s, and 72 °C for 1 min. Measurement of the fluorescent signal was carried out during annealing. Reactions were performed in triplicates, and a reaction mixture with RNase-free water instead of template cDNA was employed as non-template control. Relative expression levels were calculated as $2^{-\Delta C_T}$, where ΔC_T values corresponded to the difference of the C_T -values of the endogenous control and target genes.

3.11.GC-FID analysis of fatty acid profiles

Cells were washed once with PBS, then harvested in 100 µL PBS by scraping. Samples were centrifuged for 5 min at 1,500 rpm in a benchtop centrifuge at room temperature, and supernatants were discarded. Cell pellets were resuspended in 150 µL PBS. 50 µL cell suspension was transferred to a clear crimp vial for GC-FID measurement. 150 µL of methanol containing 2 W/V% NaOH was added to the 50 µL cell suspension in the crimp vials. Samples were incubated at 90 °C for 30 min, then cooled to room temperature. 400 µL of methanol containing 13–15% of boron trifluoride was added to the samples, and the vials were incubated at 90 °C for 30 min. After cooling to room temperature, 200 µL of saturated NaCl solution and 300 µL of n-hexane were added. Fatty acid methyl esters (FAMEs) were extracted to the upper phase containing nhexane, and this phase was transferred to a vial for GC analysis. GC analysis was carried out in a Shimadzu GC-2014 gas chromatograph equipped with a Zebron ZB-88 capillary column (60 cm × 0.25 mm i.d., 0.20 μm film thickness) with an 88% (propyl-nitrile)-arylpolysiloxane stationary phase and a flame ionization detector (FID). For chromatographic separation of FAMEs, the following oven time-temperature program was used: the flow velocity was 35 mL/min, the initial temperature was 100 °C and reached 210 °C with an increase of 5 °C/min. 1 µL of extracted sample was injected into the GC [125].

3.12. Subjects and genotyping

Association studies presented in the thesis were carried out by other members of the research group. 282 patients diagnosed with T2DM in the 2^{nd} Department of Internal Medicine, Semmelweis University (51.2% female, 48.8% male, disease onset at the age of 62.4 ± 12.6 y) were recruited in the study of the rs1054411 promoter polymorphism of the *SCD1* gene and 425 patients diagnosed with T2DM in the 2^{nd} Department of Internal Medicine, Semmelweis University (57.7% female, 42.3% male, disease onset at the age of 48.0 ± 12.4 y) in the study of the M224L (rs2234970) polymorphism. The control group consisted of 370 and 463 volunteers, respectively, with no medical history of any metabolic disease (study of the rs1054411 promoter polymorphism: 61.4% female, 38.6% male, mean age: 33.1 ± 21.6 y; and study of the M224L SNP: 58.9% female, 41.1% male, mean age: 39.2 ± 13.0 y). The diagnosis of diabetes was made based on fasting blood

sugar values, oral glucose tolerance test (OGTT), and HbA_{1C} value according to WHO regulations. Individuals with autoimmune, infectious, or metabolic disorders other than type 2 diabetes were excluded from the study. Genetic analysis of the participants was approved by the Local Ethical Committee (ETT TUKEB ad.328/KO/2005, ad.323-86/2005-1018EKU from the Scientific and Research Ethics Committee of the Medical Research Council). The study was conducted in accordance with the principles of the Declaration of Helsinki. Participants signed a written informed consent before sample collection for genetic analysis. To avoid the risk of spurious association caused by population stratification, subjects of Hungarian origin were exclusively included to ensure the comparison of homogenous populations. Buccal epithelial cells were collected by swabs. The first step of DNA isolation was incubation of the buccal samples at 56 °C overnight in 0.2 mg/mL Proteinase K cell lysis buffer. Subsequently, proteins were denatured using a saturated NaCl solution. DNA was then precipitated by isopropanol and 70% ethanol. DNA pellet was resuspended in 100 μ L 0.5 × TE (1 × TE: 10 mM Tris pH = 8.0; 1 mM EDTA) buffer. Concentration of the samples was measured by NanoDrop1000 spectrophotometer.

Both polymorphisms of the *SCD1* gene were genotyped using TaqMan assays. For rs1054411 promoter polymorphism, a pre-designed TaqMan assay was used: C_34192814_10, Thermo Fisher Scientific, Waltham, MA, USA. qPCR assay was performed in 5 μL final volume containing approximately 4 ng genomic DNA, 1 × TaqPathTM ProAmpTM Master Mix, and 1 × TaqMan[®] SNP Genotyping Assay using QuantStudio 12 K Flex Real-Time PCR System (Thermo Fisher Scientific, Waltham, MA, USA).

For the M224L (rs2234970) polymorphism, an own-designed TaqMan assay was used which contained the two primers and the allele-specific fluorescent probe labelled by JOE for the C allele and labelled by FAM for the A allele (listed in Table 6). Real-time PCR assay was performed in 10 μL final volume containing approximately 4 ng genomic DNA, 1 × TaqPathTM ProAmpTM Master Mix, 0.5 μM primers and 0.3 μM allele-specific probes using QuantStudio 12K Flex Real-Time PCR System (Thermo Fisher Scientific, Waltham, MA, USA). In both cases, the thermocycle was started by activating the hot start DNA polymerase and denaturing genomic DNA at 95 °C for 10 min. This was followed by 40 cycles of denaturation at 95 °C for 15 s, and combined annealing and

extension at 60 °C for 1 min. Real-time detection was carried out during the latter step to verify the results of the subsequent post-PCR plate reads and automatic genotype calls.

Table 6. TaqMan primers and probes.

OligonucleotideSequence (5' \rightarrow 3')PrimersSenseCACAAGCGTGGGCAGGATAntisenseGGTGTCTGGTCTGTCAATGTAGGTProbesC allele specificJOE-AAGCACATCAGCAGCAAGCCAGGTT-BHQ1A allele specificFAM-AAGCACATCATCAGCAAGCCAGG-BHQ1

3.13. Statistical analysis

Immunoblots were evaluated by densitometry using Image Studio[®] 5.2 software (LI-COR Biotechnology, Lincoln, NE, USA). The results are shown as relative band densities normalized to Actin as a reference. Relative band densities, luciferase activities and mRNA levels are presented in the diagrams as mean values \pm S.D. and were compared by ANOVA with the Tukey's multiple comparison post hoc test, using the GraphPad Prism 6.0 software (GraphPad Software, Boston, MA, USA). Differences with a p < 0.05 value were considered to be statistically significant. Genotype—phenotype association was assessed by χ^2 -test comparing the genotype distribution of the patient and the control groups.

4. Results

4.1. Effects of fatty acids on SCD1 level

First, we investigated the effects of various FAs common in the European diet on the expression of SCD1.

4.1.1. Impact of different dietary FAs on SCD1 expression at the protein level

In order to investigate the effect of different FAs on the intracellular level of SCD1 enzyme, human embryonic kidney (HEK293T) and human hepatocyte carcinoma (HepG2) cells were treated with BSA-conjugated oleate, palmitate, stearate, linoleate, vaccenate and elaidate at a final concentration of 100 µM for 24 hours and their SCD1 content was assessed by immunoblotting (Figure 5 A, C) and evaluated by densitometry (Figure 5 B, D). The results obtained in HEK293T cells (Figure 5 A, B) confirmed the data from previous studies as the cis-MUFA oleate reduced the amount of intracellular SCD1 to one fifth of the untreated control level, and the cis-PUFA linoleate caused almost complete disappearance of SCD1 protein. Furthermore, as expected, the saturated FAs, palmitate and stearate increased SCD1 protein level, although statistical significance was only observed for stearate. Interestingly, the two TFAs did not change the amount of SCD1 in the same direction: while vaccenate almost halved it, elaidate approximately doubled it. This divergent effect resulted in a remarkable, fourfold difference in the detected SCD1 protein content between cells treated with each of the two TFAs. On the other hand, the SCD1 protein level modulating effect of most FAs was not spectacular in HepG2 cells (Figure 5 C, D), as the amount of SCD1 appeared unchanged after oleate, palmitate, stearate and vaccenate treatments. However, linoleate showed a rather similar, marked decreasing effect as in HEK293T cells, and although elaidate did not double the protein amount, it increased it so much that the difference between the effects of the two TFAs in this cell line was also significant.

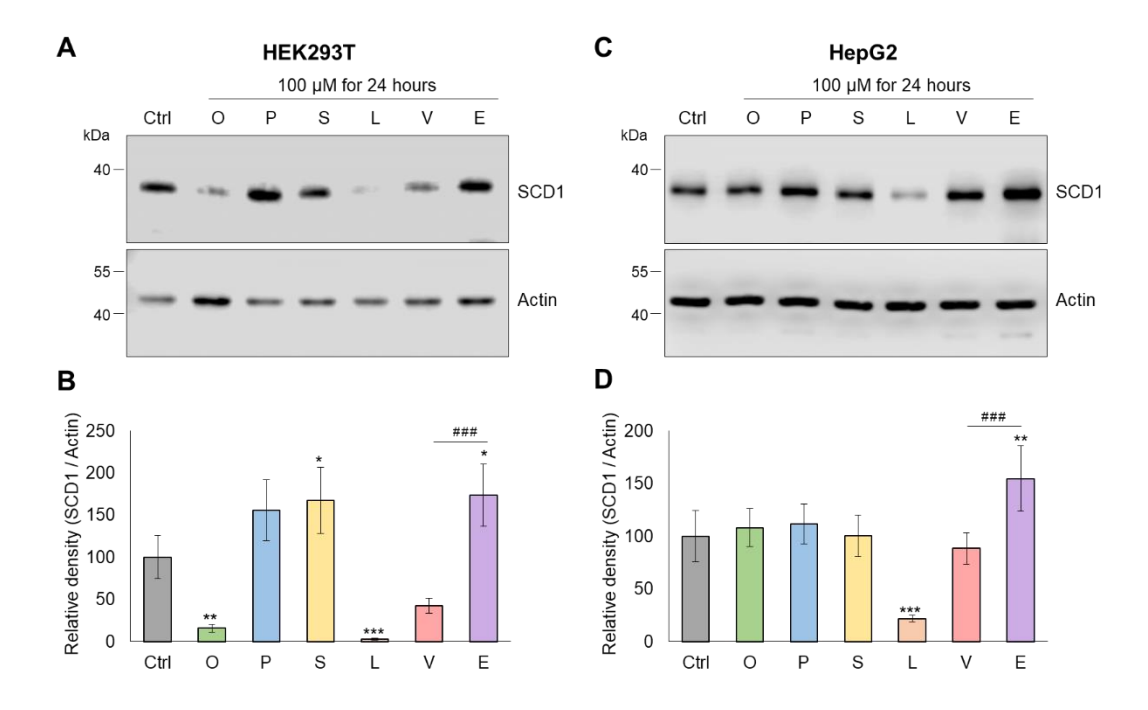


Figure 5. SCD1 protein expression in FA-treated HEK293T and HepG2 cells. Each cell line was treated with BSA-conjugated FAs at a final concentration of 100 μ M for 24 hours. Changes in intracellular SCD1 levels in response to individual FAs were followed by immunoblotting. **A** and **C** show these results for each cell line after using anti-SCD1 and the housekeeping anti-Actin antibody. Band intensities of immunoblots from four (HEK293T) and five (HepG2) independent experiments were measured by densitometry and SCD1/Actin ratios are presented as bar graphs (**B**, **D**). Statistical analysis was performed with the Tukey-Kramer Multiple Comparisons Test. Data are shown as mean values \pm SD. Ctrl: control; O: oleate; P: palmitate; S: stearate; L: linoleate; V: vaccenate; E: elaidate; *p < 0.05; **p < 0.01; *** and **##p < 0.001.

4.1.2. Changes in *SCD1* mRNA level in response to various dietary FAs

Since it is conceivable that the changes in intracellular SCD1 protein amount in response to FAs may already be reflected at mRNA level, we used qPCR to compare the amount of *SCD1* mRNA in treated and untreated cells (Figure 6). After 24 hours FA treatment (at a final concentration of 100 μM), DNA-free total RNA was isolated from HEK293T and HepG2 cells and reverse transcribed into cDNA. Housekeeping *GAPDH* served as an endogenous control. In HEK293T cells, oleate, linoleate and vaccenate significantly reduced *SCD1* expression, while palmitate, stearate and elaidate did not seem to have measurable effects (Figure 6 A). HepG2 cells show a slight response to FA treatment not only at the protein level but also at the mRNA level; however, the effect of

linoleate and elaidate was also significant at the mRNA level and in the same direction as seen in the immunoblots (Figure 6 B). Moreover, a significant difference between the effect of the two TFAs was observed in both cell lines, consistent with the results of the corresponding protein levels.

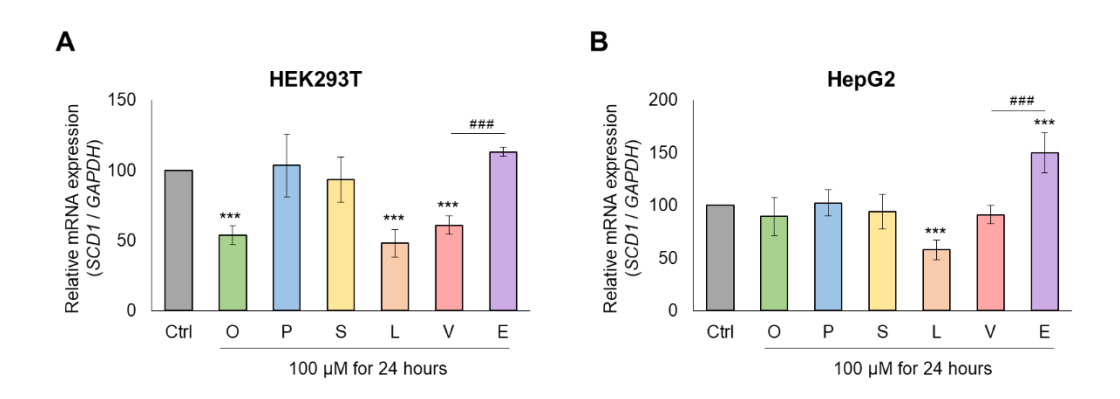


Figure 6. Impact of different FAs on the *SCD1* **mRNA expression in HEK293T and HepG2 cells.** After mRNA isolation and reverse transcription into cDNA, mRNA expression of FA-treated HEK293T (**A**) and HepG2 (**B**) cells was assessed by qPCR. FA treatment and sample preparation were performed as described in *Methods*. qPCR was carried out using SCD1 and GAPDH sequence specific primers as indicated in *Methods*. The diagram depicts the results of six independent measurements. Statistical analysis was performed with the Tukey-Kramer Multiple Comparisons Test. Ctrl: control; O: oleate; P: palmitate; S: stearate; L: linoleate; V: vaccenate; E: elaidate. Data are shown as mean values \pm S.D. *** or *###p < 0.001.

4.1.3. Effects of dietary FAs through *SCD1* promoter

The observed modulation of SCD1 expression by FAs can be attributed to changes in mRNA stability or transcriptional regulation. To investigate whether the promoter responds differently to the FAs of our choice, a 1094 base pair long section of the 5' regulatory region of *SCD1* was cloned into pGL3-Basic vector. HEK293T and HepG2 cells transiently transfected with this pGL3B-SCD1 promoter construct were treated with BSA-conjugated FAs at a final concentration of 100 μ M and the resulting luciferase activities were measured (Figure 7). pGL3B control verified that the cloned 5' regulatory region worked as a proper promoter, as the relative luciferase activity increased at least 20-fold in both cell lines transfected with the pGL3B-SCD1 construct (Figure 7 A, B). Although linoleate was effective in decreasing luciferase activity in both cell lines, oleate did not seem to suppress it as expected from the protein and mRNA results. However, the

effects of palmitate and stearate correlated well with the findings obtained at protein and mRNA levels, as they significantly increased the promoter activity in both cell types. Although vaccenate seemed to have no effect on the promoter activity, the other TFA, elaidate, increased the relative luciferase activity by 2- (Figure 7 A) and 1.5-fold (Figure 7 B), respectively, thus the earlier seen significant difference between the two TFAs was also reflected at the level of transcriptional regulation in both cell lines.

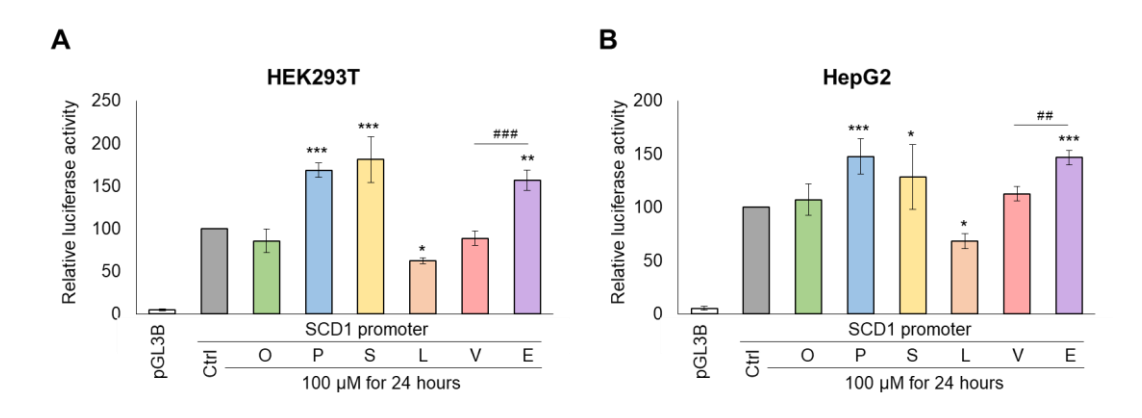


Figure 7. Effect of dietary FAs on *SCD1* promoter activity in HEK293T and HepG2 cells. Transiently transfected HEK293T (A) and HepG2 (B) cells with pGL3B or pGL3B-SCD1 promoter construct were treated with FAs at a final concentration of 100 μM for 24 hours. pCMV-β-gal vector served as transfection control. Luciferase and β-galactosidase activities were measured from harvested cells as described in *Methods* and their ratios are displayed as bar graphs. Diagrams depict the results of three independent measurements normalized to the untreated *SCD1* promoter. Data are shown as mean values \pm S.D. Statistical analysis was performed by using the Tukey-Kramer Multiple Comparisons Test. Ctrl: control; O: oleate; P: palmitate; S: stearate; L: linoleate; V: vaccenate; E: elaidate; *p < 0.05; ** and *#*p < 0.01; *** and *#*p < 0.001.

4.2. Variations of *SCD1* gene

Little is known about the effects of natural genetic variations in human *SCD1*. We sought to answer how the most common SNPs in the regulatory and promoter regions affect the transcriptional regulation of this gene.

4.2.1. SNPs of SCD1 promoter

Searching the NCBI dbSNP and Ensembl databases, four polymorphisms were found in the *SCD1* promoter region with a minor allele frequency (MAF) greater than 5% (Table 7 and Figure 8 A). The Variant Effect Predictor (VEP) of Ensembl determined all four

polymorphisms as modifiers, *i.e.*, each of them could potentially lead to functional differences in the regulation of *SCD1* expression.

Table 7. SNPs in *SCD1* **promoter.** MAF: minor allele frequency based on 1000 Genomes Project global frequency data; VEP: Variant Effect Predictor.

SNP ID	Position	Alleles		MAF (%)	VEP
	Position	major	minor	IVIAT (%)	VLP
rs1054411	-11	С	G	28	modifier
rs670213	- 895	Т	С	33	modifier
rs2275657	- 964	G	С	44	modifier
rs2275656	-1057	G	С	45	modifier

In order to validate these *in silico* predictions, each SNP was generated in the pGL3B-SCD1 promoter construct by site-directed mutagenesis and after transient transfection, tested in luciferase reporter assay in HEK293T and HepG2 cells. No significant difference can be observed between the relative luciferase activity caused by the major and minor alleles of the four SNPs in either cell line (Figure 8 B, C).

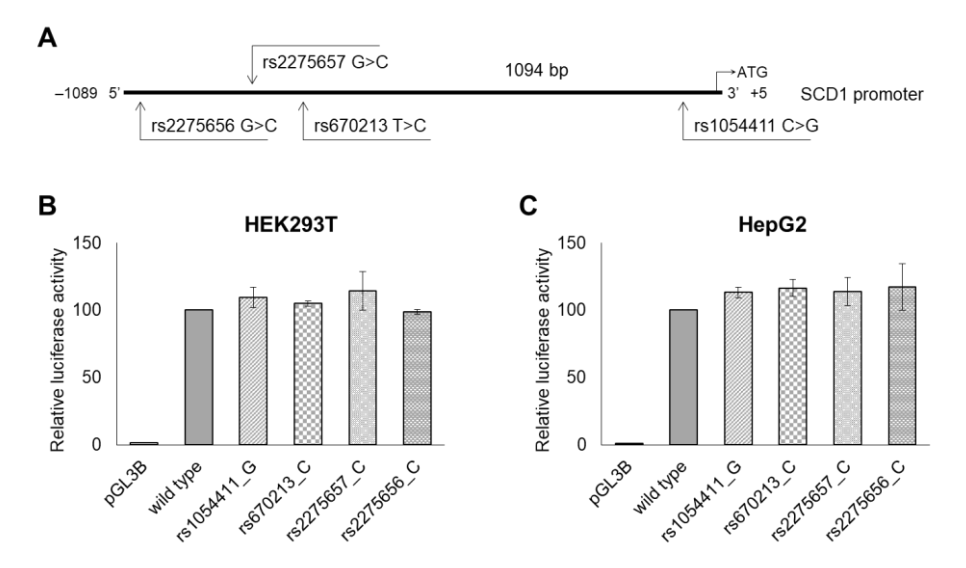


Figure 8. Location and function of *SCD1* promoter polymorphisms. Position, reference SNP cluster (rs) IDs and the nucleotide changes of the four polymorphisms with minor allele frequency greater than 5% depicted in the subcloned region of *SCD1* promoter (**A**). Transient transfection of HEK293T (**B**) and HepG2 (**C**) cells with pGL3B and wild type or polymorphic pGL3B-SCD1 promoter constructs was performed as described in *Methods*. pCMV-β-gal vector served as transfection control. Luciferase and β-galactosidase enzyme activities were measured as indicated in *Methods*. Their relative ratios are shown as bar graphs. Data are shown as mean values \pm S.D. Statistical analysis was performed by using the Tukey-Kramer Multiple Comparisons Test.

4.2.1.1. Effect of promoter SNPs on FA-dependent modulation of *SCD1* expression

Promoter activity was also tested in the presence of FAs (Figure 9). HEK293T cells were treated with BSA-conjugated FAs after transfection with pGL3B-SCD1 promoter constructs, and *SCD1* promoter activities were examined in a luciferase reporter system. Among the four SNPs investigated, rs1054411 enhanced significantly the promoter activity in the presence of all FAs used. Exposure to elaidate gave the most spectacular result – the G allele of the rs1054411 increased the luciferase activity almost threefold in the presence of this TFA (Figure 9 F).

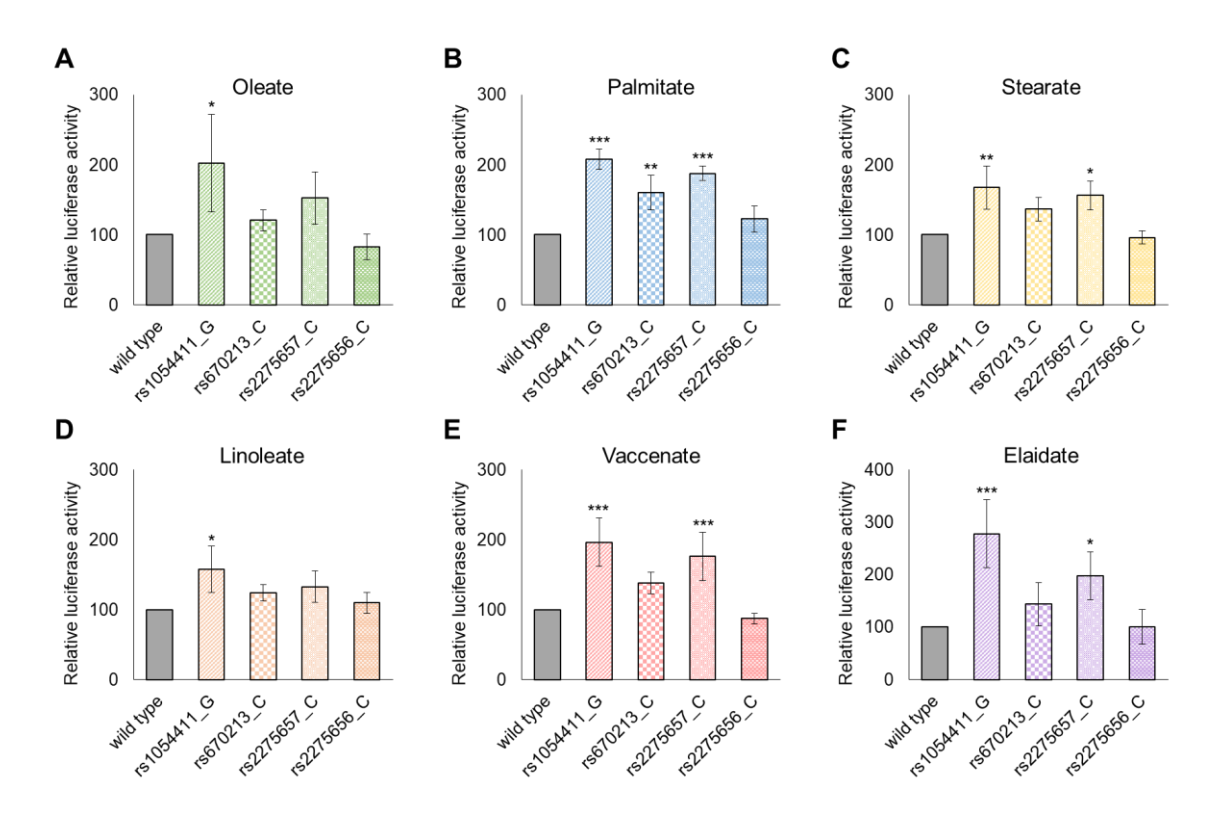


Figure 9. Modulatory effect of the four most common promoter polymorphisms on FA-dependent *SCD1* **expression in HEK293T cells.** Transient transfection with wild type and SNP-containing pGL3B-SCD1 promoter constructs and FA treatment was performed as described in *Methods*. pCMV-β-gal vector served as transfection control. Luciferase and β-galactosidase enzyme activities were measured as indicated in *Methods*. Their relative ratios are shown as bar graphs. The diagram depicts the results of at least three independent measurements normalized to the relative luciferase activity of oleate-(**A**), palmitate-(**B**), stearate-(**C**), linoleate-(**D**), vaccenate-(**E**) or elaidate-treated (**F**) wild type *SCD1* promoter containing reporter construct. Data are shown as mean values \pm S.D. Statistical analysis was performed by using the Tukey-Kramer Multiple Comparisons Test. O: oleate; P: palmitate; S: stearate; L: linoleate; V: vaccenate; E: elaidate; *p < 0.05; **p < 0.01; ***p < 0.001.

C alleles of rs670213 and rs2275657 did not have a great impact on *cis*-unsaturated FA-sensitivity (oleate and linoleate, Figure 9 A and D, respectively). Rs2275657_C increased significantly the luciferase activity in the presence of the other four FAs, *i.e.*, saturated palmitate and stearate (Figure 9 B, C) and *trans* vaccenate and elaidate (Figure 9 E, F), while a significant increment could only be observed with palmitate (Figure 9 B) in the case of rs670213_C variant. The relative luciferase activity of the C variant of rs2275656 followed that of the wild type promoter, indicating a minimal impact of this polymorphism on the promoter activity in the presence of any FAs.

The most effective SNP, rs1054411 was also tested in HepG2 cells with the same protocol (Figure 10). In this cell line, the minor, G allele caused a significantly enhanced promoter activity not only in the presence of elaidate, but also when lineleate or vaccenate were administered.

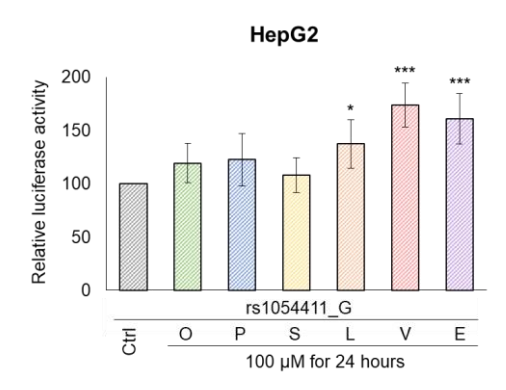


Figure 10. Impact of rs1054411 SNP on *SCD1* promoter activity in HepG2 cells. Transient transfection with wild type and SNP-containing pGL3B-SCD1 promoter constructs and FA treatment was performed as described in *Methods*. pCMV-β-gal vector served as transfection control. Luciferase and β-galactosidase enzyme activities were measured as indicated in *Methods*. Their relative ratios are shown as bar graphs. The diagram depicts the results of six independent measurements normalized to the relative luciferase activity of wild type *SCD1* promoter containing reporter construct. Data are shown as mean values \pm S.D. Statistical analysis was performed by using the Tukey-Kramer Multiple Comparisons Test. Ctrl: control; O: oleate; P: palmitate; S: stearate; L: linoleate; V: vaccenate; E: elaidate; *p < 0.05; ****p < 0.001.

4.2.1.2. TF binding modifications of *SCD1* promoter SNPs: an *in silico* analysis

JASPAR transcription factor binding site prediction program was used to determine *in silico* whether any TF binding site is affected by the investigated nucleotide variations in the promoter. Each SNP was analyzed in its 20-nucleotide vicinity. The most relevant TFs were selected with two restrictions: (i) to exclude TFs with low binding affinity to the 41 nucleotide sequences tested, the relative TF binding score had to be greater than 80% for at least one allele, and (ii) to consider only those TFs whose binding could be actually affected by the SNPs, the relative score difference between the two alleles had to be at least 15%. Along these criteria, rs1054411 resulted in five, rs670213 and rs2275657 in two TFs and rs2275656 in seven TFs whose binding to the *SCD1* promoter is likely to be modified by the polymorphic alleles (Table 8).

Table 8. List of transcription factors whose binding to *SCD1* promoter may be affected by the polymorphisms studied. Data are results of JASPAR transcription factor binding site prediction program. Depending on whether the minor allele increases or decreases the probability of TF binding, the difference between the relative scores of the two alleles is indicated by a positive or negative value, respectively.

SNP ID	TF name TF ID Strand Relation			elative score (%	ive score (%)	
SINP ID	ir name	יון זו	Stranu	major allele	minor allele	Difference
	NFATC3	MA0625.2	+	61.45	80.39	18.94
	SOX18	MA1563.1	_	65.39	81.67	16.28
rs1054411	SPI1	MA0080.1	_	81.85	66.40	-15.45
	ETV5	MA0765.1	_	85.96	69.13	-16.83
	ETS1	MA0098.1	+	98.14	76.54	-21.60
rs670213	TFAP2A	MA0003.1	+	92.89	73.99	-18.90
150/0215	RHOXF1	MA0719.1	+	80.65	63.97	-16.68
#c2275657	NFATC3	MA0625.2	_	64.77	83.72	18.94
rs2275657	USF1	MA0093.1	_	70.16	85.55	15.39
	TFAP2A	MA0003.1	+	78.11	97.01	18.90
	NR2C2	MA1536.1	_	64.15	80.59	16.43
	NR5A1	MA1540.1	_	77.70	93.60	15.89
rs2275656	PITX2	MA1547.2	_	80.83	65.76	-15.07
	TFE3	MA0831.1	_	82.07	65.90	-16.17
	RHOXF1	MA0719.1	_	80.74	64.06	-16.68
	TFAP2A	MA0003.1	-	88.76	69.86	-18.90

Among all the predicted hits, the influence of rs1054411 on ETS1 binding appeared to the most plausible, as this TF has the highest relative score for the wild type promoter (rs1054411_C: 98.14%) and the highest difference between the scores of the two alleles (rs1054411_G is 21.60% less likely to form an ETS1 TF binding site). Figure 11 depicts the consensus sequence of ETS1 response element. Since the fifth nucleotide, C is highly conserved, we reasoned that the C/G nucleotide exchange might indeed modify the binding affinity of the TF.

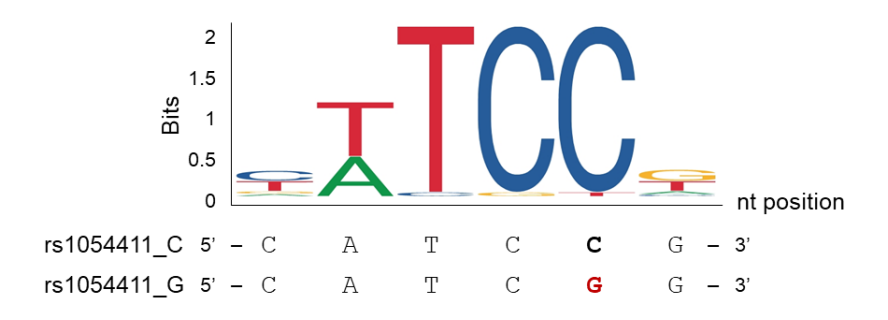


Figure 11. Consensus sequence of ETS1 TF binding site. The polymorphic nucleotide of rs1054411, highlighted in bold and red, is within the highly conserved consensus region of the ETS1 response element.

4.2.1.3. Allele-specific effect of ETS1 on SCD1 promoter activity

Based on literature data, the regulatory mechanisms of ETS1 TF are highly diverse. To investigate whether FAs also modulate ETS1 expression, HEK293T cells were treated with various FAs and endogenous *ETS1* mRNA and protein levels were assessed as described in *Methods*. Although unfortunately the poor sensitivity of commercially available ETS1 antibodies did not allow proper analysis of the protein, it has been revealed that ETS1 mRNA levels were not affected by any of the FAs tested (Figure 12 A). To overcome this problem, an ETS1 expression construct with pcDNA3.1(–) vectorial background was purchased and the experiment was repeated in HEK293T cells overexpressing ETS1. In this model, the protein levels were not affected by the FAs (Figure 12 B, C).

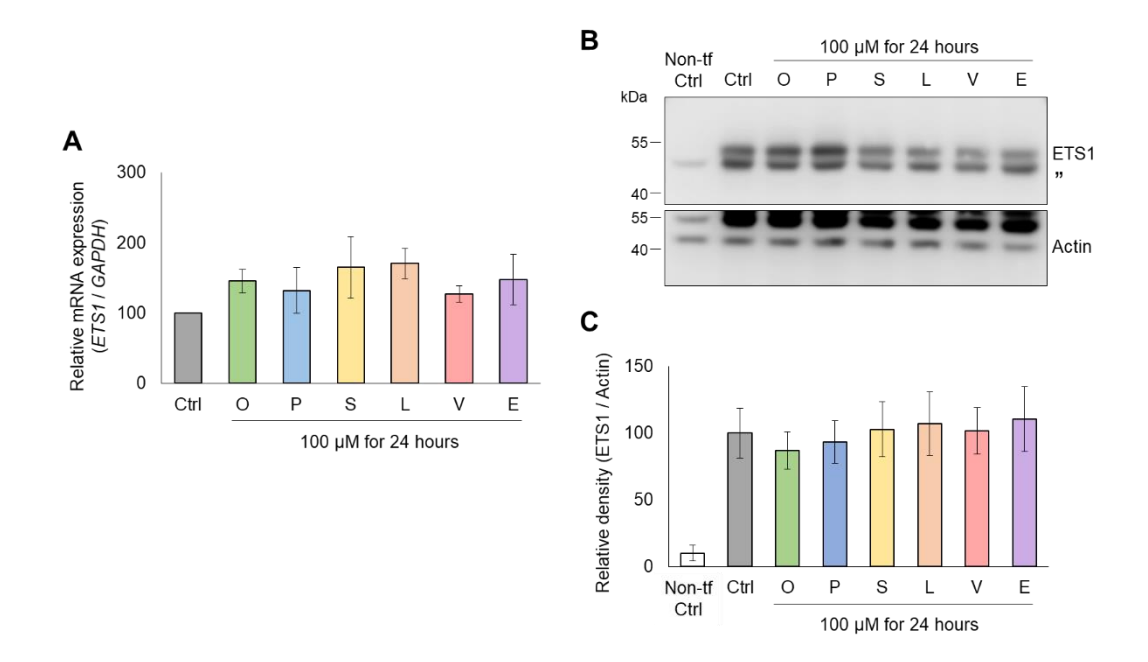


Figure 12. FA-dependent ETS1 expression in HEK293T cells. Endogenous ETS1 mRNA level in control and FA-treated cells, measured by qPCR (A). ETS1 mRNA expression is normalized to the housekeeping GAPDH expression. Representative immunoblot result from ETS1 overexpression experiment (B). Protein levels were examined after harvesting FA-treated cells, using anti-ETS1 and anti-Actin antibodies." indicates a non-specific band on the immunoblot. Band intensities were determined by densitometry of six independent immunoblot results and ETS1/Actin ratios are depicted as bar graphs (C). Transfection, treatments and measurements were carried out as described in Methods. Statistical analysis was performed with the Tukey-Kramer Multiple Comparisons Test. Data are shown as mean values \pm S.D. Non-tf Ctrl: non-transfected control; Ctrl: control; O: oleate; P: palmitate; S: stearate; L: linoleate; V: vaccenate; E: elaidate.

After confirming that FAs do not disturb the expression of ETS1, the prediction that ETS1 binding is interfered by the rs1054411 polymorphism was verified *in vitro* in a luciferase reporter system. Wild type and rs1054411_G variant promoter activities were determined after co-transfection with different amounts of the ETS1 expression construct as described in *Methods*. *SCD1* promoter activity was enhanced with increasing amounts of ETS1 plasmid and protein (Figure 13 B) for both variants, but to different extents (Figure 13 A). A significant, 1.5-fold increase in wild type promoter activity was seen even with 25 ng ETS1 expression plasmid, and the increase was more than twofold with 200 ng ETS1 plasmid. The activity of the rs1054411_G variant followed a gentler slope, as its increase reached statistical significance at 50 ng ETS1 plasmid and barely doubled at 200 ng. The difference between the two promoter activities was significant from 25 ng

ETS1 plasmid. These findings confirm the *in silico* predictions that rs1054411_G variant would reduce the TF-binding capacity of the promoter.

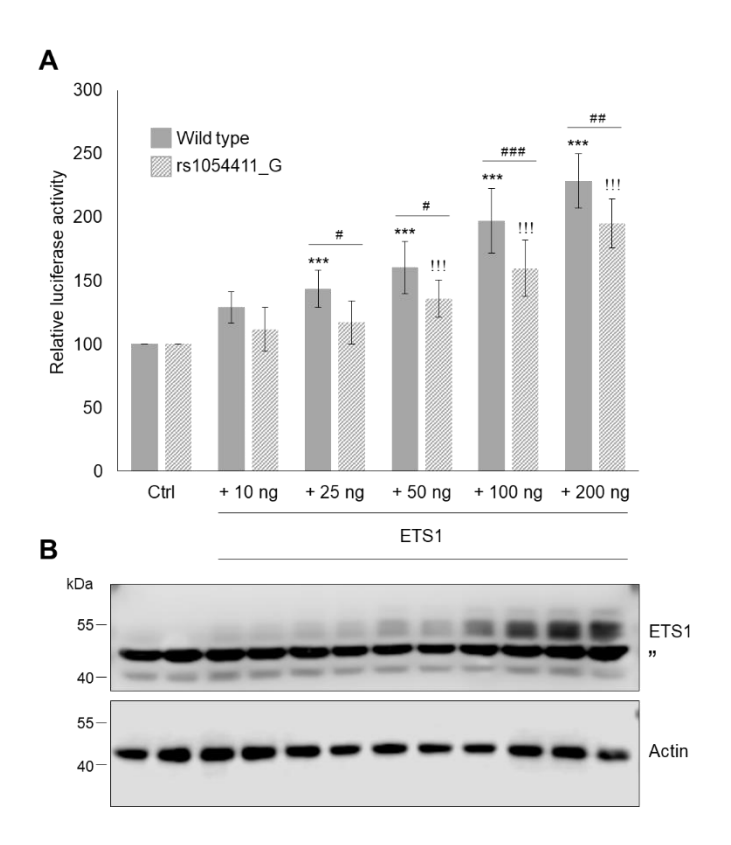


Figure 13. Impact of rs1054411 SNP on the ETS1-mediated stimulation of *SCD1* **promoter activity.** Luciferase reporter assay was used to determine the allele-specific effect of increasing amounts of ETS1 (**A**). pCMV-β-gal vector served as transfection control. Luciferase and β-galactosidase enzyme activities were measured as indicated in *Methods* and their relative ratios are shown as bar graphs. The diagram presents the results of three to twelve independent measurements normalized to ETS1-free wild type or rs1054411_G pGL3-SCD1 promoter construct, respectively. Data are shown as mean values \pm S.D. Statistical analysis was performed by using the Tukey-Kramer Multiple Comparisons Test. Ctrl: control; *p < 0.05; *#p < 0.01; ***, *## or !!!p < 0.001. Immunoblot of ETS1 protein expressed in HEK293T cells co-transfected with increasing amounts of ETS1 plasmid and one of the SCD1 promoter constructs (**B**). "indicates a non-specific band on the immunoblot. Co-transfection and immunoblotting are detailed in *Methods*.

4.2.1.4. Modulation of the FA-induced activity of rs1054411_G promoter variants by ETS1

We addressed the question whether there is an interaction between the effects of FA treatment and ETS1 overexpression on the activity of major or minor allele of *SCD1* promoter concerning the rs1054411 SNP. To this end, a combination of co-transfection and FA treatment was carried out in HEK293T cells. 100 ng ETS1 construct was used because this amount resulted in the most significant difference between the two alleles (Figure 13), and the cells were treated with elaidate, as this FA caused the greatest promoter activation with rs1054411_G allele (Figure 9 F). Cells were transfected with an *SCD1* promoter construct with or without ETS1 expression vector, then incubated in the presence or absence of elaidate, and the relative luciferase activities were measured as described in *Methods*. In line with the previous results, both ETS1 overexpression and elaidate treatment increased the promoter activity for both variants, and the effect of the FA was stronger on the activity of the minor promoter variant. Importantly, however, the abundance of ETS1 enhanced the inducing effect of elaidate, while reduced the difference between the elaidate-induced activity of the two promoter variants (Figure 14).

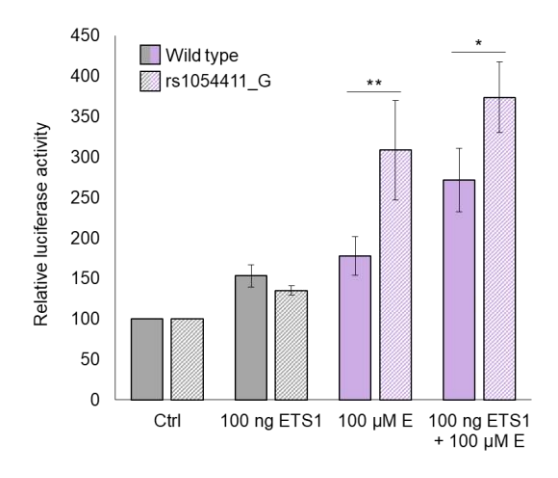


Figure 14. Interaction between the effect of elaidate treatment and ETS1 overexpression on the activity of rs1054411_C and _G alleles of *SCD1* promoter. Cotransfection and FA-treatment of HEK293T cells are detailed in *Methods*. pCMV-β-gal vector served as transfection control. Luciferase and β-galactosidase activities were measured as indicated in *Methods* and their ratios are shown as bar graphs. The diagram depicts the results of three independent measurements normalized to ETS1-free and FA-untreated wild type or rs1054411_G pGL3-SCD1 promoter construct, respectively. Data are shown as mean values \pm S.D. Statistical analysis was performed by using the Tukey-Kramer Multiple Comparisons Test. Ctrl: control; E: elaidate; *p < 0.05; **p < 0.01.

4.2.2. Variations of the coding region

4.2.2.1. Effect of M224L missense SCD1 SNP on the protein level

The major A allele (Met224) of *SCD1* gene was cloned into pcDNA3.1(–) expression plasmid, and the minor G variant (Leu224) was created by site-directed mutagenesis from this construct as detailed in *Methods*. Possible effect of the amino acid exchange on the amount of the protein was tested in transfected HEK293T and HepG2 cells by immunoblotting. Endogenous SCD1 expression could only be detected in HepG2 cells (Figure 15 D, E, F) but not in the non-transfected HEK293T cells or HEK293T cells transfected with the empty vector (Figure 15 A, B, C).

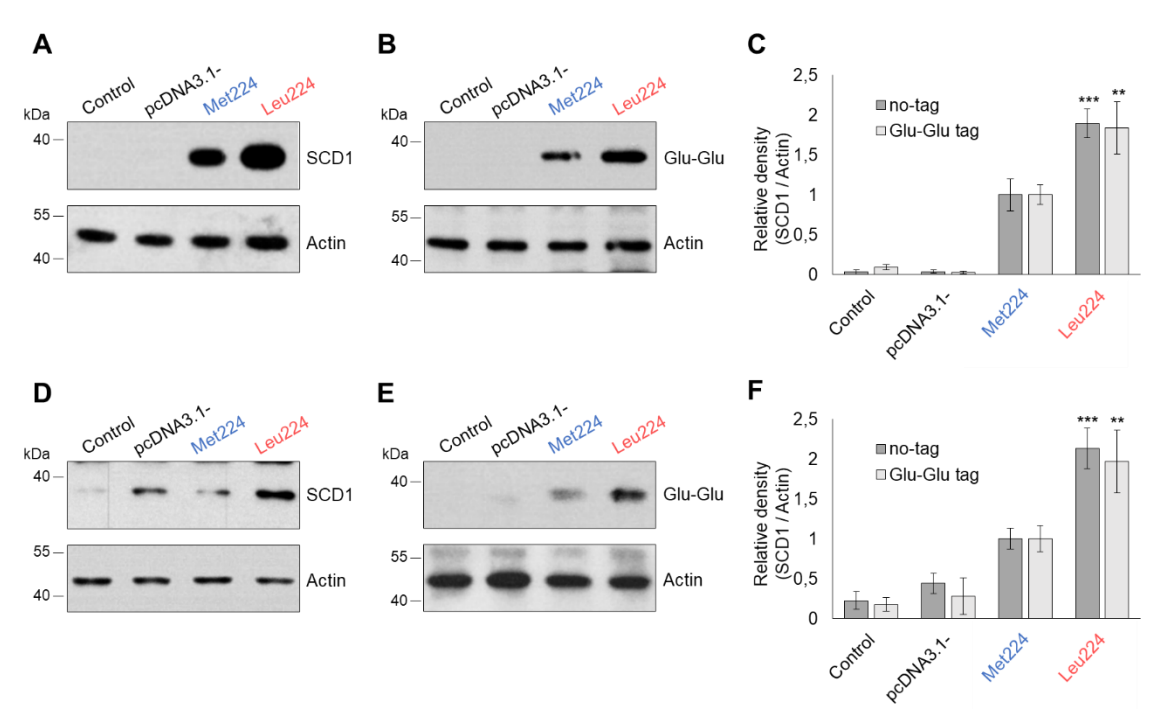


Figure 15. Protein expression of unlabeled and Glu-Glu tagged M224L SCD1 variants in two cell lines. Immunoblots of SCD1 in transiently transfected HEK293T cells, 24 hours after transfection, using with anti-SCD1 (A) or anti-Glu-Glu tag (B) antibodies. Immunoblots of SCD1 in HepG2 cells in the same experimental conditions, using anti-SCD1 (D) or anti-Glu-Glu tag (E) antibodies. In each case, Actin served as a loading control. Band intensities were determined by densitometry of three independent immunoblot results and SCD1/Actin ratios are depicted as bar graphs (C, F). Statistical analysis was performed with the Tukey-Kramer Multiple Comparisons Test. Data are shown as mean values \pm S.D. **p < 0.01; ***p < 0.001.

A significant difference could be observed between the levels of overexpressed Met224 and Leu224 proteins in both cell lines, in favor of the latter variant (Figure 15 A,

D). To rule out the possibility that the difference was due to a different affinity of the antibody for the two variants, the experiment was also performed using C terminal Glu-Glu tagged versions of both variants. The immunoblot with the anti-tag antibody consistently showed the same pattern: there was a marked difference in band densities, and the quantification revealed that the amount of Leu224 variant was about twice that of Met224 (Figure 15 B, E).

4.2.2.2. Influence of M224L missense SCD1 SNP on the mRNA level

The elevated Leu224 SCD1 protein level can be attributed to an increased amount of mRNA, giving way to enhanced translation and/or a longer half-life of the protein. To address the first possibility, the amount of *SCD1* mRNA in transfected HEK293T was determined by qPCR using primers specific to endogenous and overexpressed *SCD1* cDNA or primers specific to the Glu-Glu tagged version. The mRNA levels of the leucine-coding C variant were seen to be significantly higher in both cases: a 1.889-fold difference for the untagged and a 1.972-fold difference for the tagged versions were detected in favor of the Leu224 variant (Figure 16).

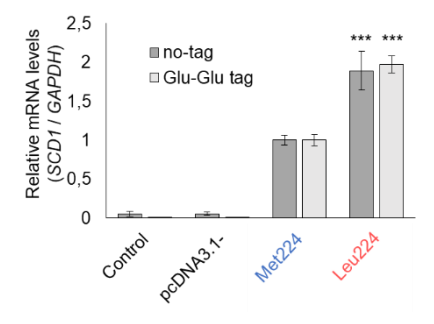


Figure 16. *SCD1* expression in transiently transfected HEK293T cells determined by qPCR. After transfection, DNA contamination-free total RNA was isolated from harvested cells and reverse transcribed into cDNA as detailed in *Methods*. qPCR was carried out using either *SCD1* or Glu-Glu tag and *GAPDH* sequence specific primers as indicated in *Methods*. The diagram depicts the results of three independent measurements. Statistical analysis was performed with the Tukey-Kramer Multiple Comparisons Test. Data are shown as mean values \pm S.D. ***p < 0.001.

Since the single A/C nucleotide replacement is the only difference between the two mRNA variants, we assumed that the observed difference in mRNA levels was due to altered mRNA stability. To address this hypothesis, the structure of the two mRNA variants was predicted *in silico* with the RNAfold online tool. According to the prediction,

the mRNA of the minor (C) allele forms an extra hairpin loop in the center, which may contribute to increased stability and thus increased translation (Figure 17 A). The program calculates the structures based on MFE (Figure 17 B), and the mountain plot indicates slight differences also in the flanking region of the SNP, further increasing the probability that the two mRNA variants have different stability.

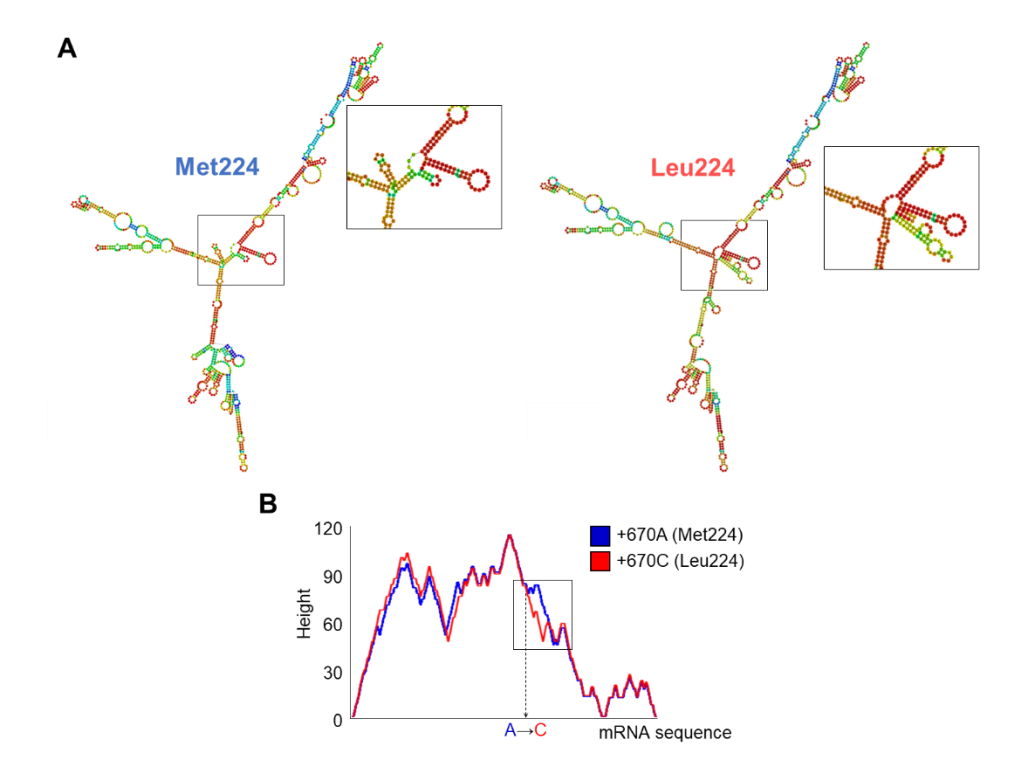


Figure 17. In silico prediction of the secondary MFE structures of +670A and +670C SCD1 using the RNAfold online tool. Spatial structure of the SCD1 mRNAs (A). The different segments near the SNP are magnified. Mountain plot of MFE (B). Mountain plot represents a secondary structure in a plot of height versus position, where the height is given by the number of base pairs enclosing the base at a given position. Loops correspond to plateaus (hairpin loops are peaks), helices to slopes.

To validate the *in silico* prediction that mRNA stability is allele-specific in favor of the minor allele, an *in vitro* experiment was designed: using a transcription inhibitor, actinomycin D, degradation of the two tagged mRNA variants was monitored in a twelve-hour time window. qPCR analysis was carried out using Glu-Glu tag specific primers. The difference between the two variants could be observed as early as 1 hour after transcription arrest and became more significant over time (Figure 18). The mRNA of the A allele almost halved 2 hours after transcription arrest, while that of the C allele did not reach 50% of the initial level even after 12 hours.

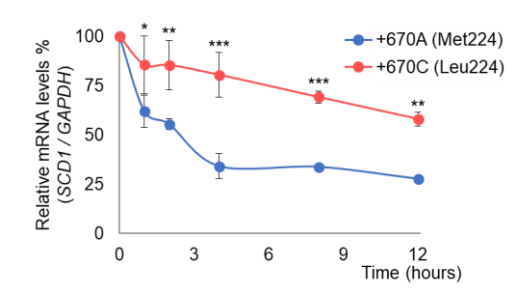


Figure 18. Allele-specific mRNA degradation of the two *SCD1* variant monitored by qPCR. HEK293T cells were transiently transfected with the methionine-expressing +670A and the leucine-expressing +670C variants of SCD1. 5 μ g/mL actinomycin D treatment for 0, 1, 2, 4, 8 and 12 hours, harvesting, total RNA isolation and reverse transcription into cDNA was accomplished as detailed is *Methods*. qPCR was carried out using either *SCD1* or Glu-Glu tag and *GAPDH* sequence specific primers as indicated in *Methods*. Diagram depicts the average of three parallels. Statistical analysis was performed with the Tukey-Kramer Multiple Comparisons Test. Data are shown as mean values \pm S.D. *p < 0.05; **p < 0.01; ***p < 0.001.

4.2.2.3. Protein stability of M224L SCD1 variants

In addition to increased mRNA stability, another possible explanation for the elevated SCD1 protein levels observed in the Leu224 variant is a more stable protein structure that prolongs the half-life of the minor protein variant. To address this possibility, intracellular degradation of Met224 and Leu224 was compared using cycloheximide, a translation inhibitor and immunoblotting. In line with previous studies, the amount of the major SCD1 variant with a reportedly short half-life was almost halved after 1 hour of translation arrest (Figure 19 A). Its amount continued to decrease, and Met224 SCD1 became barely detectable by the end of the six-hour time window. In contrast, the amount of Leu224 hardly decreased in the first two hours, which resulted in a clearly visible, significant difference between the quantity of the two variants. The marked, although statistically less significant difference between the two protein variants persisted throughout the experiment, and the Leu224 variant could be clearly detected even at the end.

Since the SNP is located in the third transmembrane region of the enzyme, it was not unexpected that the I-TASSER online software did not predict any major change in the 3D protein structure after substituting Met224 to Leu224 (Figure 19 B). However, an alteration in the normalized B-factor values in this section of the protein indicates a decreased conformational entropy of leucin residue at position 224 (Figure 19 C).

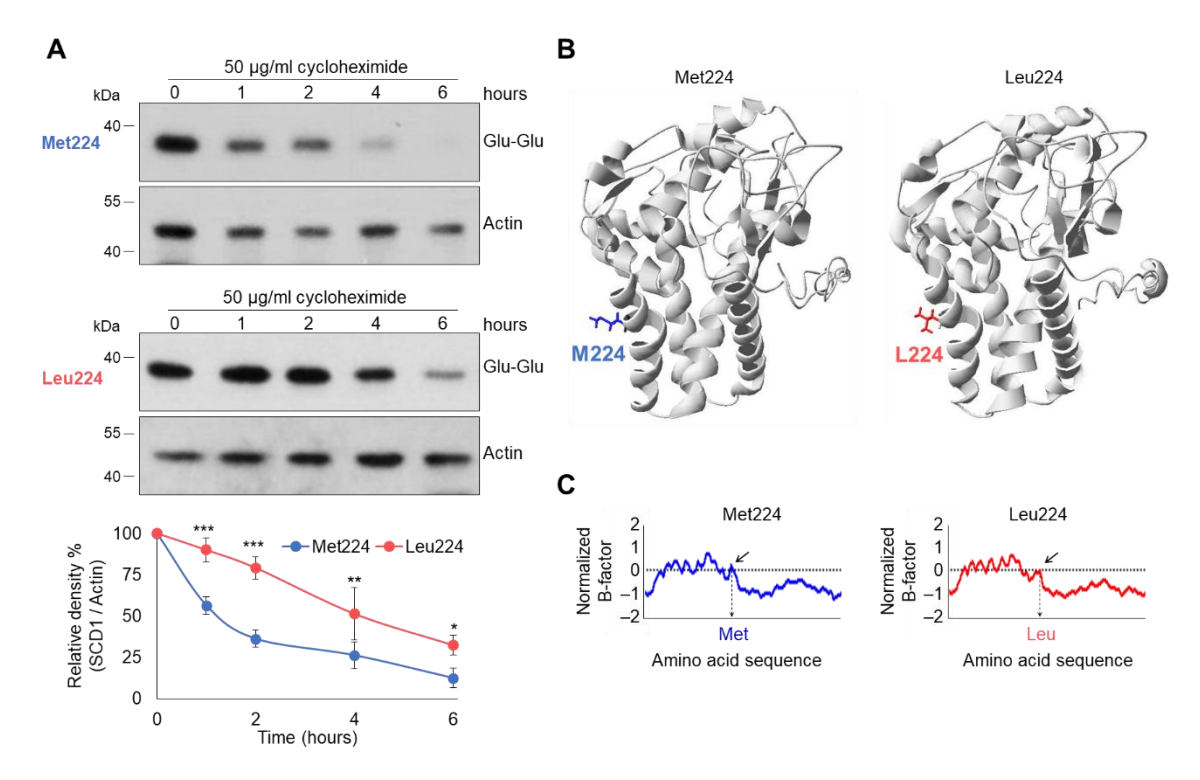


Figure 19. Stability of M224L SCD1 variants. Examination of intracellular degradation of SCD1 with methionine or leucine at position 224 (**A**). Transiently transfected HEK293T cells were treated with 50 µg/mL translation inhibitor, cycloheximide for 0, 1, 2, 4 and 6 hours. Harvested cells were analyzed by immunoblotting, using anti-Glu-Glu tag and anti-Actin antibodies. Exact protocols are detailed in *Methods*. Representative result of four independent experiments is shown. Band intensities were determined by densitometry and SCD1-Glu-Glu/Actin ratios are depicted as bar graphs. Statistical analysis was performed with the Tukey-Kramer Multiple Comparisons Test. Data are shown as mean values \pm S.D. *p < 0.05; **p < 0.01; ***p < 0.001. Resolved crystal structure of Met224 human SCD1 from Protein Data Bank compared with I-TASSER online tool predicted secondary structure of Leu224 variant (**B**). Images were rendered using DeepView/Swiss-Pdb Viewer version 4.0.2. Comparison of normalized B-factor values for Met224 and Leu224 SCD1 variants (**C**). The normalized-B factor (B-factor of each residue/B-factor of whole average) was plotted as the function of the amino acid residues.

4.2.2.4. Impact of FAs on the M224L protein variants

We were interested whether FAs can affect the two M224L variants differently. Thus, the protein levels were assessed in transfected HEK293T cells treated with various FAs (Figure 20 A, B). The major (Met) variant was essentially unresponsive to FAs, except for oleate, which, confirming the literature data, decreased the intracellular amount of Met224 SCD1. Surprisingly, oleate had no reducing but even a slight increasing effect on the amount of the Leu224 variant. In further contrast to the major variant, the amount of

Leu224 was elevated in the presence of all FAs used. Statistically significant increment was observed in the case of palmitoleate (3-fold), linoleate (4-fold) and stearate (6-fold). Moreover, all FAs elevated the level of Leu224 protein compared not only to its untreated control, but to the Met224 variant after the corresponding FA-treatment. However, the latter difference was statistically significant only for stearate.

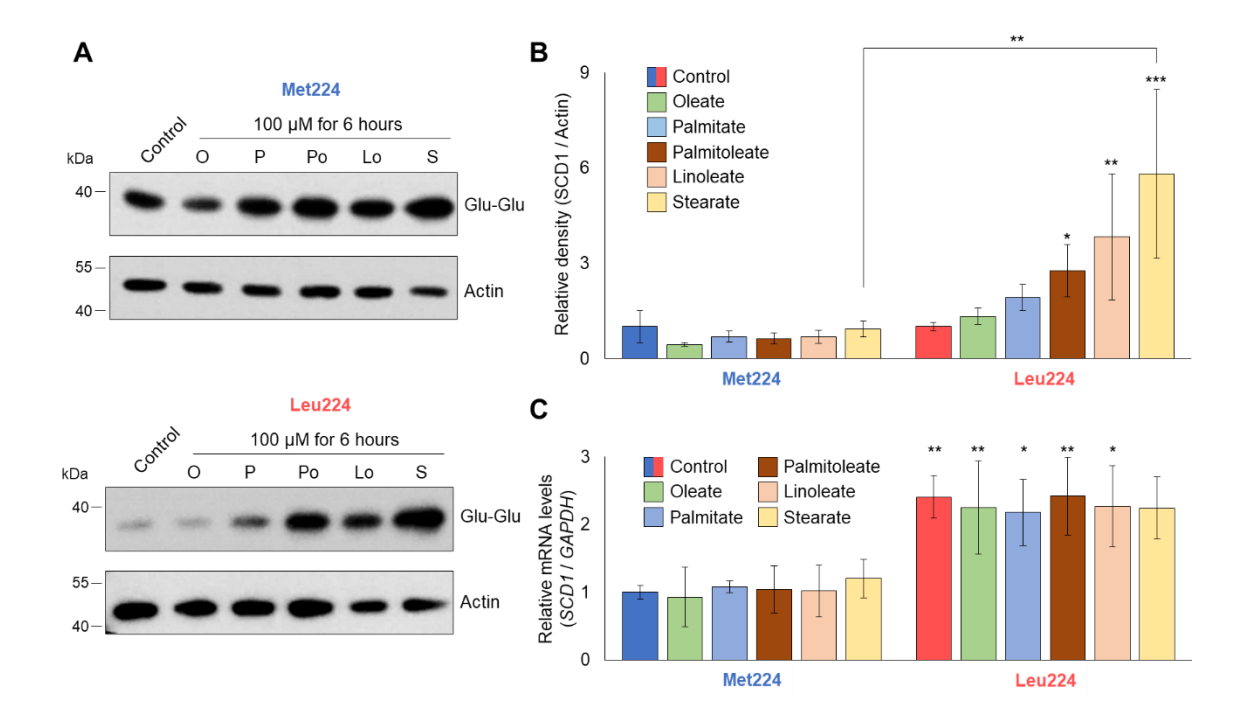


Figure 20. Impact of different FAs on M224L variants of SCD1. Representative immunoblots of five independent experiments (A) and densitometric evaluation of all five blots (B). HEK293T cells were transiently transfected and 24 hours later treated with BSA-conjugated oleate (O), palmitate (P), palmitoleate (PO), linoleate (LO) and stearate (S) for 6 hours at a final concentration of 100 µM. Protein content of the harvested cells were monitored by immunoblotting, using anti-Glu-Glu tag and anti-Actin antibodies. Transfection, FA treatment and immunoblotting were carried out as detailed in *Methods*. In each case, housekeeping Actin served as a loading control. SCD1/Actin ratios from quantitating band intensities by densitometry, are depicted as bar graphs. Statistical analysis was performed with the Tukey-Kramer Multiple Comparisons Test. Data are shown as mean values \pm S.D. *p < 0.05; **p < 0.01; ***p < 0.001. Impact of FAs on mRNA levels of the SCD1 variants (C). Transfected HEK293T cells were treated with BSA-conjugated FAs, similarly to the previous experiment. cDNA was reverse transcribed from total RNA isolated from harvested cells, qPCR was carried out using Glu-Glu tag and GAPDH sequence specific primers as indicated in Methods. Diagram depicts the average of three parallels. Statistical analysis was performed with the Tukey-Kramer Multiple Comparisons Test. Data are shown as mean values \pm S.D. *p < 0.05; **p < 0.01.

The effect of FAs on the mRNA levels was tested in similar experiments using qPCR analysis Glu-Glu-tag specific oligos. During the six-hour treatment, no FA seemed to alter the amount of mRNA for either variant of *SCD1* (Figure 20 C).

4.2.2.5. Enzymatic activity of M224L desaturase variants

From the results of our previous experiments, it can be clearly seen that FAs affect differently the intracellular amount of the two SCD1 protein variants. To demonstrate that the overexpressed desaturase is functional, and that elevated protein levels in case of Leu224 SCD1 also imply increased desaturation, the FA content of transfected HEK293T cells was analyzed by GC-FID. SCD1-dependent desaturation was inferred from the ratio between the sum of the two major MUFAs and the sum of the two major SFAs (eq 1).

(1)
$$\frac{\text{palmitoleate (C16:1 } \textit{cis}\Delta 9) + \text{oleate (C18:1 } \textit{cis}\Delta 9)}{\text{palmitate (C16:0)} + \text{stearate (C18:0)}}$$

The empty pcDNA3.1(–) vector did not change the FA content of transfected cells (Figure 21). In contrast, cells expressing the Met224 SCD1 showed a significant, 1.2-fold increase in the unsaturated: saturated FA ratio, indicating that the overexpressed enzyme is indeed functional (Figure 21 C).

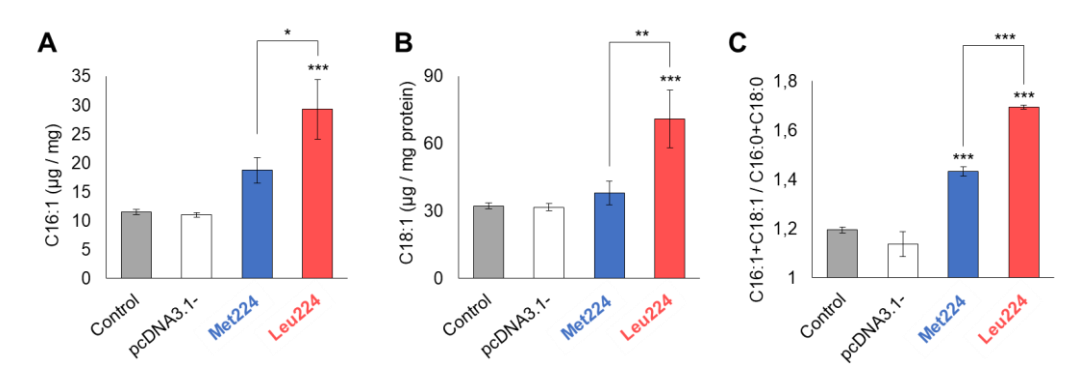


Figure 21. Changes in FA content of cells transfected with M224L SCD1 variants. HEK293T cells were harvested 24 hours after transfection and FA contents were analyzed by GC-FID as described in *Methods*. Absolute amount of the two main products of SCD1, C16:1 palmitoleate (**A**) and C18:1 oleate (**B**) was measured and depicted as bar graphs. Ratio of the sum of major unsaturated and the sum of major saturated FAs (**C**). Data were normalized to the total protein content of the samples and are shown as mean values \pm S.D. Diagram depicts the average of three parallels. Statistical analysis was performed with the Tukey-Kramer Multiple Comparisons Test. *p<0.05; **p<0.01; ***p<0.001.

Moreover, as expected from the higher protein levels, transfection with Leu224 SCD1 expression construct caused an even greater increase in the unsaturated: saturated FA ratio, *i.e.*, a 1.4-fold increment compared to control and a 1.18-fold compared to the Met224 variant. Additionally, the amount of the two main products of the desaturase, C16:1 palmitoleate (Figure 21 A) and C18:1 oleate (Figure 21 B) also reflected a significant increase in favor of the Leu224 variant.

4.2.2.6. Is the increase in protein level caused by the polymorphism due to the missing methionine or the leucine present?

To investigate whether the extended half-life of Leu224 SCD1 is caused more by the absence of a methionine side chain or by the appearance of a leucine side chain, we also created an artificial Ala224 variant by site-directed mutagenesis (changing the methionine-coding AUG to the alanine-coding GCG triplet) and compared its stability with that of the two natural variants in the experimental system described previously. Although the artificial Ala224 variant presented with lower mRNA levels (Figure 23 C), its protein level was no significantly different from that of Met224 (Figure 22).

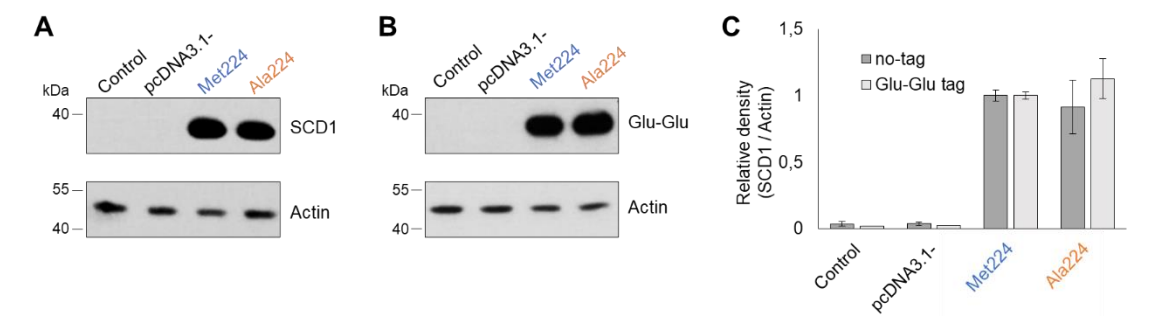


Figure 22. Comparison of intracellular Met224 and Ala224 SCD1 protein levels. HEK293T cells were transiently transfected with untagged (**A**) and tagged (**B**) SCD1 constructs: Met224 and Ala224 variants. 24 hours after transfection, cells were harvested and the protein amounts were monitored by immunoblotting. In each case, housekeeping Actin served as a loading control. Representative immunoblots of three independent experiments are shown. SCD1/Actin ratios from quantitating band intensities by densitometry, are depicted as bar graphs (**C**). Statistical analysis was performed with the Tukey-Kramer Multiple Comparisons Test. *p < 0.05; **p < 0.01; ***p < 0.001.

After translation arrest with cycloheximide, the artificial Ala224 proved to be more stable and had a longer half-life (Figure 23 A). Nevertheless, in terms of its sensitivity to FAs, it showed no difference from the natural reference Met224, as the FAs did not affect the amount of either protein variants significantly (Figure 23 B).

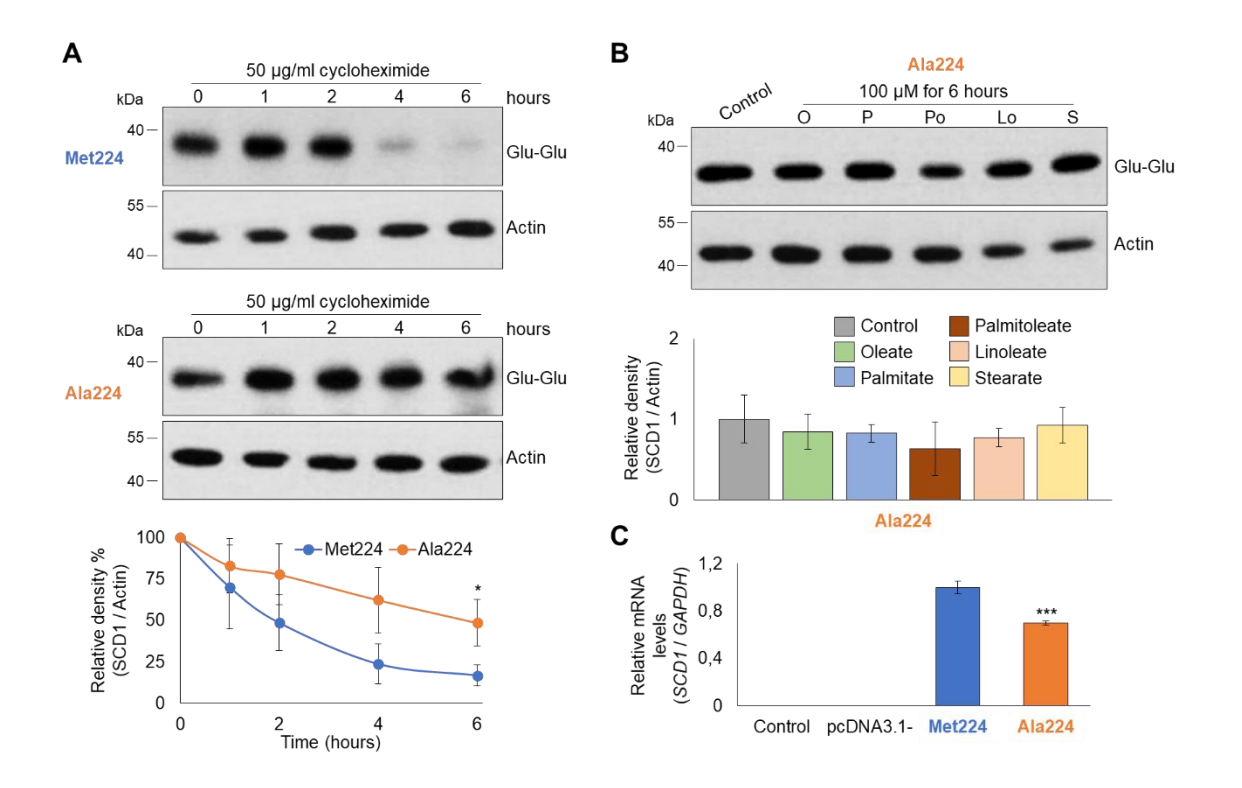


Figure 23. Expression and FA-sensitivity of Ala224 SCD1. Protein synthesis in transiently transfected HEK293T cells was arrested with 50 mg/mL cycloheximide for 0. 1, 2, 4 and 6 hours (A). Protein amounts were monitored by immunoblotting. Representative result of four independent experiments is shown. Band intensities were determined by densitometry and SCD1-Glu-Glu/Actin ratios are depicted as bar graphs. Impact of FAs on the Ala224 variant (**B**). Transiently transfected cells were treated with 100 µM BSA-conjugated oleate, palmitate, palmitoleate, linoleate and stearate. Immunoblot analysis of cell lysates was carried out using anti-Glu-Glu tag and anti-Actin antibodies. Representative result of three independent experiments is shown. The band intensities were determined by densitometry and SCD1-Glu-Glu/Actin ratios are shown as bar graphs. qPCR analysis of Ala224 (C). RNA isolation, reverse transcription to cDNA and qPCR of samples from transiently transfected HEK293T cells were carried out as determined in Methods. The diagram presented depicts the results of three independent measurements. Statistical analysis was performed with the Tukey-Kramer Multiple Comparisons Test. Data are shown as mean values \pm S.D. *p < 0.05; **p < 0.01; ***p < 0.001.

4.3. Association studies

Two selected polymorphisms, *i.e.*, one of the four promoter polymorphisms and the only missense polymorphism of the coding region, were tested for association with type 2 diabetes mellitus on a small population. The association studies presented in this section were carried out by our research team. They are part of our overall research on SCD1 and

are included in this thesis because they are relevant to the discussion and interpretation of my results.

Possible association between rs1054411 C/G promoter polymorphism and T2DM and between the missense M224L A/C SNP and T2DM was assessed by case–control setups. Results are summarized in Table 9 and Table 10, respectively. The observed genotype distribution in the control group was in agreement with the expected values based on the Hardy–Weinberg equilibrium (χ^2 -test p = 0.911). Association analysis was carried out by using both allele- and genotype-wise approaches including the dominant model (*i.e.*, Genotype combination).

Table 9. Comparison of allele, genotype, and genotype combination frequencies of rs1054411 promoter SNP in control and T2DM groups. T2DM: type 2 diabetes mellitus.

	Control (N = 370)		T2D (N = 2		
	N	%	N	%	
Allele					
С	437	59	351	62	
G	303	41	213	38	
χ^2	p = 0.24	147			
Genot	ype				
C/C	127	34	107	38	
C/G	183	49	137	49	
G/G	60	16	38	13	
χ^2	p = 0.4943				
Genotype combination					
C+	310	84	244	87	
C-	60	16	38	13	
χ^2	p = 0.3319				

Allele frequencies were congruent with the European population data available in 1000Genomes (MAF: 41 vs. 40%). However, in our control group, the minor allele was slightly overrepresented compared to both ALFA (MAF: 35%) and global frequencies (MAF: 28%). As Table 9 shows, the frequency of the G allele was slightly but not significantly lower in the patient group in all the three comparisons (when comparing the control and patient groups using χ^2 -test, neither the allele or genotype, nor the genotype

combination frequency reaches the significance level of p < 0.05). Due to the limited number of samples that could be included in the study, the lack of statistically significant result does not exclude a putative role of the SNP in the genetic risk of T2DM.

Table 10. Comparison of allele, genotype, and genotype combination frequencies of M224L SNP in control and T2DM groups. T2DM: type 2 diabetes mellitus.

	Control (N = 463)		T2DM (N = 425)			
	N	%	N	%		
Allele						
Met	574	62	502	59		
Leu	352	38	348	41		
χ^2	p = 0.20	071				
Genotype						
Met/Met	181	39	152	36		
Met/Leu	212	46	198	47		
Leu/Leu	70	15	75	18		
χ^2	p = 0.4601					
Genotype combination						
–Leu	181	39	152	36		
+Leu	282	61	273	64		
χ^2	p = 0.3061					

Allele frequencies were in line with the data available in GnomAD. As shown in Table 10, frequency of the leucine-coding allele was slightly but not significantly higher in the patient group in all comparisons.

5. Discussion

Development of complex genetic diseases arises from the interplay of genetic and environmental factors. These conditions encompass a range of metabolic disorders, including obesity, the metabolic syndrome, type 2 diabetes mellitus, along with closely associated cardiovascular diseases and cancers. Deranged lipid metabolism plays a crucial role in these metabolic diseases, so a balanced supply of saturated and unsaturated FAs is of great significance for the prevention. In addition to regular physical activity, adequate hydration, and avoiding detrimental habits, the right amount and composition of food is crucial. There is a consensus that excessive consumption of animal fats abundant in SFAs is harmful to health, compared to vegetable oils rich in MUFAs and PUFAs. However, the genetic background governing the enzyme networks that metabolize and respond to these dietary fats remains poorly understood.

5.1. Importance of different types of FAs and their relationship with SCD1 enzyme

Besides SFAs, the presence of bent-shaped UFAs is indispensable for appropriate triglyceride and phospholipid synthesis, the latter maintaining optimal membrane fluidity and flexibility, and transmembrane signaling. However, during de novo synthesis, only SFAs can be produced, so even with a sufficient amount of UFA taken in during nutrition, the endogenous FA balance would normally incline to SFAs. Excessive SFAs can induce lipotoxicity through disturbing normal cell functions, causing redox imbalance [126], impaired lipid signaling, membrane and organelle dysfunction, inflammation or even apoptosis [127, 128]. Protecting effects of UFAs against SFA-induced lipotoxicity are widely investigated. A recent study for instance, showed both in vitro in INS-1E rat insulinoma cell line and in vivo in male C57BL/6 mice on high-fat diet that MUFAs and PUFAs, such as EPA, DHA and AA, but mainly oleic acid (in vitro) and olive oil (in vivo) effectively protect islet β -cells from SFA-induced cellular lipotoxicity [129]. The function of desaturase enzymes, introducing double bonds in SFAs, is pivotal for achieving the appropriate FA ratio. Although our cells can insert double bonds into the FA chains at various positions up to 9, a saturated chain can only get desaturated between the carbons 9 and 10 by SCD enzymes, which therefore catalyze the rate determining step for the synthesis of all unsaturated FAs. Although SCDs require electrons from NAD(P)H, it has been shown that their activity is determined by the level of the SCD enzyme itself rather than the capacity of the associated electron transfer chain [130]. This work focuses on SCD1, the major isoform of the two human SCDs. Since this enzyme is expressed in nearly all cell types, its health impacts are rather diverse, *i.e.*, in addition to protecting certain cells against SFA-induced lipotoxicity, its overexpression or overactivity in the major metabolic tissues may be also detrimental to health through favoring triglyceride synthesis and thus obesity [84]. Adipose tissue hypertrophy can lead to general inflammation and high levels of FFAs, which in turn leads to obesity-induced systemic lipotoxicity [131] (Figure 4).

However, neither the exact mechanism of the protective effects of UFAs against lipotoxicity, nor the differences between the effects of various FAs are fully understood. As expected and consistent with our findings, SFAs typically elevate the cellular abundance of SCD1 (Figure 5, 6 and 7). This promotes their conversion into UFAs, facilitating their consumption by lipid synthesis and thereby reducing their accumulation and diminishing their harmful effects. Cis-UFAs substantially reduce SCD1 expression [132], although the mechanism of action of MUFAs and PUFAs may differ. On the one hand, polyunsaturated linoleate is believed to disrupt desaturation by modulating transcription, and it has been found to consistently suppress SCD1 expression across all three levels investigated (promoter activity, mRNA, and protein levels) in both HEK293T and HepG2 cell lines. This aligns with the identification and characterization of a PUFAresponsive element in the upstream regulatory region of human and mouse SCD1 genes [80, 84, 133]. On the other hand, although a large number of studies have demonstrated the ability of monounsaturated oleate to suppress SCD1 [134], the exact mechanism remains uncertain. Oleate notably diminished the level and activity of SCD1, but the findings regarding its impact on SCD1 mRNA levels, and promoter activity, are inconsistent. This suggests that oleate may act through mRNA and/or protein stabilization rather than transcriptional repression [135]. Notably, the well-established suppressive effect of oleate on SCD1 was not observed across all three regulatory levels examined in HepG2 cells. However, the effects of other FAs were also relatively modest in this cell line, possibly due to a relatively high tolerance of HepG2 cells toward FAs [136].

Health effects of TFAs are controversial. On the one hand, human studies identified a positive association between TFA consumption and the onset of lipid metabolismlinked conditions, such as the metabolic syndrome, type 2 diabetes mellitus, cardiovascular disease, and cancer [137]. On the other hand, other studies indicate that TFAs may exhibit protective effects against palmitate toxicity in cell cultures similar to those of oleate [41]. Compared to the most lipotoxic SFAs, TFAs induce inflammation and ER stress to a much lesser extent, suggesting that they are less harmful [138, 139]. TFAs surely exert distinct effects on metabolism and fundamental physiological processes compared to other dietary FAs, however, the question is whether naturally occurring and industrial TFAs have the same health effects. Several human studies indicate that the unfavorable impacts are predominantly associated with industrial TFAs [140, 141], while naturally occurring TFAs could be harmless or even beneficial for metabolic health [142, 143]. However, other epidemiological and clinical studies indicate no difference between the harmful effects of the two types of TFAs as both can contribute to metabolic and cardiovascular diseases [144, 145]. The controversy of the above in vivo results urged us to attempt to elucidate the potential differences between the two types of TFAs. We chose to compare their effects on SCD1 expression first, because any difference in the modulation of this key enzyme of FA metabolism would have a major impact on overall lipid homeostasis and thus on inflammation, stress, insulin sensitivity and viability in a variety of cells. It has been reported earlier that the iTFA elaidate increases the level of FA desaturation in HASMC, HUVEC and HepG2 cells [132, 146], and raises the level of SCD1 mRNA in trophoblast and HASMC cells [132, 147], while the rTFA vaccenate showed no similar effects [132, 146, 148]. We found it necessary to systematically compare the effects of the two TFAs on SCD1 expression in two cell lines (HEK293T and HepG2) by assessing changes in the mRNA and protein levels and in the promoter activity in a luciferase reporter system. Our findings were in accordance with the available, albeit limited, scientific data described above and supported the difference between the two TFAs. We found that elaidate markedly induces SCD1, which is reflected in all three parameters investigated, and this contrasts with the ineffectiveness of vaccenate (Figure 5, 6 and 7).

5.2. Polymorphisms of *SCD1*

Even though the role of SCD1 is pivotal in both SFA-induced lipotoxicity and obesity, there is scarce literature addressing polymorphisms that can influence its expression or activity. According to the promoter region, no SNPs have been functionally investigated yet – except that rs670213 polymorphism has been proven to be unrelated to metabolic risk [102, 103]. On the other hand, M224L (rs2234970), a missense polymorphism in the coding region of SCD1 with a relatively high frequency in all studied populations to date (Leu224 allele: 24–53%) has been studied and its association with pathological conditions was addressed in four studies [98-101].

5.2.1. Promoter SNPs

We searched for the most common promoter SNPs in silico and tested them in vitro in a luciferase reporter system both in the absence (Figure 8) and presence (Figure 9 and 10) of various dietary FAs. Among the four common promoter SNPs investigated, rs1054411 was found to be functional in the presence of FAs and as a modifier of a TF binging site. Our in silico analysis identified ETS1 as a TF with allele-specific binding to the SCD1 promoter region carrying the SNP rs1054411 (Table 8 and Figure 11). ETS1 is a proto-oncogene from the ETS protein family, regulating the expression of a wide range of proteins. As ETS1 can affect cell development, differentiation, survival and death, it is not surprising that increased ETS1 expression or activity has been associated with a diverse set of cancers. It was shown to influence angiogenesis through the regulation of proteins controlling endothelial cell migration and invasion [149, 150]. In addition to its role in tumor progression and invasion, ETS1 has been found to be involved in cellular metabolism [151], as it has been revealed to up-regulate key enzymes in FA metabolism [152]. Since the role of FAs in regulating ETS1 has not yet been clarified, we considered it important to investigate this potential connection. On the one hand, our experiments did not reveal any effects of FAs on ETS1 expression (Figure 12), on the other hand, we confirmed in vitro our in silico prediction that in the presence of the rs1054411_G allele, ETS1 has a 20% reduced affinity to the promoter (Figure 13). Moreover, with a combination of co-transfection and FA treatment, we demonstrated interaction between TF binding and the presence of FAs, as ETS1 reduced the enhancing effect of elaidate on

rs1054411_G allele-specific promoter activity by about half, *i.e.*, 73% vs 37% (Figure 14).

5.2.2. M224L SNP

Studies investigating the M224L missense SNP of the coding region revealed association between the minor Leu224 variant and an increased risk of cardiovascular diseases through higher unsaturated: saturated ratio of C:18 FAs [101]. Moreover, the Leu224 variant has also been shown to be an aggravating factor in stage II colorectal cancer [100]. However, the major Met224 allele was associated with insulin resistance in the skeletal muscle through increased intramyocellular lipid accumulation in an Indian population [99], while the SNP did not show any correlation with effects of dietary DHA treatment in patients with the metabolic syndrome [98]. According to these studies, the M224L SNP appears to be linked to various medical conditions, however the molecular mechanisms underlying these effects are unclear. Therefore, we aimed to elucidate how this SNP influences the mRNA and protein levels, as well as the activity of SCD1 in a cellular model.

Our experiments showed markedly higher expression and activity of the Leu224 variant (Figure 15, 16, and 21). Since we meant to reveal whether the observed results can be attributed to the lack of leucine or to the appearance of methionine at the polymorphic position, we created an artificial, alanine-containing variant as a new amino acid in the investigated locus can serve as an indifferent reference in functional assays [153]. Regarding that the two natural variants were identical except for the A/C difference within the triplet coding for the 224th amino acid, the elevated mRNA level of the Leu224 (C) variant can be explained by an increased mRNA stability. Based on literature data, a single nucleotide change, even a synonymous SNP, may modify mRNA stability [154]. The *in silico* analysis strengthened our hypothesis, predicting an extra hairpin loop in the flanking region of the polymorphic site in the minor variant (Figure 17) and we confirmed a hindered mRNA degradation *in vitro* with the actinomycin D treatment (Figure 18). Since the artificial Ala224 mutant did not show an elevated mRNA level (Figure 23 C), the increased mRNA stability can be attributed to the appearance of a C in the Leu-coding allele.

In addition to the increased mRNA stability of the Leu224 variant, the hindrance of protein degradation (Figure 19 A) also contributes to the higher intracellular SCD1 levels. Although no considerable difference can be seen in the protein structures predicted in silico (Figure 19 B), there is abundant evidence in the literature that missense polymorphisms causing different amino acid substitutions at different loci affect the rate of degradation [155-158]. However, since a slower protein degradation could be detected in case of the artificial Ala224 variant (Figure 23 A), the protein stabilizing effect seems to be due to the elimination of the methionine side chain. Taking all these into consideration, it seems that the similar intracellular amount of the major Met224 and the artificial Ala224 variants of the protein (Figure 22) is due to two opposite effects: the lower mRNA level (Figure 23 C) is compensated by a longer protein half-life of Ala224 (Figure 23 A). The intracellular amount of the Leu224 variant can further be elevated by supplementation with certain FAs (Figure 20 A, B). This phenomenon seems to be a consequence of increased protein stability as the mRNA levels did not change (Figure 20 C). This effect of FAs is dependent on the presence of the leucine 224 as the protein level of the artificial Ala224 variant showed no significant change in response to FAs (Figure 23 B). We hypothesize that the Leu224 variant, with its decreased conformational entropy in the third transmembrane region (Figure 19 C), exhibits an increased sensitivity to various fatty acyl chains.

5.3. Summarizing considerations

Although neither of the investigated polymorphisms showed significant association with type 2 diabetes mellitus in our study (Table 9, 10), their role in the development of adverse metabolic conditions cannot be ruled out completely. Our association studies had rather low statistical power due to the small number of samples. Based on our *in silico* analysis and *in vitro* experiments, the potential correlation of the rs1054411 promoter polymorphism and M224L missense variant with diabetes would be worth investigating in larger populations and by involving additional phenotypic and clinical data, such as the composition of dietary intake and serum FA profile. Future research should also analyze haplotypes from both functional and associative perspectives.

Summing up, we demonstrated that the two most common TFAs, the industrial elaidate and the natural vaccenate, have significantly different, partly opposite effects on SCD1 expression: while vaccenate reduces or does not change the expression, a significant increment was observed upon elaidate supplementation in two cell lines. Among the promoter polymorphisms investigated, rs1054411, which did not alter the basal *SCD1* expression, significantly influenced the effect of various dietary FAs on *SCD1* promoter activity and also modulated the effect of the ETS1 TF (Figure 24).

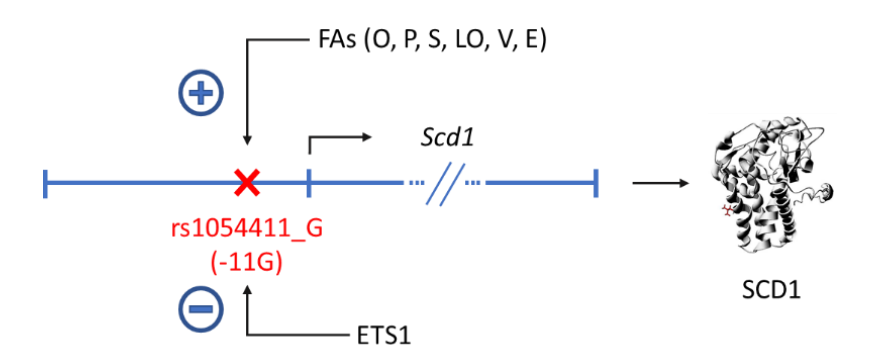


Figure 24. Effect of rs1054411 promoter polymorphism on SCD1 expression. In the presence of the G allele, FAs elevate SCD1 expression, while ETS1 binding to the promoter is reduced. O: oleate, P: palmitate, S: stearate, LO: linoleate, V: vaccenate, E: elaidate.

The M224L SNP in the coding region influences SCD1 protein level, *i.e.*, the Leu224 version shows an enhanced mRNA stability and an increased protein stabilizing effect of FAs, and it is the lack of Met224 that causes a hindered protein degradation (Figure 25). Elevated SCD1 expression is linked to various health conditions, whether as a cause or a consequence [84, 134]. SCD1 is considered a promising target for the treatment of metabolic diseases, and efforts are ongoing to develop liver-specific SCD1 inhibitors [159]. Genetic variations significantly affect efficacy of treatment [160, 161], thus functional polymorphisms of SCD1 may alter the effectiveness or even the necessity of SCD1 inhibitors. Therefore, the development of personalized therapeutic strategies based on genetic profiling is a promising future direction for the management of lipid metabolism-related diseases.

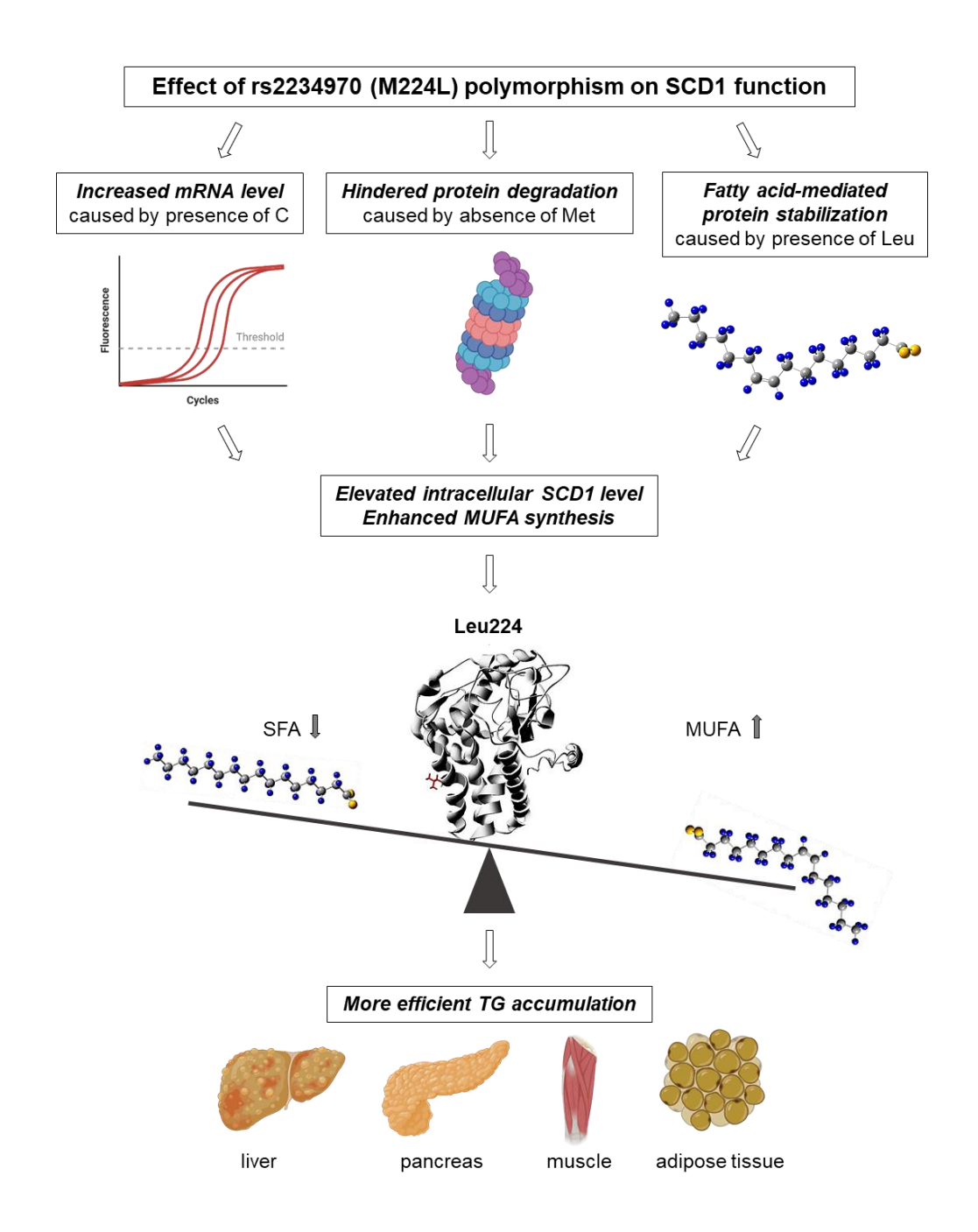


Figure 25. Effect of M224L polymorphism on SCD1 function (Created in BioRender).

6. Conclusions

We studied the transcriptional control and genetic polymorphisms of human stearoyl-CoA desaturase 1, the enzyme catalyzing the rate limiting step of converting SFAs into UFAs. The expression of the enzyme is regulated at many levels and depends on numerous factors. Our main findings are the following.

- 1. We investigated the impact of different types of FAs on SCD1 expression in HEK293T and HepG2 cells. We found a significant difference between the two TFAs: vaccenate decreased while elaidate markedly increased SCD1 levels, and this was due to transcriptional effects as consistently observed in protein and mRNA levels as well as in promoter activity assays.
- 2. We set out to assess the impacts of the most common polymorphisms of the *SCD1* gene, thus firstly, we created four polymorphic reporter constructs to investigate the effects of rs1054411, rs670213, rs2275657 and rs2275656 promoter SNPs.
 - a. Although the four promoter polymorphisms themselves does not influence the enzyme's promoter activity, the presence of certain FAs can modify the SNP-containing promoter activities. While the other SNPs have more diverse effects, rs1054411 enhances significantly the promoter activity in the presence of all FAs used.
 - b. We confirmed *in silico* and *in vitro* as well that compared to the wild type, rs1054411_G allele significantly (more than 20%) reduces ETS1 TF binding to the promoter. We also observed that ETS1 enhances the inductive effect of elaidate in the case of both alleles of the promoter.
- 3. To characterize the M224L (rs2234970) missense SNP in the coding region of SCD1, we created expression vector constructs. We demonstrated increased mRNA stability, desaturation index and FA-mediated protein stability, caused by the presence of the minor allele, and hindered protein degradation, due to the absence of the major allele.
- 4. Although neither of the examined polymorphisms showed significant association with T2DM, and the genotyping should be complemented with a larger sample size, the role of these polymorphisms in the development of metabolic conditions cannot be ruled out completely.

7. Summary

Stearoyl-CoA desaturase 1 enzyme, which catalyzes the synthesis of unsaturated FAs, is a key regulator of defense against lipotoxicity. However, altered activity or expression of SCD1 is a potential risk factor for metabolic disorders such as type 2 diabetes mellitus through its effect on fat storage.

The aim of the present thesis was to determine the nutritional and genetic factors that influence SCD1 enzyme levels, separately and in combination. The impact of different saturated and *cis* or *trans* unsaturated FAs on the endogenous and transiently transfected SCD1 was monitored in HEK293T and HepG2 cells. Four promoter variants (rs1054411_G, rs670213_C, rs2275657_C and rs2275656_C) and the single missense polymorphism in the coding region (M224L, *i.e.*, rs2234970) were generated by site-directed mutagenesis. The effect of SCD1 promoter variants on the TF binding site was investigated *in silico* using the JASPAR database and *in vitro* with a luciferase reporter system. Intracellular mRNA and protein levels were determined by qPCR and immunoblotting, respectively. Desaturase functions were measured by GC-FID.

SCD1 responds differently to different types of FAs at promoter, mRNA and protein levels. The two most common TFAs, industrial elaidate and natural vaccenate, have significantly different effects on SCD1 expression. The four most common promoter polymorphisms were found to be ineffective alone, but in the presence of FAs, they already modulated *SCD1* promoter activity. Both *in silico* and *in vitro* analyses revealed that in the presence of the minor allele of the rs1054411 promoter variant, the probability of ETS1 TF binding to the *SCD1* promoter was reduced by 20%. The Leu224 polymorphic enzyme was more abundant in cells due to slower protein degradation and more stable mRNA structure, which could be further enhanced by FAs. Significantly increased intracellular amounts of the SCD1 enzyme products (C18:1 and C16:1) proved the functionality of the highly expressed Leu224 variant.

Our results suggest that the levels of SCD1, a key regulator of lipid metabolism, may be influenced by a combination of common polymorphisms and available FAs. This highlights the need to map gene-environment interactions to understand both the normal function and the pathomechanism of lipid metabolism-related diseases.

8. Bibliography

- 1. The nomenclature of lipids (Recommendations 1976) IUPAC-IUB Commission on Biochemical Nomenclature. Biochem J. 1978;171(1):21-35.
- 2. Tvrzicka E, Kremmyda LS, Stankova B, Zak A. Fatty acids as biocompounds: their role in human metabolism, health and disease--a review. Part 1: classification, dietary sources and biological functions. Biomed Pap Med Fac Univ Palacky Olomouc Czech Repub. 2011;155(2):117-30.
- 3. Kihara A. Very long-chain fatty acids: elongation, physiology and related disorders. J Biochem. 2012;152(5):387-95.
- 4. Lim JN, Oh JJ, Wang T, Lee JS, Kim SH, Kim YJ, Lee HG. trans-11 18:1 vaccenic acid (TVA) has a direct anti-carcinogenic effect on MCF-7 human mammary adenocarcinoma cells. Nutrients. 2014;6(2):627-36.
- 5. Ferlay A, Bernard L, Meynadier A, Malpuech-Brugere C. Production of trans and conjugated fatty acids in dairy ruminants and their putative effects on human health: A review. Biochimie. 2017;141:107-20.
- 6. Sommerfeld M. Trans unsaturated fatty acids in natural products and processed foods. Prog Lipid Res. 1983;22(3):221-33.
- 7. Oteng AB, Kersten S. Mechanisms of Action of trans Fatty Acids. Adv Nutr. 2020;11(3):697-708.
- 8. Guillocheau E, Legrand P, Rioux V. Trans-palmitoleic acid (trans-9-C16:1, or trans-C16:1 n-7): Nutritional impacts, metabolism, origin, compositional data, analytical methods and chemical synthesis. A review. Biochimie. 2020;169:144-60.
- 9. Kuhnt K, Baehr M, Rohrer C, Jahreis G. Trans fatty acid isomers and the trans-9/trans-11 index in fat containing foods. Eur J Lipid Sci Technol. 2011;113(10):1281-92.
- 10. Baccouch R, Shi Y, Vernay E, Mathelie-Guinlet M, Taib-Maamar N, Villette S, Feuillie C, Rascol E, Nuss P, Lecomte S, Molinari M, Staneva G, Alves ID. The impact of lipid polyunsaturation on the physical and mechanical properties of lipid membranes. Biochim Biophys Acta Biomembr. 2023;1865(2):184084.
- 11. Harayama T, Shimizu T. Roles of polyunsaturated fatty acids, from mediators to membranes. J Lipid Res. 2020;61(8):1150-60.
- 12. Vanni S, Riccardi L, Palermo G, De Vivo M. Structure and Dynamics of the Acyl Chains in the Membrane Trafficking and Enzymatic Processing of Lipids. Acc Chem Res. 2019;52(11):3087-96.
- 13. Marza E, Long T, Saiardi A, Sumakovic M, Eimer S, Hall DH, Lesa GM. Polyunsaturated fatty acids influence synaptojanin localization to regulate synaptic vesicle recycling. Mol Biol Cell. 2008;19(3):833-42.
- 14. Christie WW, Harwood JL. Oxidation of polyunsaturated fatty acids to produce lipid mediators. Essays Biochem. 2020;64(3):401-21.
- 15. Ganguly R, Pierce GN. Trans fat involvement in cardiovascular disease. Mol Nutr Food Res. 2012;56(7):1090-6.
- 16. Bendsen NT, Christensen R, Bartels EM, Astrup A. Consumption of industrial and ruminant trans fatty acids and risk of coronary heart disease: a systematic review and meta-analysis of cohort studies. Eur J Clin Nutr. 2011;65(7):773-83.
- 17. Jackson CL. Lipid droplet biogenesis. Curr Opin Cell Biol. 2019;59:88-96.

- 18. Jo J, Gavrilova O, Pack S, Jou W, Mullen S, Sumner AE, Cushman SW, Periwal V. Hypertrophy and/or Hyperplasia: Dynamics of Adipose Tissue Growth. PLoS Comput Biol. 2009;5(3):e1000324.
- 19. Kanda H, Tateya S, Tamori Y, Kotani K, Hiasa K, Kitazawa R, Kitazawa S, Miyachi H, Maeda S, Egashira K, Kasuga M. MCP-1 contributes to macrophage infiltration into adipose tissue, insulin resistance, and hepatic steatosis in obesity. J Clin Invest. 2006;116(6):1494-505.
- 20. Callegari IOM, Oliveira AG. The Role of LTB4 in Obesity-Induced Insulin Resistance Development: An Overview. Front Endocrinol (Lausanne). 2022;13:848006.
- 21. Rehman K, Akash MS. Mechanisms of inflammatory responses and development of insulin resistance: how are they interlinked? J Biomed Sci. 2016;23(1):87.
- 22. Rehman K, Akash MSH, Liaqat A, Kamal S, Qadir MI, Rasul A. Role of Interleukin-6 in Development of Insulin Resistance and Type 2 Diabetes Mellitus. Crit Rev Eukaryot Gene Expr. 2017;27(3):229-36.
- 23. Aguirre V, Uchida T, Yenush L, Davis R, White MF. The c-Jun NH(2)-terminal kinase promotes insulin resistance during association with insulin receptor substrate-1 and phosphorylation of Ser(307). J Biol Chem. 2000;275(12):9047-54.
- 24. Gual P, Le Marchand-Brustel Y, Tanti JF. Positive and negative regulation of insulin signaling through IRS-1 phosphorylation. Biochimie. 2005;87(1):99-109.
- 25. Krebs DL, Hilton DJ. SOCS: physiological suppressors of cytokine signaling. J Cell Sci. 2000;113 (Pt 16):2813-9.
- 26. Jager J, Gremeaux T, Cormont M, Le Marchand-Brustel Y, Tanti JF. Interleukin-1beta-induced insulin resistance in adipocytes through down-regulation of insulin receptor substrate-1 expression. Endocrinology. 2007;148(1):241-51.
- 27. Konstantynowicz-Nowicka K, Harasim E, Baranowski M, Chabowski A. New evidence for the role of ceramide in the development of hepatic insulin resistance. PLoS One. 2015;10(1):e0116858.
- 28. Miquilena-Colina ME, Lima-Cabello E, Sanchez-Campos S, Garcia-Mediavilla MV, Fernandez-Bermejo M, Lozano-Rodriguez T, Vargas-Castrillon J, Buque X, Ochoa B, Aspichueta P, Gonzalez-Gallego J, Garcia-Monzon C. Hepatic fatty acid translocase CD36 upregulation is associated with insulin resistance, hyperinsulinaemia and increased steatosis in non-alcoholic steatohepatitis and chronic hepatitis C. Gut. 2011;60(10):1394-402.
- 29. Kazantzis M, Stahl A. Fatty acid transport proteins, implications in physiology and disease. Biochim Biophys Acta. 2012;1821(5):852-7.
- 30. Nakamura S, Takamura T, Matsuzawa-Nagata N, Takayama H, Misu H, Noda H, Nabemoto S, Kurita S, Ota T, Ando H, Miyamoto K, Kaneko S. Palmitate induces insulin resistance in H4IIEC3 hepatocytes through reactive oxygen species produced by mitochondria. J Biol Chem. 2009;284(22):14809-18.
- 31. Lambertucci RH, Hirabara SM, Silveira Ldos R, Levada-Pires AC, Curi R, Pithon-Curi TC. Palmitate increases superoxide production through mitochondrial electron transport chain and NADPH oxidase activity in skeletal muscle cells. J Cell Physiol. 2008;216(3):796-804.
- 32. Seifert EL, Estey C, Xuan JY, Harper ME. Electron transport chain-dependent and -independent mechanisms of mitochondrial H2O2 emission during long-chain fatty acid oxidation. J Biol Chem. 2010;285(8):5748-58.

- 33. Ghosh J, Das J, Manna P, Sil PC. Taurine prevents arsenic-induced cardiac oxidative stress and apoptotic damage: role of NF-kappa B, p38 and JNK MAPK pathway. Toxicol Appl Pharmacol. 2009;240(1):73-87.
- 34. Gao D, Nong S, Huang X, Lu Y, Zhao H, Lin Y, Man Y, Wang S, Yang J, Li J. The effects of palmitate on hepatic insulin resistance are mediated by NADPH Oxidase 3-derived reactive oxygen species through JNK and p38MAPK pathways. J Biol Chem. 2010;285(39):29965-73.
- 35. Zambo V, Simon-Szabo L, Szelenyi P, Kereszturi E, Banhegyi G, Csala M. Lipotoxicity in the liver. World J Hepatol. 2013;5(10):550-7.
- 36. Shimizu Y, Hendershot LM. Oxidative folding: cellular strategies for dealing with the resultant equimolar production of reactive oxygen species. Antioxid Redox Signal. 2009;11(9):2317-31.
- 37. Volmer R, van der Ploeg K, Ron D. Membrane lipid saturation activates endoplasmic reticulum unfolded protein response transducers through their transmembrane domains. Proc Natl Acad Sci U S A. 2013;110(12):4628-33.
- 38. Kitai Y, Ariyama H, Kono N, Oikawa D, Iwawaki T, Arai H. Membrane lipid saturation activates IRE1alpha without inducing clustering. Genes Cells. 2013;18(9):798-809.
- 39. Sommerweiss D, Gorski T, Richter S, Garten A, Kiess W. Oleate rescues INS-1E beta-cells from palmitate-induced apoptosis by preventing activation of the unfolded protein response. Biochem Biophys Res Commun. 2013;441(4):770-6.
- 40. Listenberger LL, Han X, Lewis SE, Cases S, Farese RV, Jr., Ory DS, Schaffer JE. Triglyceride accumulation protects against fatty acid-induced lipotoxicity. Proc Natl Acad Sci U S A. 2003;100(6):3077-82.
- 41. Sarnyai F, Somogyi A, Gor-Nagy Z, Zambo V, Szelenyi P, Matyasi J, Simon-Szabo L, Kereszturi E, Toth B, Csala M. Effect of cis- and trans-Monounsaturated Fatty Acids on Palmitate Toxicity and on Palmitate-induced Accumulation of Ceramides and Diglycerides. Int J Mol Sci. 2020;21(7).
- 42. Galbo T, Perry RJ, Jurczak MJ, Camporez JP, Alves TC, Kahn M, Guigni BA, Serr J, Zhang D, Bhanot S, Samuel VT, Shulman GI. Saturated and unsaturated fat induce hepatic insulin resistance independently of TLR-4 signaling and ceramide synthesis in vivo. Proc Natl Acad Sci U S A. 2013;110(31):12780-5.
- 43. Boslem E, MacIntosh G, Preston AM, Bartley C, Busch AK, Fuller M, Laybutt DR, Meikle PJ, Biden TJ. A lipidomic screen of palmitate-treated MIN6 beta-cells links sphingolipid metabolites with endoplasmic reticulum (ER) stress and impaired protein trafficking. Biochem J. 2011;435(1):267-76.
- 44. Veret J, Coant N, Berdyshev EV, Skobeleva A, Therville N, Bailbe D, Gorshkova I, Natarajan V, Portha B, Le Stunff H. Ceramide synthase 4 and de novo production of ceramides with specific N-acyl chain lengths are involved in glucolipotoxicity-induced apoptosis of INS-1 beta-cells. Biochem J. 2011;438(1):177-89.
- 45. Longato L, Tong M, Wands JR, de la Monte SM. High fat diet induced hepatic steatosis and insulin resistance: Role of dysregulated ceramide metabolism. Hepatol Res. 2012;42(4):412-27.
- 46. Powell DJ, Turban S, Gray A, Hajduch E, Hundal HS. Intracellular ceramide synthesis and protein kinase Czeta activation play an essential role in palmitate-induced insulin resistance in rat L6 skeletal muscle cells. Biochem J. 2004;382(Pt 2):619-29.

- 47. Wierzbicki M, Chabowski A, Zendzian-Piotrowska M, Harasim E, Gorski J. Chronic, in vivo, PPARalpha activation prevents lipid overload in rat liver induced by high fat feeding. Adv Med Sci. 2009;54(1):59-65.
- 48. Ly LD, Xu S, Choi SK, Ha CM, Thoudam T, Cha SK, Wiederkehr A, Wollheim CB, Lee IK, Park KS. Oxidative stress and calcium dysregulation by palmitate in type 2 diabetes. Exp Mol Med. 2017;49(2):e291.
- 49. Ghafourifar P, Klein SD, Schucht O, Schenk U, Pruschy M, Rocha S, Richter C. Ceramide induces cytochrome c release from isolated mitochondria. Importance of mitochondrial redox state. J Biol Chem. 1999;274(10):6080-4.
- 50. Maedler K, Oberholzer J, Bucher P, Spinas GA, Donath MY. Monounsaturated fatty acids prevent the deleterious effects of palmitate and high glucose on human pancreatic beta-cell turnover and function. Diabetes. 2003;52(3):726-33.
- 51. Henique C, Mansouri A, Fumey G, Lenoir V, Girard J, Bouillaud F, Prip-Buus C, Cohen I. Increased mitochondrial fatty acid oxidation is sufficient to protect skeletal muscle cells from palmitate-induced apoptosis. J Biol Chem. 2010;285(47):36818-27.
- 52. Milanski M, Degasperi G, Coope A, Morari J, Denis R, Cintra DE, Tsukumo DM, Anhe G, Amaral ME, Takahashi HK, Curi R, Oliveira HC, Carvalheira JB, Bordin S, Saad MJ, Velloso LA. Saturated fatty acids produce an inflammatory response predominantly through the activation of TLR4 signaling in hypothalamus: implications for the pathogenesis of obesity. J Neurosci. 2009;29(2):359-70.
- 53. Calder PC. Long-chain fatty acids and inflammation. Proc Nutr Soc. 2012;71(2):284-9.
- 54. Wong SW, Kwon MJ, Choi AM, Kim HP, Nakahira K, Hwang DH. Fatty acids modulate Toll-like receptor 4 activation through regulation of receptor dimerization and recruitment into lipid rafts in a reactive oxygen species-dependent manner. J Biol Chem. 2009;284(40):27384-92.
- 55. Kong W, Yen JH, Vassiliou E, Adhikary S, Toscano MG, Ganea D. Docosahexaenoic acid prevents dendritic cell maturation and in vitro and in vivo expression of the IL-12 cytokine family. Lipids Health Dis. 2010;9:12.
- 56. Calder PC. Omega-3 fatty acids and inflammatory processes: from molecules to man. Biochem Soc Trans. 2017;45(5):1105-15.
- 57. Lee H, Park WJ. Unsaturated fatty acids, desaturases, and human health. J Med Food. 2014;17(2):189-97.
- 58. Marquardt A, Stohr H, White K, Weber BH. cDNA cloning, genomic structure, and chromosomal localization of three members of the human fatty acid desaturase family. Genomics. 2000;66(2):175-83.
- 59. Leonard AE, Kelder B, Bobik EG, Chuang LT, Parker-Barnes JM, Thurmond JM, Kroeger PE, Kopchick JJ, Huang YS, Mukerji P. cDNA cloning and characterization of human Delta5-desaturase involved in the biosynthesis of arachidonic acid. Biochem J. 2000;347 Pt 3(Pt 3):719-24.
- 60. Reynolds LM, Dutta R, Seeds MC, Lake KN, Hallmark B, Mathias RA, Howard TD, Chilton FH. FADS genetic and metabolomic analyses identify the Δ5 desaturase (FADS1) step as a critical control point in the formation of biologically important lipids. Sci Rep. 2020;10(1):15873.
- 61. Park HG, Park WJ, Kothapalli KS, Brenna JT. The fatty acid desaturase 2 (FADS2) gene product catalyzes Delta4 desaturation to yield n-3 docosahexaenoic acid and n-6 docosapentaenoic acid in human cells. FASEB J. 2015;29(9):3911-9.

- 62. Ge L, Gordon JS, Hsuan C, Stenn K, Prouty SM. Identification of the delta-6 desaturase of human sebaceous glands: expression and enzyme activity. J Invest Dermatol. 2003;120(5):707-14.
- 63. Pedrono F, Blanchard H, Kloareg M, D'Andrea S, Daval S, Rioux V, Legrand P. The fatty acid desaturase 3 gene encodes for different FADS3 protein isoforms in mammalian tissues. J Lipid Res. 2010;51(3):472-9.
- 64. Plaisier CL, Horvath S, Huertas-Vazquez A, Cruz-Bautista I, Herrera MF, Tusie-Luna T, Aguilar-Salinas C, Pajukanta P. A systems genetics approach implicates USF1, FADS3, and other causal candidate genes for familial combined hyperlipidemia. PLoS Genet. 2009;5(9):e1000642.
- 65. Rioux V, Legrand P. Fatty Acid Desaturase 3 (FADS3) Is a Specific Δ13-Desaturase of Ruminant trans-Vaccenic Acid. Lifestyle Genom. 2019;12(1-6):18-24.
- 66. Karsai G, Lone M, Kutalik Z, Brenna JT, Li H, Pan D, von Eckardstein A, Hornemann T. FADS3 is a Delta14Z sphingoid base desaturase that contributes to gender differences in the human plasma sphingolipidome. J Biol Chem. 2020;295(7):1889-97.
- 67. Shanklin J, Guy JE, Mishra G, Lindqvist Y. Desaturases: emerging models for understanding functional diversification of diiron-containing enzymes. J Biol Chem. 2009;284(28):18559-63.
- 68. Nagao K, Murakami A, Umeda M. Structure and Function of Delta9-Fatty Acid Desaturase. Chem Pharm Bull (Tokyo). 2019;67(4):327-32.
- 69. Behrouzian B, Buist PH. Mechanism of fatty acid desaturation: a bioorganic perspective. Prostaglandins Leukot Essent Fatty Acids. 2003;68(2):107-12.
- 70. Wu X, Zou X, Chang Q, Zhang Y, Li Y, Zhang L, Huang J, Liang B. The evolutionary pattern and the regulation of stearoyl-CoA desaturase genes. Biomed Res Int. 2013;2013:856521.
- 71. Wang H, Klein MG, Zou H, Lane W, Snell G, Levin I, Li K, Sang BC. Crystal structure of human stearoyl-coenzyme A desaturase in complex with substrate. Nat Struct Mol Biol. 2015;22(7):581-5.
- 72. Heinemann FS, Ozols J. Stearoyl-CoA desaturase, a short-lived protein of endoplasmic reticulum with multiple control mechanisms. Prostaglandins Leukot Essent Fatty Acids. 2003;68(2):123-33.
- 73. Igal RA, Sinner DI. Stearoyl-CoA desaturase 5 (SCD5), a Delta-9 fatty acyl desaturase in search of a function. Biochim Biophys Acta Mol Cell Biol Lipids. 2021;1866(1):158840.
- 74. Fagerberg L, Hallstrom BM, Oksvold P, Kampf C, Djureinovic D, Odeberg J, Habuka M, Tahmasebpoor S, Danielsson A, Edlund K, Asplund A, Sjostedt E, Lundberg E, Szigyarto CA, Skogs M, Takanen JO, Berling H, Tegel H, Mulder J, Nilsson P, Schwenk JM, Lindskog C, Danielsson F, Mardinoglu A, Sivertsson A, von Feilitzen K, Forsberg M, Zwahlen M, Olsson I, Navani S, Huss M, Nielsen J, Ponten F, Uhlen M. Analysis of the human tissue-specific expression by genomewide integration of transcriptomics and antibody-based proteomics. Mol Cell Proteomics. 2014;13(2):397-406.
- 75. Orosz G, Szabo L, Bereti S, Zambo V, Csala M, Kereszturi E. Molecular Basis of Unequal Alternative Splicing of Human SCD5 and Its Alteration by Natural Genetic Variations. Int J Mol Sci. 2023;24(7).

- 76. Sinner DI, Kim GJ, Henderson GC, Igal RA. StearoylCoA desaturase-5: a novel regulator of neuronal cell proliferation and differentiation. PLoS One. 2012;7(6):e39787.
- 77. Zambo V, Orosz G, Szabo L, Tibori K, Sipeki S, Molnar K, Csala M, Kereszturi E. A Single Nucleotide Polymorphism (rs3811792) Affecting Human SCD5 Promoter Activity Is Associated with Diabetes Mellitus. Genes (Basel). 2022;13(10).
- 78. Enoch HG, Catala A, Strittmatter P. Mechanism of rat liver microsomal stearyl-CoA desaturase. Studies of the substrate specificity, enzyme-substrate interactions, and the function of lipid. J Biol Chem. 1976;251(16):5095-103.
- 79. Zhang L, Ge L, Parimoo S, Stenn K, Prouty SM. Human stearoyl-CoA desaturase: alternative transcripts generated from a single gene by usage of tandem polyadenylation sites. Biochem J. 1999;340 (Pt 1)(Pt 1):255-64.
- 80. Zhang L, Ge L, Tran T, Stenn K, Prouty SM. Isolation and characterization of the human stearoyl-CoA desaturase gene promoter: requirement of a conserved CCAAT cis-element. Biochem J. 2001;357(Pt 1):183-93.
- 81. Mauvoisin D, Rocque G, Arfa O, Radenne A, Boissier P, Mounier C. Role of the PI3-kinase/mTor pathway in the regulation of the stearoyl CoA desaturase (SCD1) gene expression by insulin in liver. J Cell Commun Signal. 2007;1(2):113-25.
- 82. Mauvoisin D, Prevost M, Ducheix S, Arnaud MP, Mounier C. Key role of the ERK1/2 MAPK pathway in the transcriptional regulation of the Stearoyl-CoA Desaturase (SCD1) gene expression in response to leptin. Mol Cell Endocrinol. 2010;319(1-2):116-28.
- 83. Waters KM, Miller CW, Ntambi JM. Localization of a polyunsaturated fatty acid response region in stearoyl-CoA desaturase gene 1. Biochim Biophys Acta. 1997;1349(1):33-42.
- 84. Mauvoisin D, Mounier C. Hormonal and nutritional regulation of SCD1 gene expression. Biochimie. 2011;93(1):78-86.
- 85. Saito E, Okada T, Abe Y, Kuromori Y, Miyashita M, Iwata F, Hara M, Ayusawa M, Mugishima H, Kitamura Y. Docosahexaenoic acid content in plasma phospholipids and desaturase indices in obese children. J Atheroscler Thromb. 2011;18(4):345-50.
- 86. Lee AR, Han SN. Pinolenic Acid Downregulates Lipid Anabolic Pathway in HepG2 Cells. Lipids. 2016;51(7):847-55.
- 87. Lee KN, Pariza MW, Ntambi JM. Conjugated linoleic acid decreases hepatic stearoyl-CoA desaturase mRNA expression. Biochem Biophys Res Commun. 1998;248(3):817-21.
- 88. Antal O, Peter M, Hackler L, Jr., Man I, Szebeni G, Ayaydin F, Hideghety K, Vigh L, Kitajka K, Balogh G, Puskas LG. Lipidomic analysis reveals a radiosensitizing role of gamma-linolenic acid in glioma cells. Biochim Biophys Acta. 2015;1851(9):1271-82.
- 89. Kato H, Sakaki K, Mihara K. Ubiquitin-proteasome-dependent degradation of mammalian ER stearoyl-CoA desaturase. J Cell Sci. 2006;119(Pt 11):2342-53.
- 90. Mziaut H, Korza G, Ozols J. The N terminus of microsomal delta 9 stearoyl-CoA desaturase contains the sequence determinant for its rapid degradation. Proc Natl Acad Sci U S A. 2000;97(16):8883-8.
- 91. Mziaut H, Korza G, Benraiss A, Ozols J. Selective mutagenesis of lysyl residues leads to a stable and active form of delta 9 stearoyl-CoA desaturase. Biochim Biophys Acta. 2002;1583(1):45-52.

- 92. Lengi AJ, Corl BA. Comparison of pig, sheep and chicken SCD5 homologs: Evidence for an early gene duplication event. Comp Biochem Physiol B Biochem Mol Biol. 2008;150(4):440-6.
- 93. Zhang J, Song F, Zhao X, Jiang H, Wu X, Wang B, Zhou M, Tian M, Shi B, Wang H, Jia Y, Wang H, Pan X, Li Z. EGFR modulates monounsaturated fatty acid synthesis through phosphorylation of SCD1 in lung cancer. Mol Cancer. 2017;16(1):127.
- 94. Murakami A, Nagao K, Juni N, Hara Y, Umeda M. An N-terminal di-proline motif is essential for fatty acid-dependent degradation of Delta9-desaturase in Drosophila. J Biol Chem. 2017;292(49):19976-86.
- 95. Liu Z, Yin X, Mai H, Li G, Lin Z, Jie W, Li K, Zhou H, Wei S, Hu L, Peng W, Lin J, Yao F, Tao H, Xiong XD, Li K. SCD rs41290540 single-nucleotide polymorphism modifies miR-498 binding and is associated with a decreased risk of coronary artery disease. Mol Genet Genomic Med. 2020;8(3):e1136.
- 96. Li D, Ji L, Liu L, Liu Y, Hou H, Yu K, Sun Q, Zhao Z. Characterization of circulating microRNA expression in patients with a ventricular septal defect. PLoS One. 2014;9(8):e106318.
- 97. Sepramaniam S, Tan JR, Tan KS, DeSilva DA, Tavintharan S, Woon FP, Wang CW, Yong FL, Karolina DS, Kaur P, Liu FJ, Lim KY, Armugam A, Jeyaseelan K. Circulating microRNAs as biomarkers of acute stroke. Int J Mol Sci. 2014;15(1):1418-32.
- 98. AbuMweis SS, Panchal SK, Jones PJH. Triacylglycerol-Lowering Effect of Docosahexaenoic Acid Is Not Influenced by Single-Nucleotide Polymorphisms Involved in Lipid Metabolism in Humans. Lipids. 2018;53(9):897-908.
- 99. Michael N, Gupta V, Sadananthan SA, Sampathkumar A, Chen L, Pan H, Tint MT, Lee KJ, Loy SL, Aris IM, Shek LP, Yap FKP, Godfrey KM, Leow MK, Lee YS, Kramer MS, Henry CJ, Fortier MV, Seng Chong Y, Gluckman PD, Karnani N, Velan SS. Determinants of intramyocellular lipid accumulation in early childhood. Int J Obes (Lond). 2020;44(5):1141-51.
- 100. Fernandez LP, Ramos-Ruiz R, Herranz J, Martin-Hernandez R, Vargas T, Mendiola M, Guerra L, Reglero G, Feliu J, Ramirez de Molina A. The transcriptional and mutational landscapes of lipid metabolism-related genes in colon cancer. Oncotarget. 2018;9(5):5919-30.
- 101. Rudkowska I, Julien P, Couture P, Lemieux S, Tchernof A, Barbier O, Vohl MC. Cardiometabolic risk factors are influenced by Stearoyl-CoA Desaturase (SCD) -1 gene polymorphisms and n-3 polyunsaturated fatty acid supplementation. Mol Nutr Food Res. 2014;58(5):1079-86.
- 102. Arregui M, Buijsse B, Stefan N, Corella D, Fisher E, di Giuseppe R, Coltell O, Knuppel S, Aleksandrova K, Joost HG, Boeing H, Weikert C. Heterogeneity of the Stearoyl-CoA desaturase-1 (SCD1) gene and metabolic risk factors in the EPIC-Potsdam study. PLoS One. 2012;7(11):e48338.
- 103. Merino DM, Ma DW, Mutch DM. Genetic variation in lipid desaturases and its impact on the development of human disease. Lipids Health Dis. 2010;9:63.
- 104. Peter A, Weigert C, Staiger H, Rittig K, Cegan A, Lutz P, Machicao F, Haring HU, Schleicher E. Induction of stearoyl-CoA desaturase protects human arterial endothelial cells against lipotoxicity. Am J Physiol Endocrinol Metab. 2008;295(2):E339-49.

- 105. Igal RA. Stearoyl-CoA desaturase-1: a novel key player in the mechanisms of cell proliferation, programmed cell death and transformation to cancer. Carcinogenesis. 2010;31(9):1509-15.
- 106. Nashed M, Chisholm JW, Igal RA. Stearoyl-CoA desaturase activity modulates the activation of epidermal growth factor receptor in human lung cancer cells. Exp Biol Med (Maywood). 2012;237(9):1007-17.
- 107. Hulver MW, Berggren JR, Carper MJ, Miyazaki M, Ntambi JM, Hoffman EP, Thyfault JP, Stevens R, Dohm GL, Houmard JA, Muoio DM. Elevated stearoyl-CoA desaturase-1 expression in skeletal muscle contributes to abnormal fatty acid partitioning in obese humans. Cell Metab. 2005;2(4):251-61.
- 108. Jones BH, Maher MA, Banz WJ, Zemel MB, Whelan J, Smith PJ, Moustaid N. Adipose tissue stearoyl-CoA desaturase mRNA is increased by obesity and decreased by polyunsaturated fatty acids. Am J Physiol. 1996;271(1 Pt 1):E44-9.
- 109. Stefan N, Peter A, Cegan A, Staiger H, Machann J, Schick F, Claussen CD, Fritsche A, Haring HU, Schleicher E. Low hepatic stearoyl-CoA desaturase 1 activity is associated with fatty liver and insulin resistance in obese humans. Diabetologia. 2008;51(4):648-56.
- 110. Bodis K, Kahl S, Simon MC, Zhou Z, Sell H, Knebel B, Tura A, Strassburger K, Burkart V, Mussig K, Markgraf D, Al-Hasani H, Szendroedi J, Roden M, Group GDSS. Reduced expression of stearoyl-CoA desaturase-1, but not free fatty acid receptor 2 or 4 in subcutaneous adipose tissue of patients with newly diagnosed type 2 diabetes mellitus. Nutr Diabetes. 2018;8(1):49.
- 111. Kumar VB, Vyas K, Buddhiraju M, Alshaher M, Flood JF, Morley JE. Changes in membrane fatty acids and delta-9 desaturase in senescence accelerated (SAMP8) mouse hippocampus with aging. Life Sci. 1999;65(16):1657-62.
- 112. Jeyakumar SM, Vajreswari A. Stearoyl-CoA desaturase 1: A potential target for non-alcoholic fatty liver disease?-perspective on emerging experimental evidence. World J Hepatol. 2022;14(1):168-79.
- 113. Tabaczar S, Wolosiewicz M, Filip A, Olichwier A, Dobrzyn P. The role of stearoyl-CoA desaturase in the regulation of cardiac metabolism. Postepy Biochem. 2018;64(3):183-9.
- 114. Pan G, Cavalli M, Wadelius C. Polymorphisms rs55710213 and rs56334587 regulate SCD1 expression by modulating HNF4A binding. Biochim Biophys Acta Gene Regul Mech. 2021;1864(8):194724.
- 115. Mutch DM, Lowry DE, Roth M, Sihag J, Hammad SS, Taylor CG, Zahradka P, Connelly PW, West SG, Bowen K, Kris-Etherton PM, Lamarche B, Couture P, Guay V, Jenkins DJA, Eck P, Jones PJH. Polymorphisms in the stearoyl-CoA desaturase gene modify blood glucose response to dietary oils varying in MUFA content in adults with obesity. Br J Nutr. 2022;127(4):503-12.
- 116. Gong J, Campos H, McGarvey S, Wu Z, Goldberg R, Baylin A. Genetic variation in stearoyl-CoA desaturase 1 is associated with metabolic syndrome prevalence in Costa Rican adults. J Nutr. 2011;141(12):2211-8.
- 117. Stankova B, Macasek J, Zeman M, Vecka M, Tvrzicka E, Jachymova M, Slaby A, Zak A. Polymorphisms rs2167444 and rs508384 in the SCD1 Gene Are Linked with High ApoB-48 Levels and Adverse Profile of Cardiometabolic Risk Factors. Folia Biol (Praha). 2019;65(4):159-69.

- 118. Warensjo E, Ingelsson E, Lundmark P, Lannfelt L, Syvanen AC, Vessby B, Riserus U. Polymorphisms in the SCD1 gene: associations with body fat distribution and insulin sensitivity. Obesity (Silver Spring). 2007;15(7):1732-40.
- 119. Vessby B, Gustafsson IB, Tengblad S, Berglund L. Indices of fatty acid desaturase activity in healthy human subjects: effects of different types of dietary fat. Br J Nutr. 2013;110(5):871-9.
- 120. Powell DA. An overview of patented small molecule stearoyl coenzyme-A desaturase inhibitors (2009 2013). Expert Opin Ther Pat. 2014;24(2):155-75.
- 121. Lorenz R, Bernhart SH, Honer Zu Siederdissen C, Tafer H, Flamm C, Stadler PF, Hofacker IL. ViennaRNA Package 2.0. Algorithms Mol Biol. 2011;6:26.
- 122. Yang J, Zhang Y. I-TASSER server: new development for protein structure and function predictions. Nucleic Acids Res. 2015;43(W1):W174-81.
- 123. Castro-Mondragon JA, Riudavets-Puig R, Rauluseviciute I, Lemma RB, Turchi L, Blanc-Mathieu R, Lucas J, Boddie P, Khan A, Manosalva Perez N, Fornes O, Leung TY, Aguirre A, Hammal F, Schmelter D, Baranasic D, Ballester B, Sandelin A, Lenhard B, Vandepoele K, Wasserman WW, Parcy F, Mathelier A. JASPAR 2022: the 9th release of the open-access database of transcription factor binding profiles. Nucleic Acids Res. 2022;50(D1):D165-D73.
- 124. McLaren W, Gil L, Hunt SE, Riat HS, Ritchie GR, Thormann A, Flicek P, Cunningham F. The Ensembl Variant Effect Predictor. Genome Biol. 2016;17(1):122.
- 125. Zhang Y, Zhang S, Yin J, Xu R. MiR-566 mediates cell migration and invasion in colon cancer cells by direct targeting of PSKH1. Cancer Cell Int. 2019;19:333.
- 126. Han J, Kaufman RJ. The role of ER stress in lipid metabolism and lipotoxicity. J Lipid Res. 2016;57(8):1329-38.
- 127. Obaseki E, Adebayo D, Bandyopadhyay S, Hariri H. Lipid droplets and fatty acid-induced lipotoxicity: in a nutshell. FEBS Lett. 2024;598(10):1207-14.
- 128. Yazici D, Sezer H. Insulin Resistance, Obesity and Lipotoxicity. Adv Exp Med Biol. 2017;960:277-304.
- 129. Liu W, Zhu M, Liu J, Su S, Zeng X, Fu F, Lu Y, Rao Z, Chen Y. Comparison of the effects of monounsaturated fatty acids and polyunsaturated fatty acids on the lipotoxicity of islets. Front Endocrinol (Lausanne). 2024;15:1368853.
- 130. Zambo V, Simon-Szabo L, Sarnyai F, Matyasi J, Gor-Nagy Z, Somogyi A, Szelenyi P, Kereszturi E, Toth B, Csala M. Investigation of the putative rate-limiting role of electron transfer in fatty acid desaturation using transfected HEK293T cells. FEBS Lett. 2020;594(3):530-9.
- 131. Ahmed B, Sultana R, Greene MW. Adipose tissue and insulin resistance in obese. Biomed Pharmacother. 2021;137:111315.
- 132. Minville-Walz M, Gresti J, Pichon L, Bellenger S, Bellenger J, Narce M, Rialland M. Distinct regulation of stearoyl-CoA desaturase 1 gene expression by cis and trans C18:1 fatty acids in human aortic smooth muscle cells. Genes Nutr. 2012;7(2):209-16.
- 133. Zulkifli RM, Parr T, Salter AM, Brameld JM. Regulation of ovine and porcine stearoyl coenzyme A desaturase gene promoters by fatty acids and sterols. J Anim Sci. 2010;88(8):2565-75.
- 134. AM AL, Syed DN, Ntambi JM. Insights into Stearoyl-CoA Desaturase-1 Regulation of Systemic Metabolism. Trends Endocrinol Metab. 2017;28(12):831-42.

- 135. Liu Y, Li J, Liu Y. Effects of epoxy stearic acid on lipid metabolism in HepG2 cells. J Food Sci. 2020;85(10):3644-52.
- 136. Sarnyai F, Kereszturi E, Szirmai K, Matyasi J, Al-Hag JI, Csizmadia T, Low P, Szelenyi P, Tamasi V, Tibori K, Zambo V, Toth B, Csala M. Different Metabolism and Toxicity of TRANS Fatty Acids, Elaidate and Vaccenate Compared to Cis-Oleate in HepG2 Cells. Int J Mol Sci. 2022;23(13).
- 137. Islam MA, Amin MN, Siddiqui SA, Hossain MP, Sultana F, Kabir MR. Trans fatty acids and lipid profile: A serious risk factor to cardiovascular disease, cancer and diabetes. Diabetes Metab Syndr. 2019;13(2):1643-7.
- 138. Oteng AB, Bhattacharya A, Brodesser S, Qi L, Tan NS, Kersten S. Feeding Angptl4(-/-) mice trans fat promotes foam cell formation in mesenteric lymph nodes without leading to ascites. J Lipid Res. 2017;58(6):1100-13.
- 139. Monguchi T, Hara T, Hasokawa M, Nakajima H, Mori K, Toh R, Irino Y, Ishida T, Hirata KI, Shinohara M. Excessive intake of trans fatty acid accelerates atherosclerosis through promoting inflammation and oxidative stress in a mouse model of hyperlipidemia. J Cardiol. 2017;70(2):121-7.
- 140. Stender S, Astrup A, Dyerberg J. Ruminant and industrially produced trans fatty acids: health aspects. Food Nutr Res. 2008;52.
- 141. Estadella D, da Penha Oller do Nascimento CM, Oyama LM, Ribeiro EB, Damaso AR, de Piano A. Lipotoxicity: effects of dietary saturated and transfatty acids. Mediators Inflamm. 2013;2013:137579.
- 142. Jakobsen MU, Overvad K, Dyerberg J, Heitmann BL. Intake of ruminant trans fatty acids and risk of coronary heart disease. Int J Epidemiol. 2008;37(1):173-82.
- 143. Gebauer SK, Chardigny JM, Jakobsen MU, Lamarche B, Lock AL, Proctor SD, Baer DJ. Effects of ruminant trans fatty acids on cardiovascular disease and cancer: a comprehensive review of epidemiological, clinical, and mechanistic studies. Adv Nutr. 2011;2(4):332-54.
- 144. Brouwer IA, Wanders AJ, Katan MB. Effect of animal and industrial trans fatty acids on HDL and LDL cholesterol levels in humans--a quantitative review. PLoS One. 2010;5(3):e9434.
- 145. Gebauer SK, Destaillats F, Dionisi F, Krauss RM, Baer DJ. Vaccenic acid and trans fatty acid isomers from partially hydrogenated oil both adversely affect LDL cholesterol: a double-blind, randomized controlled trial. Am J Clin Nutr. 2015;102(6):1339-46.
- 146. Da Silva MS, Julien P, Bilodeau JF, Barbier O, Rudkowska I. Trans Fatty Acids Suppress TNF-alpha-Induced Inflammatory Gene Expression in Endothelial (HUVEC) and Hepatocellular Carcinoma (HepG2) Cells. Lipids. 2017;52(4):315-25.
- 147. Yang C, Lim W, Bazer FW, Song G. Oleic acid stimulation of motility of human extravillous trophoblast cells is mediated by stearoyl-CoA desaturase-1 activity. Mol Hum Reprod. 2017;23(11):755-70.
- 148. Jaudszus A, Jahreis G, Schlormann W, Fischer J, Kramer R, Degen C, Rohrer C, Roth A, Gabriel H, Barz D, Gruen M. Vaccenic acid-mediated reduction in cytokine production is independent of c9,t11-CLA in human peripheral blood mononuclear cells. Biochim Biophys Acta. 2012;1821(10):1316-22.
- 149. Yordy JS, Li R, Sementchenko VI, Pei H, Muise-Helmericks RC, Watson DK. SP100 expression modulates ETS1 transcriptional activity and inhibits cell invasion. Oncogene. 2004;23(39):6654-65.

- 150. Yordy JS, Moussa O, Pei H, Chaussabel D, Li R, Watson DK. SP100 inhibits ETS1 activity in primary endothelial cells. Oncogene. 2005;24(5):916-31.
- 151. Verschoor ML, Verschoor CP, Singh G. Ets-1 global gene expression profile reveals associations with metabolism and oxidative stress in ovarian and breast cancers. Cancer Metab. 2013;1(1):17.
- 152. Verschoor ML, Wilson LA, Verschoor CP, Singh G. Ets-1 regulates energy metabolism in cancer cells. PLoS One. 2010;5(10):e13565.
- 153. Kereszturi E, Szmola R, Kukor Z, Simon P, Weiss FU, Lerch MM, Sahin-Toth M. Hereditary pancreatitis caused by mutation-induced misfolding of human cationic trypsinogen: a novel disease mechanism. Hum Mutat. 2009;30(4):575-82.
- 154. Lee JD, Hsiao KM, Chang PJ, Chen CC, Kuo YW, Huang YC, Hsu HL, Lin YH, Wu CY, Huang YC, Lee M, Hsu CY, Pan YT, Kuo CY, Lin CH. A common polymorphism decreases LRP1 mRNA stability and is associated with increased plasma factor VIII levels. Biochim Biophys Acta Mol Basis Dis. 2017;1863(6):1690-8.
- 155. Kusudo T, Hashida Y, Ando F, Shimokata H, Yamashita H. Asp3Gly polymorphism affects fatty acid-binding protein 3 intracellular stability and subcellular localization. FEBS Lett. 2015;589(18):2382-7.
- 156. Bandiera S, Weidlich S, Harth V, Broede P, Ko Y, Friedberg T. Proteasomal degradation of human CYP1B1: effect of the Asn453Ser polymorphism on the post-translational regulation of CYP1B1 expression. Mol Pharmacol. 2005;67(2):435-43.
- 157. Martin GG, McIntosh AL, Huang H, Gupta S, Atshaves BP, Landrock KK, Landrock D, Kier AB, Schroeder F. The human liver fatty acid binding protein T94A variant alters the structure, stability, and interaction with fibrates. Biochemistry. 2013;52(51):9347-57.
- 158. Beck ME, Zhang Y, Bharathi SS, Kosmider B, Bahmed K, Dahmer MK, Nogee LM, Goetzman ES. The common K333Q polymorphism in long-chain acyl-CoA dehydrogenase (LCAD) reduces enzyme stability and function. Mol Genet Metab. 2020;131(1-2):83-9.
- 159. Oballa RM, Belair L, Black WC, Bleasby K, Chan CC, Desroches C, Du X, Gordon R, Guay J, Guiral S, Hafey MJ, Hamelin E, Huang Z, Kennedy B, Lachance N, Landry F, Li CS, Mancini J, Normandin D, Pocai A, Powell DA, Ramtohul YK, Skorey K, Sorensen D, Sturkenboom W, Styhler A, Waddleton DM, Wang H, Wong S, Xu L, Zhang L. Development of a liver-targeted stearoyl-CoA desaturase (SCD) inhibitor (MK-8245) to establish a therapeutic window for the treatment of diabetes and dyslipidemia. J Med Chem. 2011;54(14):5082-96.
- 160. Elk N, Iwuchukwu OF. Using Personalized Medicine in the Management of Diabetes Mellitus. Pharmacotherapy. 2017;37(9):1131-49.
- 161. Masulli M, Della Pepa G, Cocozza S, Capasso M, Pignataro P, Vitale M, Gastaldelli A, Russo M, Dolce P, Riccardi G, Rivellese AA, Vaccaro O. The Pro12Ala polymorphism of PPARgamma2 modulates beta cell function and failure to oral glucose-lowering drugs in patients with type 2 diabetes. Diabetes Metab Res Rev. 2021;37(3):e3392.

9. Bibliography of own publications

List of publications related to the topic of the thesis:

- Tibori, K., Orosz, G., Zámbó, V., Szelényi, P., Sarnyai, F., Tamási, V., Rónai, Z., Mátyási, J., Tóth, B., Csala, M., & Kereszturi, É. (2022). Molecular Mechanisms Underlying the Elevated Expression of a Potentially Type 2 Diabetes Mellitus Associated SCD1 Variant. International journal of molecular sciences, 23(11), 6221. https://doi.org/10.3390/ijms23116221. IF: 5.6
- Tibori, K., Zámbó, V., Orosz, G., Szelényi, P., Sarnyai, F., Tamási, V., Rónai, Z., Csala, M., & Kereszturi, É. (2024). Allele-specific effect of various dietary fatty acids and ETS1 transcription factor on SCD1 expression. Scientific reports, 14(1), 177. https://doi.org/10.1038/s41598-023-50700-5. IF: 3.8

<u>List of publications independent of the topic of the thesis:</u>

- Sarnyai, F., Kereszturi, É., Szirmai, K., Mátyási, J., Al-Hag, J. I., Csizmadia, T., Lőw, P., Szelényi, P., Tamási, V., Tibori, K., Zámbó, V., Tóth, B., & Csala, M. (2022). Different Metabolism and Toxicity of TRANS Fatty Acids, Elaidate and Vaccenate Compared to *Cis*-Oleate in HepG2 Cells. International journal of molecular sciences, 23(13), 7298. https://doi.org/10.3390/ijms23137298.
 IF: 5.6
- Zámbó, V., Orosz, G., Szabó, L., Tibori, K., Sipeki, S., Molnár, K., Csala, M.,
 & Kereszturi, É. (2022). A Single Nucleotide Polymorphism (rs3811792)
 Affecting Human SCD5 Promoter Activity Is Associated with Diabetes
 Mellitus. Genes, 13(10), 1784. https://doi.org/10.3390/genes13101784. IF: 3.5

10. Acknowledgements

First of all, I would like to thank my supervisors, Dr. Éva Kereszturi and Dr. Miklós Csala for accepting me into their team and for their invaluable support and guidance throughout my PhD studies. I would like to express my sincere gratitude to them – the insights, encouragement and thoughtful guidance have been instrumental in shaping my research and bringing it to completion.

I would like to say a big thank you to all the members of our Lipotoxicity Research Group and the whole Molecular Biology Department. Their contribution has significantly enriched my work, and the vibrant atmosphere created by these great people have been essential in helping me navigate the challenges of my research. I am particularly grateful for Dr. Veronika Zámbó and Dr. Anna Somogyi for their support and sharing their knowledge of the fundamentals of the research techniques used in our laboratory. I would like to express my appreciation for the laboratory assistants, Béláné Szénási and Viktória Novákné who continuously have been great sources of support and have always been enthusiastic to assist in any way they could. I also wish to thank Dr. Blanka Tóth and her team at Budapest University of Technology and Economics for the GC-FID analysis.

Over and above, I would like to take the opportunity to express my heartfelt thanks and gratitude for my Mother, my Father and my Sister for supporting me, encouraging me unfailingly, giving me everything they could throughout and outside of my studies, and assuring me that no matter what difficulties I face, they trust me to be able to stay on my path. Anci, thank you so much for everything – your devotion, love and care are beyond words! I couldn't wish for a better Mother than you! I cannot express enough my thanks and gratitude to my Friends who have never missed a single chance to encourage me and express their pride in my persistence towards my goals. And last, but surely not least, I would like to grab the opportunity to thank the Love of my life, Ferenc Pardi for being by my side and holding on to us, for brightening my worst days with his single, captivating smile, for believing in me, teaching me real love, appreciation and patience, for being immensely proud of me, and (if I should ever forget about it) always helping me remember how valuable I am. I love you so very much, Baby! Thank you so much to all these prodigious people for paving my way and helping me become who I am today.